Rep. Prog. Phys. **75** (2012) 016601 (41pp) doi:10.1088/0034-4885/75/1/016601

Droplet based microfluidics

Ralf Seemann[1,2], Martin Brinkmann[2], Thomas Pfohl[2,3] and Stephan Herminghaus[2]

[1] Experimental Physics, Saarland University, D-66123 Saarbrücken, Germany
[2] Max Planck Institute for Dynamics and Self-Organization, D-37018 Göttingen, Germany
[3] Department of Chemistry, University of Basel, CH-4056 Basel, Switzerland

E-mail: ralf.seemann@physik.uni-saarland.de

Received 1 November 2010, in final form 22 September 2011
Published 22 December 2011
Online at stacks.iop.org/RoPP/75/016601

Abstract
Droplet based microfluidics is a rapidly growing interdisciplinary field of research combining soft matter physics, biochemistry and microsystems engineering. Its applications range from fast analytical systems or the synthesis of advanced materials to protein crystallization and biological assays for living cells. Precise control of droplet volumes and reliable manipulation of individual droplets such as coalescence, mixing of their contents, and sorting in combination with fast analysis tools allow us to perform chemical reactions inside the droplets under defined conditions. In this paper, we will review available drop generation and manipulation techniques. The main focus of this review is not to be comprehensive and explain all techniques in great detail but to identify and shed light on similarities and underlying physical principles. Since geometry and wetting properties of the microfluidic channels are crucial factors for droplet generation, we also briefly describe typical device fabrication methods in droplet based microfluidics. Examples of applications and reaction schemes which rely on the discussed manipulation techniques are also presented, such as the fabrication of special materials and biophysical experiments.

(Some figures may appear in colour only in the online journal)

This article was invited by C F Schmidt.

Contents

1. Introduction

In recent years, the field of microfluidics has been continuously growing due to its large potential in scientific research as well as in technical and medical applications. Owing to the large spectrum of potential use, it has become an interdisciplinary research field in its own right, gathering researchers from engineering, physical, chemical, biological, and medical faculties. As a consequence of this interdisciplinarity and enormous momentum of developments, it has become increasingly difficult to handle the continuously growing body of available literature on this topic, in particular with respect to the governing fundamental physical principles and microfluidic schemes—even the number of available review papers is impressive. This paper deals exclusively with droplet based microfluidics, which has attracted particularly wide interest lately. Our main focus is on fundamental aspects of droplet based microfluidics, trying to summarize the physical mechanisms and to identify the common governing principles of various manipulation techniques which can be found in the literature. The identification of common principles seems particularly important as microfluidics is a highly interdisciplinary field where researchers from different disciplines are struggling to find a 'common scientific language'. In order to make this review readable for both experts and beginners from all fields who are taking advantage of droplet based microfluidics, we also include a brief summary of typical device fabrication techniques and give some examples of applications and biophysical experiments. However, we do not claim completeness in these sections and rather refer to specialized reviews for a complete discussion of these topics, which would go well beyond the scope of this paper.

In the early days of microfluidics, one usually considered continuous flowing streams of completely miscible liquid phases without any thermodynamic boundary. The driving idea was to scale down volumes and channel sizes to perform (bio-)chemical reactions and analysis with minute amounts of reactants, to minimize processing times [1] and to perform experiments that were not possible before, e.g., to study the kinetics of particular chemical reactions, to fabricate special materials, or to screen biological properties. A major technical perspective is to integrate all typical lab processing on a single microfluidic device, often referred to as a 'lab-on-a-chip' [2]. For some technical or medical applications microfluidic concepts are developed to allow for a stand alone, disposable microfluidic device, such as the concept of a lab-on-a-CD [2, 3].

Promising as such perspectives may be, microfluidics also comes with a number of characteristic problems. At very small length scales, the particular boundary conditions of liquid flow at solid channel walls might influence the emerging flow pattern significantly [2–6]. Depending on the particular boundary effects, the parabolic velocity profile with zero velocity at the channel walls leads to undesired side effects such as axial dispersion of the injected liquid compounds [5, 6] which is typically controlled by the width of the cross section rather than by the much smaller height of a channel [7]. Because most microfluidic experiments are performed at low Reynolds numbers, the mixing in continuous flow microfluidics proceeds by molecular diffusion which is rather slow at typical microfluidic channel widths. The dimensions of microfluidic channels range from some micrometers to some hundred micrometers and the typical flow velocities stay below $10\,\mathrm{mm\,s^{-1}}$ resulting in Reynolds numbers Re well below 100 for water. Thus, in continuous microfluidic approaches mixing is difficult, which has stimulated a large number of concepts to facilitate mixing in continuous microfluidic systems on a short time scale mainly by geometry mediated chaotic advection [8–26].

Axial dispersion can be avoided and mixing can be facilitated in a straightforward manner by either separating the continuous phase by droplets of an immiscible fluid phase, or bubbles [27–35], as sketched in figure 1(*a*). Even though the liquid of interest (gray in the figure) wets the channel walls, the bubbles or droplets avoid significant liquid exchange between the liquid segments as only a thin wetting layer at the channel walls connects the various segments [5]. Mixing occurs very rapidly within the segments due to the resulting convective flow profile inside them [30, 36–41] and was used to, e.g., synthesize special colloidal ceramics [27, 29]. Segmented flow offers many possibilities in the handling of liquids such as distillation steps [31–35, 42, 43] and is thus desirable for many technical and fundamental applications. For in depth reviews, see [30, 36, 44].

The concept of segmented flow also has certain limitations, e.g., to conduct fast chemical reactions which form gels or precipitates which might stick to the channel wall and to avoid liquid exchange between subsequently flowing segments due to a thin wetting layer. Droplet based microfluidics uses a complementary approach and dispenses the reactants into individual droplets surrounded by an immiscible liquid phase, cf figure 1(*b*). This approach has similar merits as segmented flow but the liquid of interest does not wet the channel walls and precipitating of substances and cross contaminations between different droplets can be fully prevented if the reacting molecules or ions cannot diffuse between the drops, i.e. through the carrier phase. However, care has to be taken if molecules are soluble in both liquid phases, in particular if molecules in the droplet phase have a better solubility in the carrier fluid as these molecules can

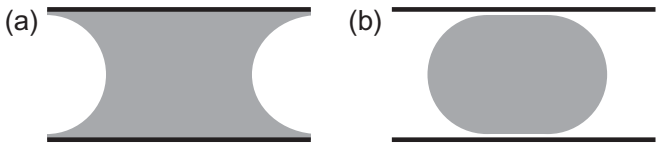

Figure 1. Schematic showing (*a*) a continuous flow that is segmented by bubbles or droplets and (*b*) droplet based microfluidics. The liquid of interest is colored gray in both cases.

easily diffuse out of the droplets [470]. The diffusion into the carrier fluid can even be enhanced in the presence of a surfactant. Inside each droplet, which is confined in and flowing though a microfluidic channel, a flow profile was found similar to the flow profile in the liquid segments as mentioned above and which guarantees fast mixing inside each droplet. This type of droplet based microfluidics requires controlled droplet formation for precise liquid dispensing, manipulation of individual droplets, and reaction control, and offers many possibilities to study fundamental and applied physical and (bio-)chemical aspects.

This paper reviews droplet based microfluidics and the focus is on the general techniques, governing physical principles, and microfluidic concepts. Aspects such as device fabrication, double emulsions, and applications in particle fabrication or biophysics are mentioned for completeness but are not reviewed in depth as they use the same or very similar microfluidic concepts.

2. Device fabrications

Any review on microfluidics would be incomplete without a few words about device fabrication and what has become known as 'soft lithography'. In this section an overview of the main fabrication techniques is provided to make the paper readable for non-experts in the field. For in depth reviews and actual trends in device fabrication, however, we refer to specialized reviews. Experienced users of microfluidics are encouraged to directly continue to section 3.

Similar type of devices and fabrication techniques are used for both continuous flow and droplet based microfluidics. But in contrast to typical applications in continuous flow microfluidics the wettability of the channels walls is crucial in droplet based microfluidics to achieve stable droplet production. Due to a typically organic carrier phase the chemical compatibility to those fluids is also very important.

There are several standard microfabrication techniques used for device fabrication ranging from contact and electron beam lithography followed by isotropic or anisotropic etching steps, and anionic bonding to form glass or silicon-glass devices [45], direct micro-machining of polymeric and metallic materials, using the polymeric photoresist structure as a channel matrix. Whilst most of these device materials offer great features with respect to chemical stability, geometric precision and durability, they are expensive and time consuming to fabricate. For scientific research, however, it is often more important to minimize the technological and temporal effort for device fabrication to quickly and easily adopt microfluidic devices to new demands and developments. Therefore soft lithographic techniques such as replica molding or embossing using masters fabricated by photolithographically or mold-machining [46–52] are widely used. A recently published technique for master fabrication outside a clean room relies on direct printing of a toner mask which can be thermally transferred to a metal master to serve as a master for etching [58].

2.1. Standard device fabrication technique in science and research

Due to its simplicity in fabrication, fairly low background fluorescence, and good bio-compatibility [47, 48, 53–55] the standard microfluidic device used in scientific research both for continuous flow and droplet based microfluidics is produced by replica molding using poly(dimethylsiloxane) (PDMS) silicon rubber. In most cases the commercially available kit 'Sylgard 184' from Dow Corning is used, consisting of a base and an agent mixed in a mass ratio of 10 : 1. To achieve certain properties such as reduced UV light scattering additives such as fluorescent dyes are mixed into the PDMS [482]. In the following the basic principle of soft lithographic device fabrication is explained for PDMS devices but applies similarly to other polymeric materials as will be discussed in section 2.3.

To fabricate PDMS devices, typically a master is produced by standard contact photolithography and a replica is generated from this master by pouring the already mixed PDMS-kit onto these masters, degassing, and heat curing. Probably, the most frequently used photoresist for the lithographic procedure is the negative resist SU-8 (Micro Resist Technology) which is available in different viscosities to directly generate a wide range of structure heights starting from about 1 μm to several hundred micrometers in one step, for further details see, e.g., [56]. For a small number of molding steps the photoresist structure can be used directly as a master for replica molding. After removing the cured PDMS replica from the master the PDMS mold is typically bonded to a glass cover and contacted by tubing which can be simply pushed through the PDMS rubber. A schematic of the typical fabrication protocol is shown in figure 2. If aqueous liquids are used for the microfluidic experiments, additional bonding of the device or sealing of the tubing may not be needed as the PDMS rubber closes all gaps very tightly. But if oily liquids are used a more rigorous bonding is required, the PDMS replica and the glass cover is OH^- terminated by a short oxygen plasma treatment prior to contacting them resulting in a covalent bond of the PDMS device and the cover.

Device fabrication techniques using PDMS as matrix material were also developed that do not require a lithographically fabricated master. Here, wires or tubing act as a three-dimensional positive mask which is embedded into the PDMS and finally removed after curing [57] resulting in cylindrical microfluidic channels. This technique, however, is limited to the fabrication of rather simple channels structures.

2.2. Special device properties for droplet based microfluidics

For stable droplet generation in a microfluidic device the wetting properties of the channel walls are crucial.

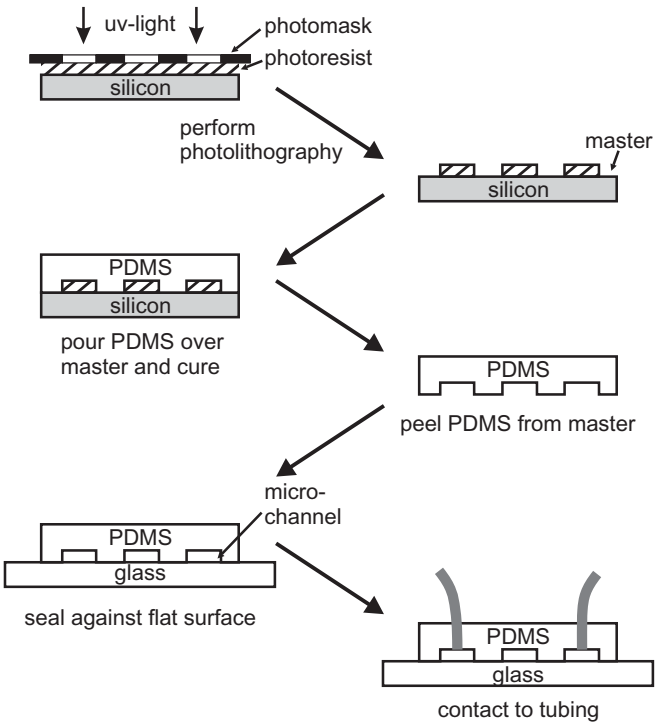

Figure 2. Schematic of typical device fabrication using contact photolithography for structuring and PDMS as the device material.

Hydrophobic channel walls are required, for instance, to generate water droplets in a surrounding oily phase. And vice versa, a hydrophilic channel wall is necessary to generate oil droplets in a surrounding aqueous phase. Thus, PDMS rubber devices will not always be the first choice or need further modifications of the channel wettability with respect to the liquid used. Sometimes even simple tricks such as soaking the PDMS device prior to usage with the continuous phase containing a high concentration of the surfactant helps us to achieve the desired wetting properties or to use certain fluids as continuous phases [59]. In case these simple measures are not sufficient to achieve the desired wetting properties, various coating techniques have been developed to tailor the wettability and the chemical compatibility of PDMS as we will discuss later in this subsection.

The elasticity of PDMS that makes its handling so easy might be unfavorable if, e.g., precise channel dimensions are needed for stable droplet formation or manipulation. Also, low aspect ratio structures, i.e. shallow microfluidic channels, may deform or even collapse at high flow rates owing to the high pressure level necessary to drive the flow [63]. To maintain the dimensions of a microfluidic channel during long device operation the chemical compatibility of the channel matrix with the used liquids is also crucial since possible swelling, dissolving of the device material, or escape of liquids diffusing through the matrix material has to be avoided. This aspect deserves particular attention in droplet based microfluidics because most experiments consider aqueous droplets flowing in a surrounding oily phase. In light of these aspects the usage of PDMS might seem quite peculiar as PDMS is only fully chemically compatible to polar liquids such as water and fluorinated oils [55, 64–67] and could yet be very permeable for those polar liquids. But for most applications the desirable properties and easy handling still predominate. An evaluation of the properties of PDMS devices can be found in [468].

Some experiments involving very small channel dimensions, very low flow rates, long storage times, or certain chemicals cannot be performed using microfluidic devices simply made of PDMS. Thus protocols were developed to coat the inner part of PDMS channels which vary the wettability and improve the chemical compatibility by a thin glass coating using sol–gel routes [68, 69]. This type of glassy coating also offers the possibility for further surface modifications using a self-assembly monolayer [70]. Alternatively, wettability and chemical compatibility can be varied by acrylic acid coatings [69], plasma polymerization [60], or deposition of polyelectrolytes [61]. Using channel coatings, not only the wettability and chemical compatibility but also the typically rectangular cross section of channels can be rounded [71].

To structure the wettability of a microfluidic device laterally, a controlled coating of individual parts of a microfluidic device using a sol–gel coating [476] or polyelectrolyte layers can be achieved by flushing the device with two liquids using flow confinement [476] or by flushing a device with droplets of various compounds through the device containing different polyelectrolyte solutions [62], respectively. In combination with a second coating step of a curable polymeric material, the diffusibility of PDMS can be used to structure the wettability locally. Oxygen chambers (chemo-masks) can be embedded into PDMS devices right at the position where a different wettability is desired. The oxygen diffuses through the PDMS during the polymer curing and locally inhibits the curing of the polymer coating [475].

2.3. Alternative device materials

In cases where the permeability of water vapor or the swelling by organic liquids forbid the usage of PDMS, alternative materials such as photo-curable polymers can be employed for soft lithographic device fabrication. Frequently used are thiolene based resins such as NOA81 or NOA83H (Norland) depending on wettability and feature resolution [67, 72, 73, 468] even with electrowetting functionality included [74]. The swelling ratio of cured thiolene resins for some typical solvents can be found in [67], in comparison with PDMS, showing that thiolene resin based microfluidic devices are very beneficial compared with PDMS devices if alkanes or even toluene are used as continuous phase fluids.

Microfluidic devices made from curable pre-polymers are typically produced in two steps. In a first step a PDMS replica is fabricated from the master as described in figure 2. From this PDMS replica a second replica is molded using, e.g., the thiolene based resin. These type of pre-polymers are either curable by UV-exposure or by a combination of UV-exposure and thermal treatment. If the reusability of the master is not critical, the thiolene devices can also be replicated directly from an SU-8 master. In addition to the particular curing protocol the general idea of device fabrication is quite similar to the one explained for PDMS devices and shall not be discussed further.

Alternative soft lithographic methods such as micromolding of thermoplastic polymers or embossing into polymers such as polymethylmetacrylate (PMMA) can be applied for the fabrication of microfluidic devices [50–52, 75, 469] and increase the number of available device materials. These types of devices and fabrication techniques are even suitable for large-scale fabrication but are not frequently used for applications in science and research. For small scale fabrication it was even demonstrated that SU-8 masters can be directly used for embossing in cycloolefin polymers without the need of, e.g., a metal master [77]. A review on bonding of thermoplastic polymer microfluidic devices can be found in [76].

3. Droplet formation

Droplet based microfluidics relies on the production of droplets with a controlled size at a high frequency. The flow of at least two liquids is controlled either by volume, using, e.g., syringe pumps or by pressure, using, e.g., hydrostatic reservoirs. Only very recently in an attempt to make microfluidic devices operation more independent it was demonstrated that a controlled flow and droplet production can be realized also by applying a vacuum [481]. The droplets are typically generated by a surface induced instability using different device geometries depending on the required droplet frequency, droplet monodispersity, or variability in droplet size. To improve the monodispersity of the generated droplets and to guarantee and prevent unwanted coalescence events during subsequent droplet manipulations surfactant is typically added to the continuous phase.

We begin with a brief overview of typically used oil/surfactant systems and continue with bulk emulsification techniques which were transferred into microfluidic devices, introducing the typical concepts which are nowadays used for *in situ* droplet formation in microfluidic devices. This overview focuses on similarities between the various concepts, their possible applications, and technological constraints. In the remainder we try to classify and discuss the concepts of droplet production in terms of universal energetic aspects that control the interfacial instabilities and also discuss some hydrodynamic aspects.

A specialized review on droplet generation by co-flow streams, flow-focusing and T-junction geometries already summarizes most of the techniques that were available by the year 2007 and how these techniques were used for particle production [185].

3.1. Carrier phases and surfactants

Typically, surfactants are added to the continuous phase to lower the interfacial energy, i.e. to facilitate the formation of new interfaces and to stabilize the formed emulsion droplets from coalescence by adsorbing at the liquid/liquid interface, cf figure 3(*a*). Often organic carrier phases such as hexadecane and mineral oil are used in combination with standard surfactant such as Tween 20 or Span 80 to form aqueous droplets. But most of these organic phases swell PDMS devices and change their geometry with time.

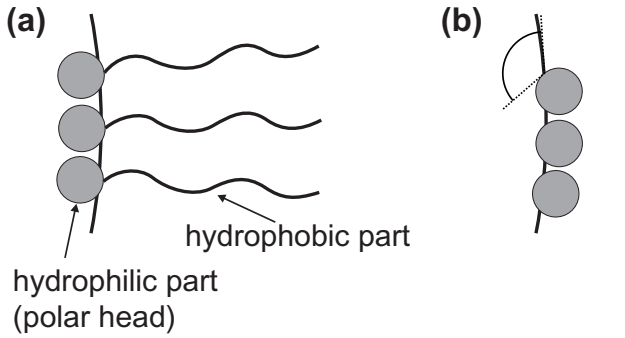

Figure 3. Schematic of the stabilizing function of a molecular surfactant (*a*) having a polar head and a hydrophobic tail and interface stabilization by solid particles (*b*), where the position at the fluid/fluid interface is given by the contact angle θ of one of the fluid phases.

The swelling can be avoided or reduced using other device materials or by applying surface coatings as discussed before in section 2 or by choosing another carrier phase. To avoid swelling effects in PDMS devices often fluorinated oils such as FC40, FC70 (DuPont) or perfluorodecalin are employed as a carrier phase which requires fluorinated surfactants such as pentadecaflouoro-1-octanol or Krytox (perfluorinated polyether, DuPont). But even though fluorinated oils do not noticeably swell PDMS it is worth mentioning that the fluorinated oils can diffuse through PDMS and leach compounds out of the PDMS material. The fairly large diffusibility of gas and vapor through some oils and in particular through fluorinated oils might be a disadvantage for some applications as cross contaminations and the selective loss of some substances cannot be avoided, but this material property can also be used to stimulate a controlled exchange of selected ions between droplets or to provide oxygen supply for cells encapsulated in aqueous droplets. In case biological substances shall be encapsulated the bio-compatibility of the organic phases, respectively, the used surfactant, also needs to be considered. Bio-compatibility can be achieved using fluorinated oils together with a surfactant combined with a perfluorinated polyether and polyethyleneglycol [78] or for organic phases such as squalane in combination with lipids, e.g. monoolein, to stabilize aqueous droplets [503]. In any case it is important to choose an appropriate oil/surfactant system and a corresponding device material to meet the respective requirements for a particular application in droplet based microfluidics.

Alternatively to molecular surfactants, emulsion droplets can be stabilized by small solid particles [79]. Provided the particles are partially wetted by the fluid phases they will attach to the fluid interface and the fluid interface adopts the wetting angle on the particle interface. In the generic case that the solid particles energetically prefer contact to one of the fluid phases, a spontaneous curvature of the fluid interface is observed, cf figure 3(*b*). However, due to the fairly large particle size and mass and the resulting slow diffusion to the liquid/liquid interface, and the fairly rigid particle stabilized liquid/liquid interface, the usage of particle stabilized emulsions is rare in microfluidics. A controlled assembly of jammed colloidal

shells at the fluid/liquid interface can be generated either by gravity in the case of aqueous drops in air [80] or by evaporation of the dispersed phase into the continuous phase in the case of water/ethanol emulsions [79, 480], and in the case of CO_2 bubbles stabilized in an aqueous solution [81].

3.2. From bulk emulsification to microfluidic droplet production

Traditional bulk processes to produce large quantities of emulsions take advantage of shear induced instabilities of the liquid interface between the continuous and the dispersed phases. Shear induced emulsification is applied in the food and cosmetic industries [82] since it has low technical demands whenever the monodispersity of the emulsion droplets is not critical. To increase the homogeneity of the generated droplet sizes, repeated fractionation of polydisperse emulsions can be applied [83]. The direct fabrication of monodisperse droplets was demonstrated in a batch process by shearing two immiscible fluids between parallel plates [84]. The first approaches to apply this technique for the droplet production in microfluidic devices employed micro-machined comb geometries [85, 86]. This geometry and its operation was and still is continuously improved to increase both monodispersity and yield of the produced droplets [87–89]. Very similar to the idea of a linear comb geometry, droplets are formed if one liquid is pushed through a porous membrane, i.e. a two-dimensional arrangement of pores, into another immiscible fluid. This technique allows us to generate large numbers of droplets whereas typically only a fraction of the membrane pores is active, i.e. liquid is only flowing through the biggest pores whereas the critical pressure to activate more pores cannot be reached without destroying the respective membrane. Improved membrane geometries significantly increase the monodispersity of the generated droplets reaching a variance of droplet size below 2% [90–92]. One of the very few examples of an implementation of a two- or three-dimensional membrane [93] into a microfluidic device for the generation of small droplets or to fragment larger droplets was fabricated in SU-8 resist, as introduced in [94].

Although methods which were originally developed in bulk could successfully be transferred into a microfluidic devices they are rather optimized for high yield than for the controlled production of monodisperse droplets, and most microfluidic 'lab chip application' relies on *in situ* drop by drop production techniques for the sake of droplet homogeneity, simplicity of device fabrication, and controllable operational parameters. The most frequently applied techniques or geometries are 'T-junctions', 'flow focusing', and 'step emulsification' which will be explained in the subsequent subsections followed by a discussion of the underlying physical principles.

3.3. T-junction

The easily controllable production of a single stream of monodisperse droplets in a microfluidic channel was first demonstrated using a T-channel geometry. The breakup of a continuous stream of one fluid is caused by shear from the cross flow of a stream of a second immiscible fluid [95].

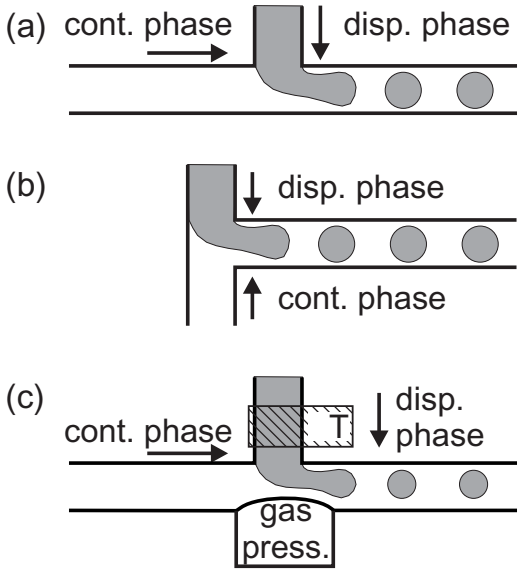

Figure 4. Schematic of various T-junction geometries. (*a*) 'regular T-junction' geometry where the dispersed phase is injected perpendicular into a stream of continuous fluid. (*b*) 'Head on' geometry where the dispersed and the continuous phases are injected from opposite sides. (*c*) 'Active T-junction' allowing variations of the geometry by air pressure and temperature control of the dispersed phase.

The generic geometry of a T-channel is shown in figure 4(*a*) as it is frequently employed to generate bubbles and droplets in microfluidic channels, e.g., [96]. The composition of the generated droplets can be varied by merging several streams of miscible liquid into one common channel before dispensing [96, 118]. In recent years a large number of papers were published that identified the physical parameters such as flow rates and viscosities [97–99], channel wall wettability [100], interfacial tension [101, 102], surfactants and their concentrations [103–106], channel dimensions [102, 107], and crossing angles of the microfluidic channels [109, 110] to derive scaling laws for droplet breakup based on experimental data [111, 112] and theoretical analysis [109, 113, 114]. In addition to passive techniques such as optimized channel geometries and operation conditions, the monodispersity of the produced drops can be actively improved by a closed loop system where the generated droplet sizes are optically monitored and used as a feedback signal to fine adjust the flow rates [117].

Several concepts have been developed to increase droplet productions rates, a straightforward approach is parallelized droplet production combining up to 32 [115] or 128 [116] T-junction geometries in a circular microfluidic device or by subsequently (multiple) splitting primary droplets, cf section 6.6. Extremely high droplet production rates up to 7.4 kHz could be also realized by two subsequent T-junctions where first air bubbles are injected into a continuous stream prior to the second T-junction where the emulsion droplets are generated in a tertiary system [483].

A variation of the above explained operation principle of a T-junction is the so called head-on device which is displayed in

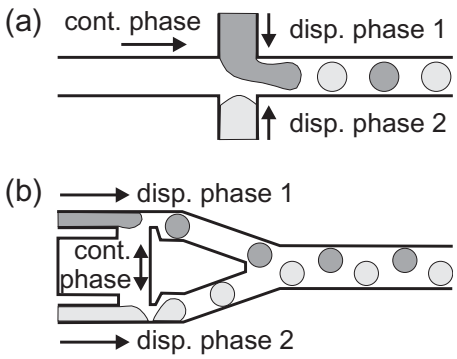

Figure 5. Schematic of various double T-junction geometries for the synchronized production of two kinds of droplets. Combination of two T-junctions as demonstrated, e.g., (*a*) in [118] and (*b*) in [132].

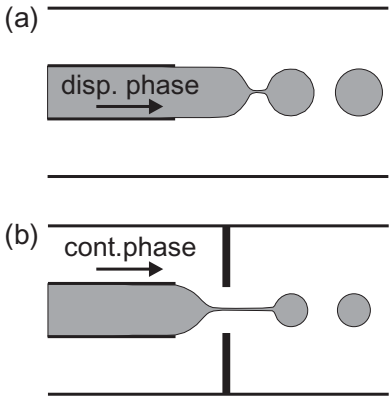

Figure 6. Schematic of co-flowing devices with flow focusing (*b*) and without flow focusing (*a*).

figure 4(*b*). Here, also a T-channel [120, 122] or a Y-channel [102] geometry is employed but the two fluids are injected from the two straight channels facing each other having similar features as the droplet production by the above described T-junction geometry.

To increase the flexibility or to expand the parameter range of reliable droplet production in T-junction devices, active elements have been introduced into T-junction geometries. Variable channel dimensions controlled by an inflatable gas chamber [123, 124] allow for the production of droplets in an extended size range. Varying the physical properties of the fluids, the size of the produced droplets can be adjusted by heating one of the connections of a T-junction by, e.g., varying surface tension or viscosity of the injected liquid [126, 127], cf figure 4(*c*). For full flexibility in the produced droplet size the droplets can be dispensed from a pressurized reservoir by opening and closing mechanical or pneumatic microvalves [128, 129]. To guarantee a precise droplet volume the continuous phase flow has to be stopped during dispensing and the droplet generation frequency is very small.

In certain applications, such as conduction chemical reactions by merging two droplets containing different reactants (as will be discussed in section 7.1.2), it is desired to generate distinct pairs of droplets. This can be achieved by a suitable combination of two T-channel geometries facing each other across a common main channel [118], cf figure 5(*a*). The synchronization which appears in some regions of flow parameters could be explained by hydrodynamic coupling [130]. Using the same basic double T-junction geometry with modified channel geometries at the outlet, a synchronized production of droplet pairs with number ratios of 1 : 5 and 5 : 1 at each junction was demonstrated [131]. A synchronized production of droplet pairs was also achieved by combining two T-junctions in a different geometry [132], cf figure 5(*b*). A passively synchronized production of droplet pairs was also demonstrated in [133] based on T-junctions with additional connections of the upstream and downstream channels.

T-junctions are widely used in droplet based microfluidics as they are easy to fabricate and easy to operate and even allow for synchronized droplet formation and are thus a good choice if the demands on the homogeneity of the generated droplet size are not too high. T-junctions allow for large droplet production frequencies of several hundred droplets per second without additional measures, depending on the particular system and geometry. The droplet production frequency is limited to large frequencies by the droplet breakup time and to small frequencies by the decreasing shear rate resulting in unstable droplet formation. The stability of the droplet formation at lower shear rates can be increased by active elements included in the T-junction device.

3.4. Flow focusing

A second, also frequently used, method to produce small droplets in microfluidic devices by viscous stress is so called 'co-flow' or 'flow focusing'. The underlying ideas and geometries of both methods are quite similar as can be seen in figure 6. In a 'co-flow' geometry two liquid streams are flowing together whereas the continuous fluid phase surrounds the dispersed liquid phase, which finally decays into droplets via Rayleigh–Plateau instability, cf figure 6(*a*) and section 4.4. In a 'flow-focusing' geometry the streams of co-flowing liquids are additionally focused through an orifice, cf figure 6(*b*). In such a flow-focusing geometry the two immiscible liquid phases undergo large elongational flow as they pass the small orifice generating smaller droplets as in a flow-focusing device of similar geometry. Since a flow-focusing geometry can be considered as a special case of a co-flow geometry the distinction in the literature is not always unambiguous.

The demands on the fabrication and operation of co-flow and flow-focusing devices are higher as compared with a T-junction geometry as more complex channel geometries and more fluidic inlets are needed. But in particular flow-focusing geometries allow us to vary the effective geometry by adjusting the flow rates of dispersed and continuous phase and thus offer a large flexibility in generated droplets size. By focusing and thinning the stream of dispersed phase through an orifice very small droplets can also be generated at high frequencies. As for the T-junctions the droplet generation is quite robust with respect to identifying appropriate operational parameters.

The co-flow technique was first developed outside of a microfluidic device to generate highly uniform gas bubbles in a liquid [134]. The concept of droplet production in co-flowing streams was first applied to liquid/liquid systems

by Umbanhowar *et al* [135] and later implemented into a quasi-two-dimensional microfluidic device and modified to a flow-focusing geometry by Anna *et al* [136]. The down-scaling of a flow-focusing device with circular channel cross section and its easy fabrication was demonstrated two years later [137], and an open channel configuration was presented for the generation of single and double emulsions using a flow-focusing geometry [138]. Applying more sophisticated microfabrication techniques round orifices were also fabricated and used for three-dimensional flow focusing. The flow rates at the round orifice are further increased compared with two-dimensional focusing resulting in an improved sensitivity of the droplet diameter on the flow parameter and increased droplet production frequency [149, 150]. To increase the production rate flow-focusing devices were parallel integrated in linear [152, 153] or circular settings [116] similar to T-junctions. For geometries with a common inlet channel for the continuous phase and a common outlet channel, a weak hydrodynamic coupling was also observed [153] which might lead to synchronized droplet generation.

The influence of numerous parameters on the formation of droplets in co-flow and flow focusing geometries was investigated such as the step-wise ramping of flow rates [139], the formation of satellite droplets [143], the effect of liquid viscosity [144], channel wettability [145], the dependence on surfactant concentration [146], kinetic aspects of emulsion stabilization [106], and the difference between pressure and volume controlled flow [140]. Also the production of monodisperse water droplets in untypical carrier phases such as highly viscous ionic liquid was demonstrated [151]. The dripping to jetting transition in a co-flowing [141] and a flow-focusing geometry [142] was studied experimentally. Based on the experimental findings scaling laws were derived to describe the flow focusing droplet production in a typical geometry [147] and in a Y-shaped geometry [148]. To understand more details of the droplet breakup mechanism in the various co-flow geometries numerical studies have also been conducted. The flow in the dispersed [146] and the continuous phase [154] was studied and also the drop formation as a result of interfacial instabilities at co-flowing [155], flow-focusing [156], and cross junction geometries [157]. Some basic principles of droplet generation and interfacial instability will be discussed in more detail in section 4.

To increase the flexibility of flow-focusing devices, e.g., to generate various droplet sizes at given flow rates or to improve the monodispersity of the generated droplets, approaches similar to the ones discussed for T-junctions were proposed to regulate the fluid flow: inflatable chambers using gas [158, 159] or liquid [160] were embedded into devices to vary the orifice dimension, cf figure 4(*c*), and also a feedback control for the fluid flow rates depending on produced droplet size [161] and a piezoelectric actuator to improve the monodispersity of the generated droplets [162] were introduced. By temperature mediated changes in fluid viscosity and surface tension the droplet size can be adjusted independent of the flow rates [163, 164], cf figure 4(*c*).

For good reason, flow focusing is one of the most frequently used techniques to generate droplets *in situ* in microfluidic devices. For a slightly increased technical effort for device production and operation, compared with T-junctions, flow focusing typically offers better monodispersity and superior frequency up to about one thousand hertz of the droplet generation. Co-flow and flow-focusing emulsification also seems to have slight preferences if delicate objects such as cells or primary emulsion droplets are included into the generated droplets.

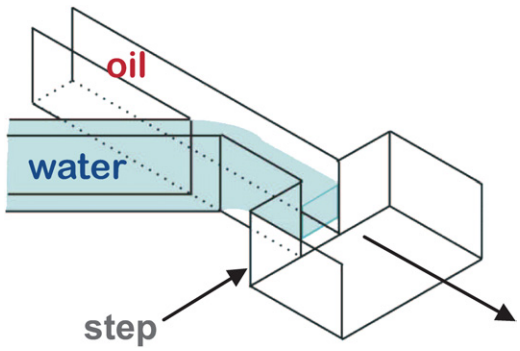

Figure 7. A step-emulsification device. In the narrow duct behind the oil/water channel junction, a quasi-two-dimensional aqueous jet has formed within the oil as the carrier phase. At the 'step' the channel widens, forcing the aqueous filament into an effectively three-dimensional setting. Decay into droplets is the immediate effect.

3.5. Step emulsification

A modified version of a co-flowing geometry is called 'step emulsification' and uses a geometric step to trigger droplet formation of a stream of a dispersed phase surrounded by a continuous phase. A typical realization is sketched in figure 7. The two liquids are brought together at a T- or Y-junction into a high aspect ratio channel. It is of no significance whether the channel is very narrow or (as in the sketch) very flat, it is the difference between the width and the height which matters. The important feature of the step-emulsification technique is that the dispersed stream is stabilized between the two walls of a high aspect ratio channel suppressing interfacial induced instabilities. The stream of the dispersed phase abruptly breaks up into droplets at the geometric step when the stabilizing channel walls end.

This type of geometry has been used by Chan *et al* [165] and later simplified and carefully characterized by Priest *et al* [166, 167]. For a step emulsification one also finds different droplet formation regimes similar to the regimes for co-flow droplet formation. The different regimes and the stabilizing effect were later confirmed independently by Saeki *et al* [168] and Humphrey *et al* [169]. The scaling of droplet size with the channel height of the shallow channel was investigated in [166, 170].

Emulsification by step geometry easily allows for an increase in the droplet production frequency by parallel dispensing of several liquid streams into droplets using the same geometric step [168], combining two of those geometries to a common inlet and outlet channel, cf figure 8. The droplet production of both inlets can be hydrodynamically coupled

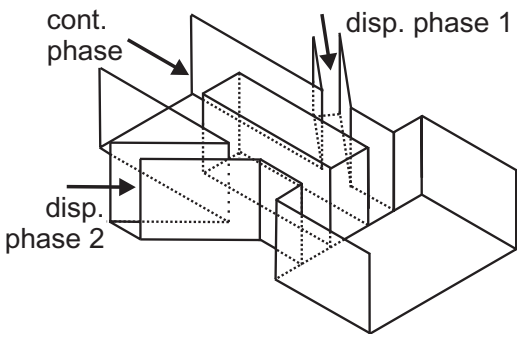

Figure 8. Sketch of a double step emulsification device. The hydrodynamic coupling of the two combined production units via the common inlet and outlet results in strictly alternating droplet formation.

resulting in an extremely robust synchronization mechanism which allows us to generate droplet pairs with different sizes and fixed number ratio of 1:1 and 1:2 [167] and more.

The step emulsification requires a fairly careful choice of flow parameter and device fabrication, respectively, the fabrication of the master might be slightly demanding due to the high aspect ratio channel and might be also slightly limited with respect to droplet formation frequency which can still be up to several hundred droplets per second, depending on the exact geometry. However, step emulsification also has many desirable properties which are hard to reach with T-junction or co-flow geometries: step emulsification offers probably the best droplet homogeneity, the possibility to generate very high dispersed phase volume ratios of up to 96%, i.e. foam like emulsions, *in situ*. The droplet production rate can be varied within more than two orders of magnitude without affecting the generated droplets size by just varying the flow rates of the dispersed and continuous liquids such that their relative flow ratio remains unchanged [166].

A combination of a geometric step and shear emulsification in a T-junction geometry is used in an edge-based droplet generation device (EDGE) [171, 172]. The dispersed phase is introduced by a wide and very shallow, quasi-two-dimensional channel into a main channel which is significantly deeper. In the shallow channel the dispersed phase is stabilized by geometry and wettability and the continuous phase flows perpendicular to the dispersed phase in the deep channel. At this stage small droplets of dispersed phase are sheared off by a continuous stream of the carrier phase [171, 172]. The pressure in the various channels during the droplet breakup is analyzed in [173]. This technique allows for large production rates at a medium monodispersity of the droplet size (coefficient of variance of 10%). This monodispersity is among the lowest of all *in situ* droplet formation techniques in microfluidic devices but might still be of interest for some applications due to the large production frequency.

3.6. Unconventional techniques and fluids

To finish the overview of the various droplet generation techniques we mention a number of rather unconventional techniques which are rarely used in microfluidics but which demonstrate additional techniques for droplet generation and manipulation and shall thus be mentioned for completeness. A co-flowing stream of a dispersed phase surrounded by a continuous phase can be actively chopped into small fragments by a pulsating air stream. When the continuous stream is flowing through a channel passage having a comb-like structure at one side [174, 175] the forward moving 'gas fingers' divide the continuous stream. The size of the fragments is given by the periodicity of the comb geometry. It is obvious that this type of droplet production is rather complex in device fabrication and operation, and the achieved droplet production frequency is rather limited.

To generate very small droplets [177, 178] which might be even below 1 μm [179] the concept of electro-spraying [180] was applied to microfluidic devices. Surprisingly the average size of the generated droplet does not monotonically decrease with an increase in the applied voltage [181]. Using electrorheological fluids as dispersed phase the homogeneity of produced droplets was shown to improve if a square wave electric field was applied [182]. The droplet generation can also be controlled by the effective wettability of the fluid phases on the channel wall and can be adjusted by electrowetting in a step-like geometry [183] similar to the geometry discussed in section 3.5 or in a co-flow geometry [121]. Needless to mention that the implementation of electrodes into a microfluidic device increases the complexity of device fabrication. The thermocapillary effect (which will be explained in section 5) can be used to stop a droplet or its production and thus provides a handle to influence the droplet generation process [184].

All these rather unconventional droplet generation techniques are rarely used for typical microfluidic applications but they nicely demonstrate how surface tension, device geometry, electrowetting, or thermocapillarity can be used to control the droplet formation process or to get an additional handle to increase, e.g., the droplet monodispersity or to vary the generated droplet size.

4. Interfacial instabilities and energetics of droplet production

Since the droplet generation technique is at the heart of droplet based microfluidics we will complement the overview of different droplet generation techniques given in the preceding section with fundamental physical considerations. To this end we will discuss and classify the interfacial instabilities underlying microfluidic droplet production with respect to the specific device geometries. So far it has been barely noticed that the elementary processes employed in droplet production are similar and can be grouped in just a few categories. In the following subsections we will first have a closer look at the energetics of these processes in order to develop a useful classification scheme for droplet generation techniques, and later on provide criteria for their appropriate choice and successful application. Finally, we will discuss the scaling of droplet sizes with respect to hydrodynamic models.

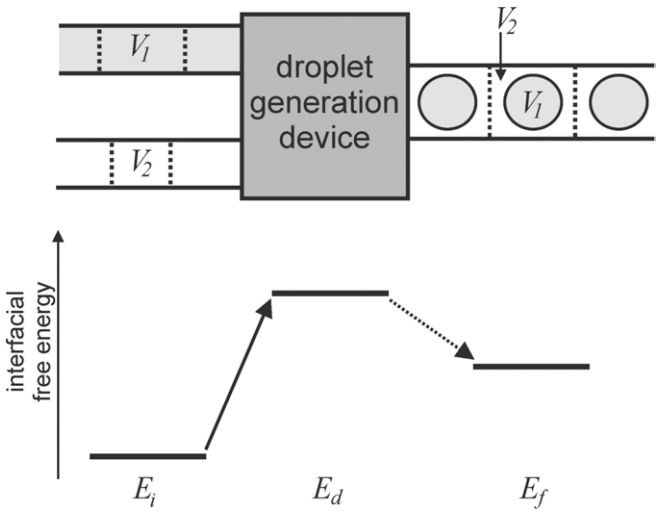

Figure 9. Schematic representation of a droplet production device. From the left, two immiscible liquids enter the setup. To the right, an emulsion leaves the device, where liquid 1 is dispersed in liquid 2. At the bottom, the content of interfacial free energy is sketched as an energy level diagram. The final energy, E_f, lies higher than the initial energy, E_i, but there is an even higher intermediate energy, E_d, somewhere within the device.

4.1. Energy assessment of droplet generation

A schematic view of a droplet generation device is shown in figure 9 (top). Two liquids are fed in from the left-hand side, one of which is to be dispersed (1). To the right, the dispersed phase is present as isolated droplets within the continuous phase. The task of the device is thus to decompose the singly connected liquid which is to be dispersed into a set of many unconnected regions of equal volume.

It is clear from the start that the dispersion process is accompanied by the injection of considerable amounts of energy into the system, in order to account for the excess free energy of the interfaces separating the dispersed from the continuous phase in the emulsion finally produced. This is sketched schematically at the bottom of figure 9 as (free) energy levels. E_i corresponds to the initial, E_f to the final state. We will readily see that there will be a higher energy level involved somewhere within the device, which we call E_d. These free energies may be defined by assigning to each 'final' droplet of volume V_1 a suitable region of continuous phase with volume V_2 which is surrounded, such that the total liquid in the channel on the right-hand side can be viewed as composed of liquid elementary cells as indicated by the dashed lines. We then can find the liquid cells in the channels to the left from which an elementary cell to the right will emerge. This is similarly indicated by dashed lines on the left-hand side. It is clear that liquid plugs of this kind cannot be identified in reality, due to the non-uniform flow velocity profiles in the channels. Nevertheless, this picture yields the correct interfacial areas per unit liquid volume, and thus is sufficiently precise for defining the energy levels as required for the discussion here.

We define the interfacial free energies with respect to a state where all channels are filled with the liquid representing the continuous phase. We can then, for instance, write down

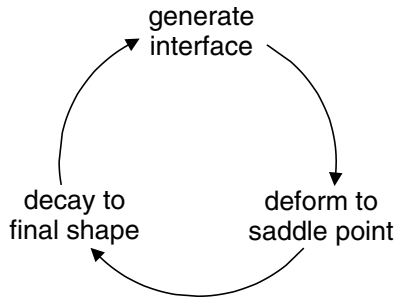

Figure 10. Principle of operation of devices which generate a series of droplets of a liquid within a second (immiscible) liquid counter phase.

the free energy of a final state consisting of spherical droplets with radius R. We obtain

$$E_f = 4\pi R^2 \gamma = \gamma (4\pi)^{1/3} (3V_1)^{2/3}, \tag{1}$$

where γ is the interfacial tension between the two liquids. For calculating the energy of the initial state, E_i, we first have to replace the continuous phase liquid (2) with the dispersed phase liquid (1) in the corresponding channel on the left-hand side. The corresponding change in interfacial free energy is proportional to $\gamma_1 - \gamma_2$, where γ_i is the interfacial tension the liquid with index i makes with the channel wall. We then obtain for the initial energy, using Young's equation [186],

$$E_i = \gamma \cos\theta \frac{S_1 V_1}{A_1}, \tag{2}$$

where θ is the contact angle the continuous phase makes at the channel wall in the presence of the dispersed phase. If there is no preference of the walls for one or the other liquid, we have $\theta = \pi/2$ and thus $E_i = 0$. S_1 and A_1 are the surface area and the volume, respectively, per unit length of the feed channel of the dispersed phase liquid. The ratio A/S of a channel is a length characterizing its size. For a circular tube as well as for a square channel, e.g., it is equal to 1/4 of the channel width. The expression $S_1 V_1 / A_1$ simply represents the interface the volume V_1 makes with the wall of the inlet channel.

4.2. Droplet formation

There are three major steps involved in the droplet generation process, as outlined in figure 10. First of all, an interface must be created between the two immiscible liquids fed into the system. Initially, this is an interface between two singly connected regions. It must therefore be considerably deformed in order to reach the final state, where the dispersed phase liquid fills many disconnected regions. Since this final state will be reached by decay from a deformed interface, there must be an intermediate state within the device with higher interfacial free energy than the final state, which spontaneously decays into the latter. This consideration completes the level diagram depicted at the bottom of figure 9. The solid arrow represents the energy fed from the system into the liquid interface, while the dashed arrow represents the spontaneous decay into the dispersed state. The intermediate energy level corresponds to a saddle point in the total interfacial energy of the system (see figure 10).

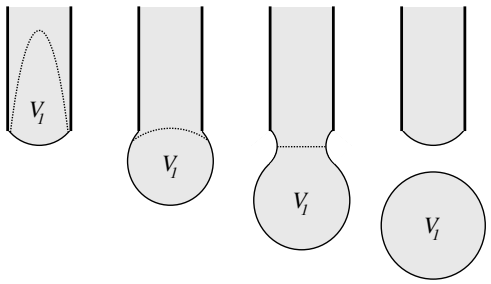

Figure 11. Generation of droplets of a liquid (1) at the outlet of a pipette in a flowing second, immiscible liquid (2). The operation is similar to the dripping instability at a faucet.

For the device to operate properly, it is important that the interface stays topologically intact while being taken from the state of its formation to the intermediate state with energy E_d. When the intermediate state is reached, the interface must become unstable with respect to a deformation mode which finally leads, after spontaneous decay, to the desired dispersed state. Reaching the intermediate state is thus defined by the occurrence of an unstable mode of interface deformation, in other words, of a saddle point on the interfacial free energy hyper-surface in Hilbert space. It is of great importance not only for the classification but also for the stability of operation of the droplet generation device to discuss the properties of this saddle point in some detail, in particular with respect to the spectrum of its unstable modes.

Let us discuss this for a simple example, which is inspired by the production of macroscopic droplets by dripping from a faucet, as was first described by Tate [187] in the 19th century and later in greater detail by Rayleigh [188]. The drop detaches from the faucet when the gravitational force acting upon it surpasses the capillary force which holds it to the opening. As a consequence, the volume of the detaching droplet scales only as the cube root of the width of the opening, making it difficult to produce very small droplets by gravity. For microfluidic applications, one thus uses stronger forces, such as, viscous drag forces. A simple setup to generate small droplets by viscous drag is the co-flow geometry as discussed in section 3.4. Details of the droplet breakup are displayed in figure 11. The droplet phase is injected through a micropipette into a homogeneous co-flow of the continuous phase [135]. The viscous drag force exerted by the outer liquid phase grows linearly with the droplet diameter, and finally detaches the droplet when it exceeds the capillary force, similar to the gravity driven dripping instability, once it has reached a critical radius, R_c. The latter is determined from the force balance, which can be roughly written as

$$6\pi R_c \eta v_2 = 2\pi r \gamma, \tag{3}$$

where η is the effective viscosity of the liquid, v_2 is the streaming velocity of the continuous phase and r is the radius of the pipette. Obviously, R_c scales linearly with the pipette radius now, enabling the down-scaling of the droplet radius to sizes suitable for microfluidic applications.

It is instructive to follow the formation of a liquid interface in this process. The dashed curve in figure 11 indicates the boundary of the liquid volume V_1 which eventually will constitute the detaching droplet. As the liquid is pushed out of the pipette, the liquid interface which is already present is increased. It retains an approximately spherical shape and is dynamically stable against all possible fluctuations. As the droplet size becomes close to critical, a liquid neck forms. This neck is elongated until it starts to thin by itself due to the capillary force acting around its perimeter. At this point, a single mode of deformation has become unstable, which corresponds to the thinning of the neck: a saddle point in the free energy surface has been reached.

As the neck pinches off, the boundary between the droplet and its successor (dashed line) shrinks to a point and finally vanishes. This discontinuity may sometimes result in additional, very small 'satellite droplets' [189], but this side effect will not concern us here. We rather focus on the observation that only in the limit of small feed velocity, v_1, will the saddle point be unstable with respect to just a single mode of deformation. This ensures an absolutely reproducible droplet volume. As the feed velocity is increased, however, a whole continuum of modes will become unstable, and a competition of pinch-off modes takes place. This makes the droplet volume more susceptible to fluctuations in the system, although there is usually still a single mode which grows fastest, and will thus determine the average droplet size.

As the flow rate of the continuous phase is increased while keeping the flow rate of the dispersed phase constant, the size of the detaching droplets becomes smaller, as suggested by equation (3). It will thus eventually reach the diameter of the outlet (dripping regime). While increasing the flow velocity of the continuous phase even further, the injected phase will no longer be able to fulfil the detachment condition. It then starts to form a liquid jet which extends from the outlet into the continuous phase, as sketched in figure 12. The situation where the radius of the jet is about equal to the radius of the nozzle is typically referred to as co-flow. However, if the radius of the jet is reduced by hydrodynamic flow focusing, the term flow focusing is often used. But from the discussion here it is already obvious that the nature of the droplet formation is identical.

Another advantage of the two liquid phases flowing besides each other for some time before the droplet instability occurs is that the surfactant molecules which are typically present in the continuous phase are given more time to decorate the liquid/liquid interface. The decreased surface tension lowers the energetic barrier at the saddle point and facilitates the droplet generation process.

To proceed with our considerations, the interfacial energy of a cylindrical jet of radius r is readily calculated, we obtain

$$E_d = 2\gamma V_1 / r. \tag{4}$$

A cylindrical jet is unstable with respect to radial undulations while flowing downstream. This 'classical' (Rayleigh–Plateau) instability has been treated for both inviscid [190, 191] and viscous [190–192] liquids. In any case, a broad spectrum of unstable modes appears, as depicted schematically at the bottom of figure 12. It extends from infinite wavelength to some cutoff wavelength of the order of the diameter of the

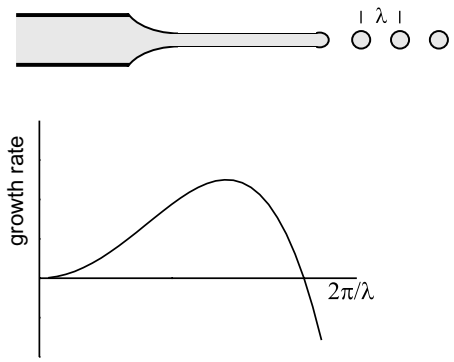

Figure 12. Top: jetting mode dispersal of a liquid (gray) injected into a second, co-streaming liquid (white). The cylindrical jet is unstable with respect to 'peristaltic' fluctuations (Rayleigh–Plateau instability). Bottom: growth rate of the amplitude of peristaltic fluctuations as a function of wave number, $2\pi/\lambda$. The fastest growing mode determines the distance of the droplets which finally form.

liquid jet. It turns out that there is always one mode for which the amplitude grows the fastest, and its wavelength selects the droplet size which finally emerges. As the sketch in figure 12 suggests, there is always a range of modes close to the maximum of the growth rate which grow similarly fast. This competition naturally limits the monodispersity of the ensemble of droplets finally produced. However, dynamical mode selection always ensures that the final droplet volume will be such that $E_f < E_d$.

This instability may as well be seeded by means of a suitable channel geometry. If a continuous stream of liquid is first guided into a channel with zigzagged side walls and stopped in there it will decay into individual droplets by the Rayleigh–Plateau instability if the zigzag geometry is chosen appropriately. But because the particular channel geometry only allows the amplitude of certain wavelengths to grow, the periodicity of the channel defines the position of the formed droplets provided the liquid thread is not too thin. The resulting droplet size depends on the size of the original liquid thread and the channel geometry and does not allow us to actively vary the droplet size [176].

4.3. Droplet formation in microfluidic devices

When confined to a microfluidic channel, the flow conditions change, and so does the dynamic behavior of the droplet forming processes in the setup just discussed. It turns out that the jet instability can be dynamically suppressed by geometric confinement. The instability of a cylindrical jet in a concentric cylindrical channel has been considered by Guillot *et al* [193]. In agreement with experiments, they predict a dripping mode for small flow rates of both the dispersed and the continuous phase and a jetting regime if one of the two flow rates is increased [193]. Since their treatment adopts a long wavelength approximation, its validity is restricted to the range of thin layers of the continuous phase, i.e. the approximation fails whenever the diameter of the jet is small compared with the diameter of the channel. In that case, the usual jet instability as discussed above is reobtained.

4.3.1. Co-flow/step emulsification. So far, the dynamical instability of the liquid surface was intimately linked to the geometry of an interface in three-dimensional space. The Rayleigh–Plateau instability, for instance, relies on the possibility of deforming a cylindrical surface such that its area is decreased while the included volume remains constant. If a microfluidic device consists of very flat channels, such that liquid interfaces within the channels are likely to extend from the bottom of the channel to its ceiling, the situation is fundamentally different. In such quasi-two-dimensional settings, any deformation of a straight liquid interface, i.e. a displacement parallel to the bottom of the channel, leads to an increase in the contour length (and thus of the total area) of that interface. In an oil-filled flat channel, a thin filament of aqueous liquid can thus flow along, e.g., the center line of the channel for arbitrary distances. All modes of deformation of its interfaces with the surrounding oil are dynamically stable, and fluctuations (either thermal or from external vibrations) are readily restored. Using flat channel geometries, it is thus possible to separate the processes of interface generation and interface destabilization (cf figure 10).

This is exploited in the step-emulsification concept [166–168, 173] as discussed before in section 3.5, cf figure 7. Because the liquid interface wants to be as small as possible, it prefers an orientation along the short dimension of the channel. This interface provides a quasi-two-dimensional arrangement of the two liquids, with the separating interface being dynamically stable. Further downstream, this channel is connected to a much wider channel, forming an abrupt step at the junction indicated in figure 7. Here the liquid (water, in the sketch) filament is forced into a three-dimensional setting and can thus not be stable anymore. The step thus triggers the decay of the formerly stable liquid filament into a more favorable, i.e. droplet-like, shape. As the droplet which is fed by the filament grows, its Laplace pressure decreases, thus draining more liquid out of the filament, in excess of the feed rate. The filament is thus thinned down and pinches off within the flat (or narrow) channel, shortly before the step; the process can then start all over again. The width of the size distribution of the droplets thus generated is typically well below 2%.

It is important to note that the pinch-off process in step emulsification can be of a very different nature to that in the dripping instability case discussed above. If the dispersed phase wets the channel walls better than does the continuous phase, pinch-off is induced by the approach of two liquid interfaces which are curved away from each other. They remain intact and stable until they touch each other in a single point. At this moment, the 'saddle point' in free energy is reached. Decay takes place along a very steep and well-defined descent in free energy, since the latter varies faster than quadratic (linear to leading order) with the interface displacement for two convex interfaces touching each other in a single point. However, although this may seem desirable for the sake of a well-controlled pinch-off process, it is unlikely to be used, since for the sake of stability of the final emulsion, the channel walls should be wetted by the continuous phase rather than by the dispersed phase as already mentioned in the section 2. Furthermore, most applications use an aqueous

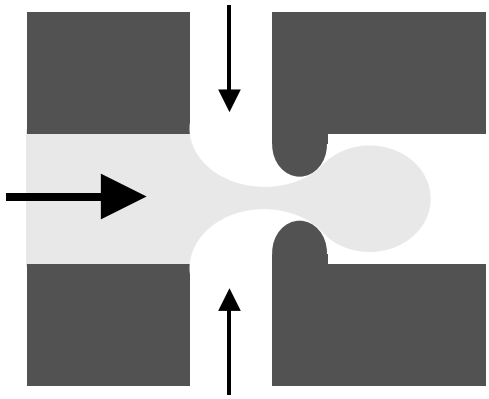

Figure 13. A frequently used device in which the continuous phase (white) is used to narrow the filament of the dispersed liquid (gray) down until pinch-off takes place.

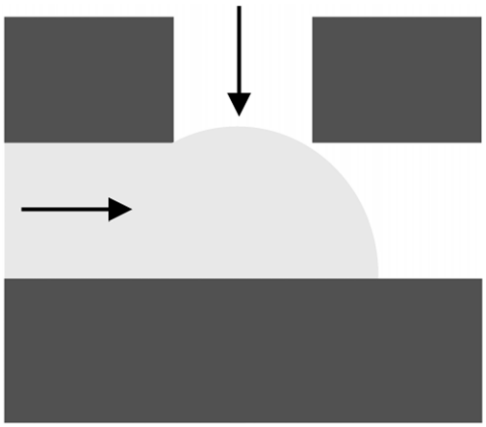

Figure 14. The simple T-junction device. The two liquids alternately obstruct each other's flow, resulting in an alternating pattern of liquid 'slugs' along the outlet channel.

phase as the dispersed phase, and almost all suitable channel materials are better wettable by oil than by water.

If the walls prefer the continuous phase, as is usually the case, the pinch-off process will finally be similar to the process in the dripping case. But the range of destabilization (i.e. the range of the saddle point in free energy) is greatly reduced by the small dimension of the narrow duct channel. Only when the liquid filament becomes thinner than the small dimension of the channel will the saddle point be reached and become effective in destabilizing the liquid interface. This makes the process potentially more stable against thermal fluctuations and external vibration.

4.3.2. Co-flow/flow focusing. A similar strategy of 'taming the saddle point' is pursued by 'flow focusing' [136, 140, 143, 144, 154]. Its principle of operation is sketched in figure 6 and in more detail in figure 13. It uses relatively flat channels all over, such that its function can be well understood in a quasi-two-dimensional view. Also here, the pinch-off process is well controlled due to the flatness of the channel. It is induced, however, directly by the flow of the continuous phase (white). When the dispersed phase (gray) blocks the narrow entrance into the channel to the right, the continuous phase, entering from top and from the bottom in the figure, starts to push the two liquid interfaces separating the dispersed phase from the continuous phase together, until they touch each other and induce pinch-off. The sketch schematically shows the situation shortly before pinch-off.

Note how intimately and co-operatively the elementary processes of interface generation, saddle point approach, and relaxation are intertwined in this device. The self-clogging of the narrow constriction naturally gives rise to a pressure increase in the side channels, which then finally leads to the pinch-off in the center of the device. The reliability of this concept can be judged from its observation in a channel which is just simply rough enough for providing somewhere a sufficiently effective constriction.

4.3.3. T-junction. Finally, let us briefly discuss also the T-junction [98, 100, 111] in which the saddle point is deprived of all imponderable softness, cf figure 4. The sketch in figure 14 shows the liquid interface shortly before reaching the 'saddle point', i.e. before touching the opposite channel wall. When this happens, the liquid interface will rearrange in order to retain its equilibrium contact angle everywhere with the wall. This will be a configuration where the liquid coming from the side channel is not continuous anymore, and will then push towards a similar pinch-off process in its turn. The pinch-off process itself is reduced here to the rearrangement between a liquid and a solid interface, which bears the least susceptibility to external noise or thermal fluctuations. At first glance, this mode thus seems to be the most reliable of all possible concepts. However, it also has some drawbacks. Instead of small droplets, it generates long plugs containing much more liquid than a droplet with a diameter corresponding to the channel width would. In order to scale down the dispersed volume elements, one would have to reduce the channel dimensions, which is connected to a serious trade off in flow resistance and production frequency. In many applications, the T-junction is thus operated in a different mode, in which the liquid tongue of one of the liquids entering the junction is readily sheared off by the flow of the other liquid. This leads to higher droplet production rates, but the pinch-off geometry cannot be defined anymore by the channel wall design.

All droplet production setups are three-dimensional in reality and topologically are equivalent to a simple T-junction. It is thus no surprise that all of them can be operated in several different modes, which are mutually similar [142]. Almost all devices, for instance, can be operated in a jetting regime, when the overall flow rate is large, but the flow rate of the dispersed phase is much smaller than the flow rate of the continuous phase. The geometric peculiarities of most setups merely serve to optimize them for a particular operation mode which is deemed advantageous for the considered application.

As a final note, we mention that equation (2) does not by itself guarantee that $E_i < E_f$. In fact, E_i can be made large and positive if the channel walls are completely wet by the continuous phase ($\theta = 0$) and the feed channel of the dispersed phase is very narrow (large ratio S_1/A_1). Indeed, it has been observed, and exploited, that $E_i > E_f$ is possible,

which leads to a spontaneous decay of the connected state of the feed liquid into droplets [176]. However, this needs not be considered as contradicting the conceptual considerations expressed in figures 9 and 10, since in that case the extra energy is fed into the system already when squeezing the liquid which is to be dispersed into the narrow feed channel, the walls of which would prefer the continuous phase. At this point, we are already well within the production process before the 'device' has been entered.

4.4. Hydrodynamic models and droplet size scaling

The in depth understanding of the droplet breakup processes is still not very mature. This applies in particular to the transition between the squeezing, dripping and jetting in T-junctions and to jetting to dripping regimes in co-flow geometries. Here, we will give a brief summary of some of the fundamental results based on fluid dynamic considerations which have been obtained for these geometries.

It is generally observed that the size of droplets and their production frequency on polydispersity depend on externally set parameter such as flow rates of the dispersed and continuous phases Q_1 and Q_2, respectively, the channel dimensions D, as well as physical quantities such as the viscosities of the dispersed and continuous phase η_1 and η_2, respectively, the interfacial tension γ between both fluid phases, and the wettability of the channel walls. At high flow velocities the mass densities ρ_1 and ρ_2 of the dispersed and continuous phase, respectively, become relevant since inertial effects come into play. The scaling of the droplet volume and production frequency for a particular flowing regime can be expressed in terms of suitably chosen dimensionless numbers which are typically given by products and ratios and of the above-mentioned physical quantities, the average flow velocities or volume fluxes of the continuous and dispersed phase, and the channel geometry, i.e. its dimensions. Similarly, the flow conditions related to a transition between different droplet production regimes can be expressed in terms of these dimensionless numbers.

4.4.1. T-junction. Due to its widespread use, a considerable amount of works has been published on T-junctions and related geometries. Droplet production in the squeezing regime is characterized by the buildup of a pressure gradient across the droplet while it is protruding into the main channel. As confirmed by experiments [111] and in numerical simulations [206] the droplet size scaling is well captured by the simple relation $V_1/D^3 = 1+\alpha\, Q_1/Q_2$, where V_1 is the droplet volume, D the diameter of the channel with square cross section, and α a constant of the order of unity. This droplet size scaling is nearly independent of the material parameter of the liquids, i.e. their viscosity and interfacial tension.

On increasing the flow rate of the continuous phase, Q_2, one enters the dripping regime. The transition between the squeezing and the dripping regime is characterized by the capillary number $Ca_2 = \gamma u_2/\eta_2$ of the continuous phase, where $u_2 = Q_2/D^2$ is the average flow velocity. Both experimental and numerical works indicate that the numerical value is close to $Ca_2 \simeq 0.015$ [111, 206].

As outlined in the previous section, the droplet formation in the dripping regime can be understood in terms of a competition between viscous shear stresses and interfacial tension forces acting on the free interface of the dispersed phase. Channels with aspect ratios in the range of 1 display a scaling of the ratio D_d/D between the droplet diameter D_d and the channel dimension D with the inverse capillary number Ca_2 [98, 127]. In this dripping regime the droplet diameter is almost independent of the flow rate Q_1 of the dispersed phase.

Modified scalings for small capillary number, i.e. small average velocities of the continuous phase, have been proposed [98, 109] which take into account the increased average velocity of the continuous phase and the buildup of a pressure gradient during droplet pinch-off. For large velocities, i.e. large Q_2, the scaling Ca_2^{-1} is recovered. A strong dependence of the droplet size on the viscosity ratio $\lambda = \eta_1/\eta_2$ is reported in [98].

At high flow rates of the continuous phase and dispersed phase the T-junction operates in the jetting regime characterized by the formation of long threads of the droplet phase before breakup. The transition between the dripping and the jetting regime can be understood from a competition of different time scales. At the point of transition the pinch-off time scale become comparable to the time scale to form a blob of the dispersed phase which can be sheared off from the side channel by the continuous phase.

Empirical laws based on numerical simulations for the droplet size scaling were given and compared with experimental results in [109, 111, 113, 114]. The droplet breakup process [205], the transition from squeezing to dripping regime [206], and the influence of viscosity [207, 208] and geometry [209] on the breakup process was also calculated numerically with partially good agreement with experimental situations.

Another aspect which we want to briefly mention here can be understood as a truly hydrodynamic effect in microfluidic droplet production. It is the coupling of droplet generation between two parallel T-junctions. Variations in the hydrodynamic resistance due to the droplets downstream of production were considered in a series of experiments and that were subsequently modeled by coupled van der Pol oscillators [130]. Analysis of the experimental data and comparison with the model predictions revealed the existence of synchronized and chaotic regimes of droplet production where highly monodisperse droplets were observed in the synchronized regime [130].

4.4.2. Co-flow. Co-flowing droplet production as introduced in sections 3.4 and 4.3 shows a rich spectrum of dynamic regimes. In the following we discuss the case of small (<1) up to moderate (≈100) Reynolds numbers $Re_\mathrm{i} = u_i\, L_i/\eta_i$ for both phases $i = 1, 2$, where u_i and L_i are typical velocities and length scale of the flow of phase i, respectively.

Similar to the T-junction the droplet production in a co-flowing device can be operated either in the dripping mode or in the jetting mode. To describe the transition between both regimes one has to distinguish the case where the volume flux Q_1 of the dispersed phase or the volume flux Q_2 of the continuous phase is increased while the flux of the remaining

phase is kept fixed [141]. In the first case, starting in dripping mode, the formation of a thinning liquid cone of the dispersed phase emanating small droplets from its tip is observed once the diameter of the droplet diameter D_d in the dripping mode has reached the diameter of the inlet D_t of the dispersed phase. In this jetting mode, the liquid thread of the dispersed phase which is stretched out by means of the viscous stress of the bypassing continuous phase decays into a train of small droplets as the thread travels further downstream. These considerations leads to a simple estimate $Ca_2 \approx 1$ for capillary number related to the dripping to jetting transition during an increase in the flow rate of the continuous phase. A number of experimental works indicate that the critical capillary length assumes a universal value close to $Ca_2 \simeq 0.1$ [141, 142].

As already pointed out in section 4.3.2, the diameter of the droplets in the jetting mode scales linearly with the diameter of the liquid thread in accordance with the linear stability analysis of the Rayleigh–Plateau instability [141], while the ratio D_j/D of the jet diameter D_j to the channel dimension D is simply controlled by the ratio of flow rates [142]. Both findings imply a scaling of droplet diameter $D_d/D \propto (Q_1/Q_2)^{1/2}$, which is corroborated by experiments [142].

In contrast to the case of an increasing flow rate Q_2 of the continuous phase, the transition between dripping and jetting during an increase in the dispersed flow rate Q_1 is accompanied by the formation of jets which are widening downstream of the orifice [141]. Experimental results suggest that this transition can be related to the Weber number $We_1 = \rho_1 D_t u_1^2/\gamma$ of the continuous phase with respect to the diameter D_t of the orifice reaching a value of the order of 1 [141]. The Weber number involves the mass density ρ of the fluid and expresses the magnitude of inertial effects relative to interfacial forces. The impact of inertial effects on droplet formation in microchannels with millimetric dimensions has been considered experimentally [107] for high flow velocities up to several meters per second. Inertial effects are also essential to an instability termed 'whipping mode' which has been described for co-flowing jets at high Reynolds number [108]. This type of instability is characterized by the growth of non-axisymmetric perturbations that render the jet absolutely unstable, i.e. any finite perturbation grows and moves upstream to the inlet.

To verify the mechanisms of droplet formation and the participating hydrodynamic processes the fluid streams of the continuous phase and the dispersed phase at the point of droplet breakup are monitored by particle image velocimetry (μPIV) [197, 198], which will be explained later in section 6.7. The majority of PIV data is available for the breakup of gas streams in T-junctions [199–201], co-flow devices [202, 203], and different flow-focusing geometries [204]. The time scales of filling the channel with a gas phase, its subsequent squeezing, and bubble pinch-off have been studied by PIV of the continuous phase [201].

5. Droplet manipulation and sorting

Droplet production, as discussed in the previous section, is very important but of course only the first step in the direction of droplet based microfluidics. For useful microfluidic processes, it is crucial that the generated trains of equally sized droplets can be reliably manipulated downstream from the production unit. In the following section we will thus summarize commonly used techniques to manipulate droplets in microfluidic devices, e.g., to passively or actively sort them based on their properties or contents, and to selectively stop individual droplets. We will continue with a brief summary of techniques to detect droplets and to measure and analyze their contents and conclude with packing behavior of emulsion droplets.

At first we will give a number of examples for passive manipulation techniques that allow us, e.g., to sort and address single droplets by means of hydrodynamic effects mainly governed by properties of the flow fields. External fields which can be switched on and off, such as electric or magnetic fields, open up the possibility to actuate and actively sort droplets by dielectric, magnetic, or electrorheological effects. Temperature gradients, e.g., induced by laser beams, can be employed to create flows and to displace droplets by means of the thermocapillary effect.

While the focus here is on the underlying common physical principles, various other aspects of droplet manipulation [381, 382] and their potential for reaction control in chemistry and biology [383–388], and applications in the food industry [389] can also be found in complementary recent review papers.

5.1. Confinement and hydraulic resistance

Similar to the voltage at an ohmic resistance, the flow velocity in channels of a certain geometry and cross section is inversely proportional to its relative hydraulic resistance and directly proportional to the pressure gradient. The additional pressure drop across the interfaces of droplets flowing in the confinement of a microfluidic channel can be utilized to direct or sort these droplets.

For simplicity let us consider elongated droplets with spherical end caps being sufficiently slow to neglect a noticeable pressure drops across a moving droplet. By the law of Laplace we observe a difference $\Delta P = P_1 - P_2$ of the pressures P_1 in the droplet and P_2 in the continuous phase across the interface which equals $\Delta P = 2\gamma/r$, where γ is the interfacial tension and r the radius of curvature of the respective end cap.

Forcing a droplet into a channel with smaller dimensions, the radius r of the end caps has to be reduced which, in turn, requires an increase in the Laplace pressure ΔP at the front of the droplet. This additional pressure difference has to come from an increase in the pressure in the continuous phase at the back of the droplet. In certain channel geometries this additional pressure will not be reached and droplets can be sorted or re-distributed [112, 238–243, 245].

Confinement induced hydrodynamic interactions in specific channel geometries can be employed to manipulate droplets [246–250], cf figure 15(*a*). Similarly, droplets may be trapped or guided on a 'rail system' by embedding lowered structures in the microfluidic channel. Droplets being attached

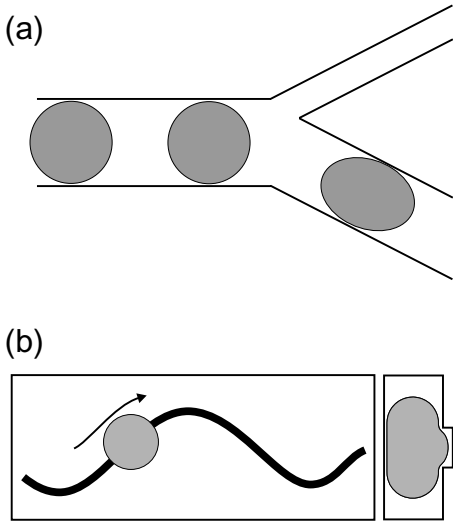

Figure 15. Schematic of the geometric manipulation. (*a*) Due to the different hydrodynamic resistance, the Laplace pressure inside the droplet, and the increase in interfacial energy, droplets will preferentially flow in the direction of the larger channel. (*b*) Due to a decrease in interfacial energy droplets can be trapped or moved on a 'rail'. Right: cross section of microfluidic channel including the rail and a trapped droplet.

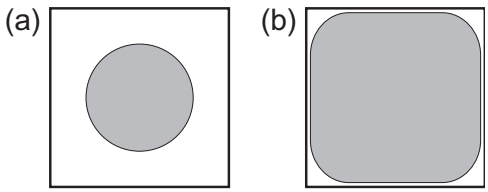

Figure 16. Cross section of a channel with (*a*) a droplet being much smaller than the channel dimensions and (*b*) a droplet being confined in the channel geometry.

to these structures can decrease their interfacial area, i.e. their interfacial energy, and stay attached to these structures, cf 15(*b*) and [251]. To free the droplets from these structures a certain threshold voltage is needed.

Taking advantage of the hydrodynamic flow profile and the hydrodynamic resistance in certain channel geometries, droplets can be passively sorted or synchronized by size at large flow rates [246, 248, 338]. An important feature is that the velocity of a droplet can differ from the average flow velocity of the continuous phase. If droplets are significantly smaller than the channel dimension, they mainly experience the maximum flow velocity in the center of the flow profile and are thus faster than the average flow velocity, cf figure 16(*a*).

Vice versa, a droplet larger than the channel is confined in the microfluidic channel and experiences 'friction' with the channel walls. The continuous phase can bypass the large drop in the form of thin liquid threads located in the corners of channels with rectangular cross section ('gutter-flow') and the thin liquid layer of carrier fluid, cf figure 16(*b*), and thus has a larger mean flow velocity as compared with the droplets. For a detailed description and scaling arguments we refer to the review [382] and references therein.

A very intuitive sorting system based on the particular flow profile in a microchannel was introduced by [249] to sort droplets according to their size. As explained above, droplets

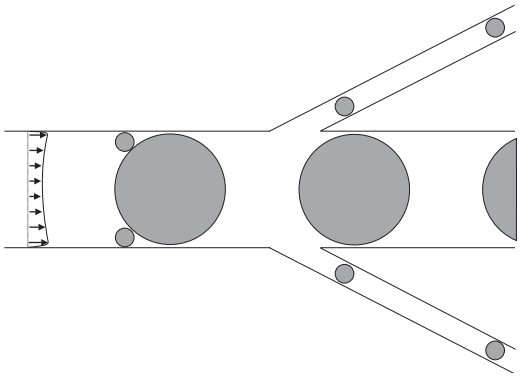

Figure 17. Schematic of the sorting and separation using the particular flow fields. The approximate flow profile of the continuous phase is sketched on the left side of the main channel.

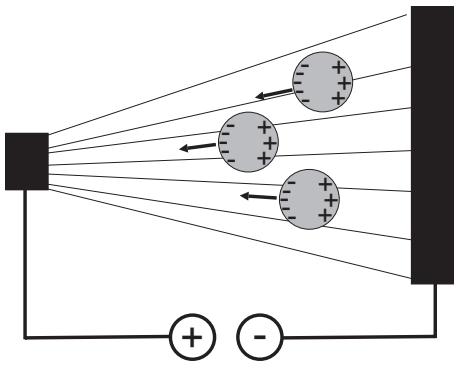

Figure 18. Schematic of the dielectrophoretic droplet manipulation.

with a diameter larger than the channel width flow slower than the average flow velocity of the continuous phase. Sufficiently small droplets traveling close to the center of the flow profile, however, move faster than the continuous phase and will be trapped at the side walls of the channel behind the large droplet traveling ahead of the small droplets. If side channels are introduced downstream from left and right which are large enough for the small droplets to pass, the small droplets are effectively separated from the stream of droplets, cf figure 17.

5.2. Dielectrophoresis

A convenient way of actuating flowing droplets is by means of electric fields that are applied locally in the channel. Since the dielectric constant of aqueous droplets is typically well above the dielectric constant of most non-polar (oily) liquids, uncharged droplets can be drawn into the direction of increasing electric field strength in a microfluidic device [210–216, 244] which provides a handle to manipulate droplets on demand, cf figure 18. In general, the term dielectrophoresis is used whenever a body made of a material with a larger dielectric constant than the ambient medium is drawn into the direction of increasing electric field strength.

The dielectrophoretic effect was first introduced for high-speed droplet sorting by Ahn *et al* [210] and is a frequently used technique to redirect droplets or cells [214, 215] or to selectively direct and merge droplets in a continuous flowing stream of liquid [212].

The standard geometry of a dielectrophoretic unit in a microfluidic device consists of parallel electrodes [216] or a grid of electrodes [211]. However, the implementation of electrodes in the fabrication process is a demanding task. In by far most applications of dielectrophoresis essentially two, more or less pointed, electrodes are inserted into a microfluidic device deflecting the droplets in a direction perpendicular to the main flow. These electrodes can be very thin and are fabricated by deposition from a metal vapor on the cover of a microfluidic device or by inserting thin metal electrodes into an already closed microfluidic device.

A more recent modification of the dielectrophoretic effect in microfluidics is optically induced dielectrophoresis (ODEP) [217–220, 232, 233]. In this technique two sides of a microfluidic device facing each other have to be coated with electrically conducting and photoconducting materials (e.g. hydrogenated amorphous silicon). Virtual electrodes generating the dielectrophoretic forces on dielectric droplets are then formed by optically projecting the electrode images onto the photoconductive material in order to generate non-uniform electric fields [217–220, 232, 233]. In this way droplets can be positioned and sorted individually in microfluidic devices using optical dielectrophoretic actuation [219, 220, 232, 233]. The advantage of optical actuation is that the movement of every droplet can be programmed individually by an adjustable laser beam. The disadvantage is that ODEP is technically demanding as it requires a special device fabrication and a laser setup.

A large flexibility in droplet handling is achieved by combining electrophoretic actuation with an appropriately shaped microfluidic network. Electrophoresis can be employed to, e.g., force a droplet into a microfluidic bypass and to control its release, and potentially to fuse it with other droplets [245]. Electrically charged droplets can be easily directed into selected channels by applying either homogeneous or inhomogeneous electric fields. This technique can be applied to droplets that are intentionally electrically charged in the course of their production or by presumably tribo-electricity while traveling in microfluidic channels [252].

5.3. Magnetic fields

Similar to droplets actuated by homogeneous or inhomogeneous electric field macroscopic magnetic particles can be oriented or directed by homogeneous or inhomogeneous magnetic fields, respectively. Placing these magnetic particles in droplets allow us to manipulate droplets on demand as the droplets follow the included magnetic particles [467]. Using this technique droplets can be forced through orifices or can even be brought to coalescence. A disadvantage of this technique is that the size of particles ranges from several micrometers to some tens of micrometers.

Stabilized suspensions of superparamagnetic colloidal particles in a liquid carrier phase exhibit a high magnetic permeability. In the presence of an inhomogeneous magnetic field such a ferrofluid will flow into the direction of increasing magnetic field strength. Similar to dielectrophoresis, the ferrofluid droplets can be directed into a desired direction by applying an inhomogeneous magnetic field whose field strength can be varied [260].

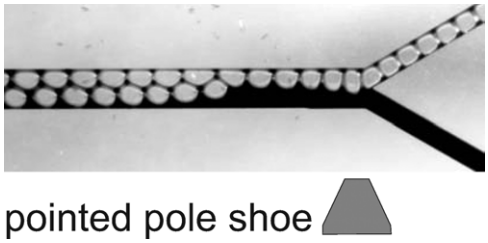

Figure 19. Droplet redirected by clogging one channel of a Y-junction with a plug formed by the continuous ferrofluid by externally applying an inhomogeneous magnetic field.

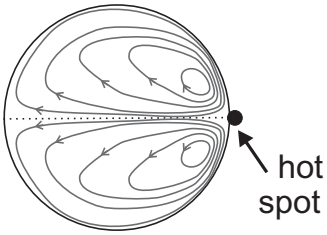

Figure 20. Schematic of the thermocapillary effect in droplets. The flow direction is towards larger surface tension. The corresponding flow profile in the surrounding fluid phase is not shown.

Alternatively, a ferrofluid can also be used as the continuous phase. In this case, the droplet manipulation is indirect as the continuous phase will locally form a barrier in a microfluidic channel at the position of highest magnetic field strength and the droplets will react to the local variation in the channel geometry [239]. In the example shown in figure 19 the ferrofluid forms a geometric barrier for the arriving droplets and forces them to move into one of the channels of a Y-junction.

5.4. Thermocapillary effect

The thermocapillary effect or Marangoni effect employs the fact that the interfacial tension is a function of temperature. For simple systems, the interfacial tension is typically decreasing with increasing temperature [234]; in surfactant stabilized systems, however, the opposite effect is found. Here, the interfacial tension may increase almost linearly with increasing temperature [235, 236].

In any case, the flow of liquid is directed towards regions of larger surface tension. Thus, a locally varying temperature results in a local imbalance of interfacial tension which induces a flow in and around the liquid droplet and, hence, induces a movement of the droplet relative to the continuous phase. The relative strength of this force increases with reduced droplet size and may become several orders of magnitude larger than forces generated by dielectrophoresis [184, 237], cf figure 20. By local heating with a focused laser spot [184, 213] one channel of, e.g., a Y-piece can be blocked and arriving droplets are directed into the selected channel. In order to account for parallel processing this technique has been extended to holographic beam patterns [253].

5.5. Electrorheological fluids

Electrical field not only induce forces onto macroscopic dielectric bodies, they may also change the viscosity of colloidal suspensions. When applying an electric field, the suspended particles may align in the direction of the electric field and thus increase the viscosity of the fluid. These electrorheological fluids can even exhibit solid-like behavior, i.e. they can sustain shear stress in the direction perpendicular to the applied electric field [271–279]. In continuous phase flow microfluidics, giant electrorheological fluids were used to fabricated micropumps [280] and mixers [281]. But also in droplet based microfluidics giant electrorheological fluids provide an additional handle to influence the function of a device. Electrorheological fluids can, e.g., be dispensed as droplets [182, 282, 283] or used as the continuous phase for droplet formation in a flow-focusing device [284, 285] which allows us to trigger droplet generation by increasing the viscosity of the electrorheological fluid when applying an electric field [284].

Electrorheological fluids can be also employed to sense droplets by capacitance measurements while flowing in microfluidic channels [265] and to merge droplets [131, 286], as the dielectric constant of the electrorheological fluid typically exceeds the other liquids involved by far, see also section 5.2. For more detailed information we refer to a specialized review on the manipulation of microfluidic droplets by electrorheological fluids [287].

5.6. Mechanical valves

The direct manipulation of liquid streams by mechanically opening and closing valves is underestimated in the literature as most of these valves are placed outside of the actual microfluidic device. However, almost every microfluidic device employs a mechanical valve to rapidly change or stop liquid streams or to inject the desired substance once the microfluidic process becomes stable. The advantage of mechanical valves is that they have no special demands on the droplet size, dielectric or magnetic properties and are thus independent of the particular emulsion system. They sort streams of droplets by selectively increasing the flow resistance of channels or by closing them entirely. The limiting factor is that mechanical valves are typically slow (a few hertz). If the valves are outside of microfluidic devices, the action of a valve is additionally delayed due to the pressure that is built up in the tubing and the microfluidic device itself. A system to freeze the position of all droplets in a microfluidic channel by closing all inlets and outlets of a microfluidic device in a short time was demonstrated in [259].

Droplets can be also redirected mechanically using vales which are embedded into microfluidic devices. Most of these valves use a second inflatable channel which is separated by a thin deformable lamellae to the microfluidic channel. The cross-sectional area of the microfluidic channel can be decreased or increased by varying the pressure in the inflatable chamber [175, 494–497], a technique first reported in [261] for the manipulation of continuous microfluidic streams and applied for microfluidic large-scale integration [262] in continuous microfluidic systems. Very recently it was demonstrated that the technique even allows us to sort droplets in two channels at a high frequency of hundreds of hertz [474].

5.7. Surface acoustic streaming

For the sake of completeness we will shortly mention actuation of liquids by sound. Directed flows in liquids can be induced by ultrasonic sound waves generated, e.g., by piezoelectric transducers. This effect, termed surface acoustic streaming, operates at very high frequencies (of about 150 MHz) and actuates the continuous phase in contact with the surface. This allow us to direct cells or droplets in different channels by varying the ultrasonic force fields [254] or surface acoustic waves [255, 256]. For a review on surface acoustic waves, see e.g. [257, 258].

5.8. Droplet detecting and sensing

For controlled manipulation and monitoring it is desirable to track the position of every individual droplet. The automatic sensing of droplets and, in particular, analyzing their content is one of the most important functionalities that needs to be optimized on the route towards fully automated on-chip droplet operation. A large number of techniques are described in the literature, each depending strongly on the particular microfluidic system and the particular physical quantity to be determined. This ranges from electrical signals such as capacity measurements and temperature variations to optical signals which can detect droplet positions and in advanced settings also determine the refractive index of the droplet phase.

In the following we will briefly explain the ideas behind commonly used detection techniques. Less known techniques depend on the particular microfluidic protocol and will therefore not be explained in detail.

5.8.1. Optical techniques. The majority of techniques to monitor and control microfluidic processes are based on optical measurements. This can be a custom made setup with an optical microscope and a high-speed camera attached to it. More specialized techniques are based on fluorescence microscopy which also allow us to distinguish different materials, in particular if some of the used fluorescence dyes either change their efficiency or emission wavelength based on the chemical surrounding. The obtained fluorescence signal can be analyzed *in situ* and used to trigger, e.g., a sorting process for high or even ultrahigh-throughput screening [330, 490, 504]. By adding certain types of quantum dots into droplets with a characteristic emission spectra, a very fine separation between several types of particles, respectively, droplets, is possible [486–489].

If sensing on-chip is desired without the use of a large optical microscope small light sensitive diodes [117, 471, 494] can be employed. In this way the size and velocity of droplets passing through a distinct spot on the microfluidic device can be measured. The light may be coupled in the microfluidic device using prisms and the microfluidic channels may act as optical waveguides [494]. But also other optical measurement

techniques based on the intensity signal of an evanescent wave are sensitive to the dielectric properties of the respective fluids and enable sensing of droplets based on the properties of the pure materials or added substances [487]. In advanced setups the refractive index of the droplets can be determined with an optical ring resonator which was embedded in the microfluidic chip [270].

5.8.2. Electrical techniques. Many alternative droplet detection techniques rely on electrical signals. It has already been shown that the position of densely packed bubbles in one and two row arrangements can be determined by capacity measurements using ferrofluids as the continuous phase [263, 264]. Similarly, droplets can be detected by capacity measurements in combination with electrorheological fluids [265]. Alternatively, droplets can be sensed by their impedance signal using thin electrodes embedded in the microfluidic channel. This method allows us to determine concentrations of ionic solutes and works also for water droplets surrounded by any oily phase [266–268].

Droplets can also be detected by an electrochemical response using a single electrode in contact with a passing droplet [269] or, alternatively, by measuring the heat loss of an area that is kept at elevated temperature [267]. This technique allows us to measure the area fraction of an electrode covered by the droplet which can be used to determine the size of the droplets *in situ*.

5.9. Static and dynamic droplet packings

One of the features of droplet based microfluidics which has rarely been referred to is the well-defined foam-like packing of droplets at sufficiently low volume fractions of the continuous phase. Such an emulsion is termed gel emulsion due to its rheological properties. The particular droplet arrangement depends on the microfluidic channel geometry and flow conditions. A active control of the packing geometry could be useful to rearrange the order of droplets in specific applications. But the behavior of densely packed droplets in microchannels is also interesting for its own scientific purpose. The packing geometry of gas bubbles in the dry limit has been studied in various geometries [288–290], similar investigations on 'dry' emulsion droplets are still missing. In this subsection we summarize the particular properties of dry emulsions, i.e. at low fractions of the continuous phase, and indicate a couple of interesting questions which can be studied with their help.

Dense assemblies of monodisperse spherical droplets packed into rectangular channels have been reported by Vanapalli *et al* [292]. In these experiments the size of the droplets is comparable to the dimensions of the channel. The packing is generated by closing a valve which then acts as a barrier for the droplets arriving from the production unit. A number of three-dimensional zigzag packings are found by confocal microscopy in agreement with simulation results and a theoretical analysis for different channel geometries [292]. Three-dimensional crystalline packing of small emulsion droplets with a diameter of 2.5 μm have been prepared in 250 μm wide channels by Shui *et al* [293]. The depth of the reservoir is 10 μm which limits the number of droplet layers to well below ten. As expected from the high surface to volume ratio of the confining channel, the emulsion droplets spontaneously arrange in a face centered cubic (fcc) packing. Surprisingly, the orientation of this fcc packing with respect to the top face of the reservoir depends on the flow rate of the continuous and dispersed phases [293]. At high flow rates of the dispersed phase the droplets tend to coalesce while small flow rates favor disordered droplet assemblies. The regimes corresponding to different orientations of the fcc packing, to disordered packings, and to droplet coalescence are summarized in a flow map diagram in terms of the flow rates of the two phases. Corresponding crystalline assemblies of monodisperse gas bubbles have been reported by van der Net *et al* [294].

In a series of experiments, Mehrotra *et al* produced droplets flowing down a linear channel with a depth of 50 μm and a width of 100 μm [295]. Depending on the size of the flowing droplets, three different packing geometries can be distinguished. Almost circular droplets are observed at small volume fractions of the dispersed phase. In an intermediate regime of volume fractions droplet shapes close to a triangle can be observed. These droplets arrange in an alternating 'zigzag'-like packing. Finally, at high volume fractions close to 1, the authors find rectangular droplet shapes which are almost aligned with the geometry of the channel and which can be compared with a bamboo packing reported also for foams in rectangular microchannels [264].

The impact of the volume fraction of the dispersed phase on packing transitions has been studied experimentally by Surenjav *et al* in [239]. In these experiments, packings of monodisperse droplets flow through a channel of linearly varying width. During the experiment the volume fraction of the continuous phase can be varied. A transition from a single row to two rows of droplets and from two to three rows is observed in a linearly widening channel. The opening angle of the channel in these experiments ranged from 5° to 10°. The reverse transition in a subsequent narrowing channel segment occurs at a smaller width compared with the width of the respective transition in the widening segment. This hysteresis in the packing transitions depends strongly on the volume fraction of the dispersed phase, ϕ . The onset of hysteresis for the single row to two row transition is found at a value of $\phi \simeq 0.85$ [239]. A similar value for the volume fraction is reported for the transitions between a two and three row packing. In view of potential combinatorial manipulation of droplets the geometric rearrangement of different droplet packings flowing around corners, and the resulting change of neighboring relations as a function of corner angle and volume fraction has also been studied experimentally by Surenjav *et al* [240].

While droplets have been attractive as individual micro-compartments for biochemical studies, droplet interfaces are recently evoking significant interest. Clearly, coalescence of droplets involves destabilization of droplet interfaces. However, when bilayer forming surfactants or lipids are used to stabilize the droplets, the aqueous droplets can be used to form self-assembled nanoscopic structures as discussed by Bayley *et al* in [296]. Such lipid bilayers provide nanoscopic

scaffolds for molecules that are inserted into them, which can then be probed either electrically or chemically. While elegant studies such as the feasibility to build wet circuitry have been demonstrated in [297–299], these are done by hand. Droplet microfluidics, with its advantages of high throughput and control, offers an obvious choice to extend such systems as shown in [300–302, 503]. The permeability of ions through a bilayer can also be used to control the coupling between chemical reactions in adjacent droplets. As shown by Thutupalli *et al* in [503] a lamella between two neighboring droplets may spontaneously collapse and form lipid bilayers at a sufficiently high volume fraction of the aqueous phase. These membranes are remarkably stable even when pumped through a microfluidic channel system. The specific capacitance of the formed bilayers can be measured statically as well as in a flowing droplet packing by contacting two adjacent droplets with Ag/AgCl electrodes. The membranes between adjacent droplets show the expected properties, such as membrane thickness and a threshold value for electroporation [503]. Also doping the bilayer, e.g., with the ion conducting membrane protein gramicidin, leads to a large increase in the conductivity. Thus, the simplicity to generate and manipulate membranes in a droplet based microfluidic system offers an ideal model system to probe membrane properties. But also the coupling of chemical reactions in neighboring droplets via the lipid membranes can be adjusted, as has been demonstrated for the Belousov–Zhabotinski reaction [503]. Here, the topology of the network of droplet contacts has a large influence on the observed spatio-temporal wave patterns.

Droplets can be manipulated in microfluidics by hydrodynamic interactions as discussed already above but, conversely, microfluidic devices also offer the great opportunity to study the hydrodynamics of droplet flows at low Reynolds numbers. In an effectively two-dimensional system (Hele–Shaw geometry) hydrodynamic interactions between particles and droplets differ substantially from the bulk behavior [304] and lead to a number of unexpected phenomena such as phonon-like excitations in non-equilibrium crystalline arrangements of droplets [305] or transitions between intermittent and ordered transport of droplets through arrays of obstacles [306].

At low flow rates of the continuous phase the shape of a flattened droplet in a Hele–Shaw cell stays close to a circular disk and the droplets can be regarded as rigid objects advected by the flow of the continuous phase. The disturbance of the flow field around the object leads to a long ranged hydrodynamic interaction while inside the droplets a treadmilling flow field emerges. The far field disturbance of a circular disk onto the ambient flow can be described by a two-dimensional dipole [307] while the treadmilling flow inside the circular droplet amounts to an effective friction of the droplet with the top and bottom walls of the cell. In [307], Beatus *et al* discuss the impact of boundary conditions on the hydrodynamic interaction between droplets in a Hele–Shaw geometry. Surprisingly, disordered assemblies of droplets display slow shock waves, cf [308]. Here, the presence of the channel boundaries is essential to explain the velocity–density coupling of the droplets. The average droplet density in the channel can be described by the one-dimensional Burgers equation [308].

6. Droplet coalescence, splitting, and mixing

To perform (bio-)chemical reactions in droplet based microfluidics and to take full advantage of the superior mixing capabilities inside flowing drops, different liquids must be combined and mixed. The best volume and reaction control is possibly provided by coalescing two formerly individual droplets which are generated with a precisely defined volume and which contain different reactants. Basically, there are four main approaches to coalesce droplets in microfluidic devices, namely droplet coalescence by channel geometry, coalescence using particular liquid properties, coalescence using the thermocapillary effect, and electrocoalescence. All these techniques differ in their capabilities and their experimental requirements and need to be chosen according to specific experimental demands as will be explained in the following. As a last subsection to droplet coalescence we also describe the direct dispensing of liquid into passing droplets which uses similar concepts. To complete the section we describe how initial or coalesced droplets can be fragmented into smaller droplets, how mixing in droplets proceeds, and how it can be determined.

6.1. Droplet coalescence using special channel geometries and flow conditions

Droplet merging by a suitably shaped channel geometry is the easiest technique but is mainly used for surfactant free droplet systems or for liquid interfaces which are only poorly stabilized by surfactants. Here the most important task is to reduce the distance between individual droplets and bring them in direct contact with each other. This can be done by various channel geometries, cf figure 21, where either the fluid resistance in a channel can be enlarged by a narrowed channel part which stops the leading droplet and provides sufficient time for a subsequent droplet to meet the previous one [317, 318, 466], cf figure 21(*a*). Alternatively droplets can be stopped and trapped by an enlargement of the channel [466], cf figure 21(*b*), or in channels with 'porous' side walls that allow the continuous phase to drain [319, 320], cf figure 21(*d*). Furthermore, coalescence can be induced by colliding two droplets in a T-junction [321] or in appropriately shaped winding channel geometries [322]. The fusion of droplets at a geometrical constriction can be controlled on demand if the flow of the continuous phase around the constriction is adjusted by a bypass which allows us to adjust the flow rate of the bypassing liquid, e.g., by a temperature controlled viscosity, as already mentioned in the context of droplet production (section 3) and as was demonstrated in [466], cf figure 21(*e*).

In addition to the temporal stopping of a droplet, it may be sufficient to slow it down, in order to guarantee that each subsequent droplet meets the previous one forming a pair. A typical geometry for this type of coalescence trigger comprises a widening channel geometry with a channel significantly larger than the droplet diameter, cf figure 21(*c*). In the widening channel geometry the continuous phase can easily flow around the droplet and the droplet slows down allowing the succeeding droplet to catch up with the first droplet. Once two droplets are in contact they might merge provided they

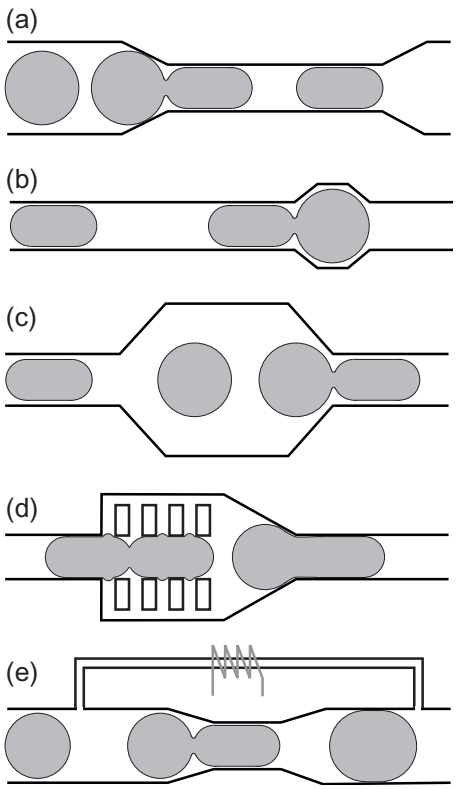

Figure 21. Schematic of different geometries to coalesce droplets by (*a*) stopping a droplet at a narrowed channel, (*b*) stopping a droplet in a widened channel, (*c*) slowing down the drop movement in a widening channel, (*d*) slowing down a droplet in a comb geometry, and (*e*) slowing down a droplet by a controlled bypass.

are given sufficient time [310–312]. If the droplets meet right after their production this techniques was also demonstrated to coalesce droplet pairs if surfactants are present [329]. A possible reason for this might be that during or right after droplet formation the droplet surface is not yet fully covered with surfactant molecules.

A counterintuitive phenomenon was found in coalescence experiments using a geometry as sketched in figure 21(*c*). In this case, the droplet coalescence occurs mostly during the re-separation of the droplets when the leading droplet begins to enter the narrow channel and not during the impact of the droplets when they initially meet [313]. This is explained by the formation of two small protrusions in the opposing parts of the interfaces during droplet separation which hastens the connection of the interfaces prior to droplet fusion in a certain range of the parameter space. This effect was also found in simulations [314] and in alternative experimental settings [315], and is explained theoretically in [316].

6.2. Droplet coalescence using particular properties of liquids

In addition to the geometry of a microfluidic channel, there are several other physical mechanisms which might lead to droplet coalescence. Fusion between droplets is observed for identical liquids with droplets of different sizes having different velocities, or equally sized droplets consisting of

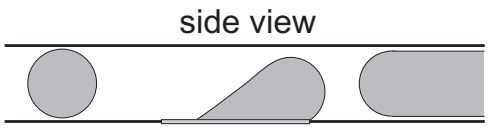

Figure 22. Schematic of wettability induced droplet fusion.

liquids having different viscosity [323]. In both cases droplet pairs are formed because one of the droplets flows faster than the other droplet due to differences in the drag force, friction at the channel walls, and internal viscous friction properties, respectively. The droplets are continuously pushed against each other, thus causing the separating oil lamella to thin down. Its eventual rupture then leads to droplet fusion. For bidisperse droplets which differ significantly in their size it could be shown that within a certain travel distance in a microfluidic channel each larger drop is merged with exactly one smaller droplet [330] provided that channel geometry and channel size is chosen appropriately and that the surfactant does not stabilize the droplets very well. Similarly, the flow velocity of elongated drops in microchannels depends on the surface tension of the liquids. Hence droplets having different surface tension will also meet and finally fuse if the contact time is sufficiently large [324].

Depending on the flow velocity, sufficiently small droplets can be alternatively stopped in a microfluidic channel at a patterned area which is wetted by the dispersed fluid. If additional droplets arrive and fuse with the trapped drop, the size of the trapped (sessile) drop increases until the hydrodynamic drag force exceeds the capillary force fixing the drop in place [325, 326], cf figure 22. The drop is then displaced from the wettable patch, allowing the process to start over again with the next droplets arriving at the wettable patch.

6.3. Droplet coalescence using the thermocapillary effect

Similar to applications in droplet manipulation, the thermocapillary effect can be employed to create a convective motion within each droplet. Induced by a hot spot, e.g., generated by a focused laser spot, this convective motion can be utilized to initiate droplet fusion. As already mentioned in section 5.4 the surface tension of surfactant stabilized interfaces may increase with increasing temperature [235, 236] and the flow of liquid is directed towards regions of larger surface tension. This flow causes a local imbalance of the interfacial tension and might lead to droplet fusion.

Droplet coalescence using the thermocapillary effect in microfluidic devices can be achieved in the following way. A first droplet is stopped at a laser spot by the thermocapillary effect until a second drop arrives. When the resulting drag force exceeds the forces applied by the thermocapillary effect, the droplet pair will move forward and pass the laser spot. The droplets fuse once the contact area passes through the laser spot, cf figure 23. Alternatively, the laser spot can be used to burn a lamella within an array of droplets [237] using the same principle. More advanced optical settings use holographic vortex traps to manipulate and fuse drops [253, 331]. Also the ohmic resistance can be used to heat

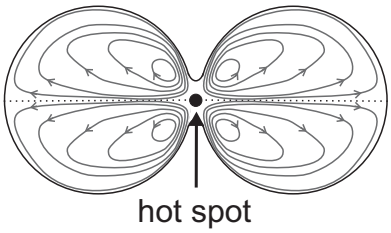

Figure 23. Schematic of droplet coalescence by the thermocapillary effect.

a drop if an electrical current is applied to a single droplet being contacted by electrodes: an arriving droplet touches two electrodes and a current flows resulting in local heating and the thermocapillary effect traps and fuses the droplets [332, 333].

6.4. Droplet coalescence using electrocoalescence

The last droplet coalescence technique which will be discussed relies on the fact that the coalescence of droplets can be achieved by applying electric fields when no significant electrical current is flowing. This process has been termed electrocoalescence and has already been used for many years in other scientific and industrial fields. In atmospheric physics, for example, electric fields force the coalescence and dissolution of raindrops. Electrocoalescence is also applied in the food industry or petrol engineering for de-foaming processes to remove, e.g., dispensed water from crude oil. A review on these bulk processes can be found in [334].

Standard settings apply a homogeneous or inhomogeneous electric field across droplets in the range 1–100 kV m^{-1}. Inside electrically conducing (aqueous) droplets there is no electric field due to the separation of mobile charges, cf figure 18. If two such droplets are close to each other the induced dipoles of both droplets align, leading to an attractive Coulomb force between them and eventually leading to droplet fusion. Whereas the attraction of individual droplets in an applied electric field is readily explained and frequently used in microfluidics, the mechanism leading to droplet coalescence remained obscure until recently.

Electrocoalescence of droplets was first applied in microfluidic settings for liquid/liquid extraction processes [335]. The fusion of individual droplet pairs by electrocoalescence was shown about one year later by Chabert *et al.* [336]. One of the first applications of electrocoalescence of continuously flowing trains of droplets was demonstrated in [337]. In this approach a rectangular reaction chamber has been fabricated in the microfluidic device and the inlet and outlet channels of the rectangular chamber are placed in diametrically opposite corners. About perpendicular to the flow direction of the droplets, an electrical field is applied by two electrodes embedded into the microfluidic device. It was also demonstrated that the electric fields can be oriented parallel to the flow direction if electrodes are formed across the channel [338], cf figure 24(*a*). Later, several variations of this geometry were used to apply electrocoalescence in microfluidic settings, e.g., in [121, 243, 244], or to study the coalescence behavior [339, 340]. A strong electric field between droplet pairs

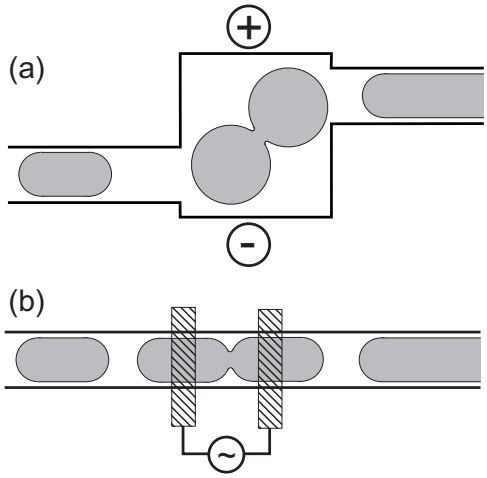

Figure 24. Schematic of electrocoalescence (*a*) using dielectrophoresis for the droplet approach and (*b*) directly contacting the droplets by electrodes.

leading to their coalescence can be also generated by alternatively charging droplets during their production [336, 341]. Electrocoalescence can also be achieved by directly contacting the droplets with electrodes cf figure 24(*b*). In this configuration droplet fusion can be achieved by applying a few volts only. Applying an ac-voltage even allows us to coalesce droplets using electrodes insulated with a thin polymeric layer, as the capacitive coupling from the metal electrode to the conducting droplet is very effective [344].

The process of electrocoalescence was explained quantitatively by a spinodal breakup [342] of a thin oil lamella between two conducting droplets in the presence of an electric field [343]. To achieve a quantitative agreement with experimental data the particular geometry of the circular contact areas of the drops was considered which imposes certain constraints on the evolving spinodal wave pattern [344]. The dependence of the coalescence voltage on droplet size, surface tension, and separation distance can be explained by this theory for various ionic concentrations of the aqueous phase and frequencies of the applied ac voltage [344].

6.5. Direct dispensing into droplets

Without the use of surfactants, liquid can be also directly dispensed from one or several side channels into passing droplets [327, 328, 466], cf figure 25. Applying the electrocoalescence effect, liquid can also be dispensed into surfactant stabilized droplets when a voltage is applied between the passing droplet and the dispensed liquid [473]. Direct dispensing into droplets at kHz rates offers great possibilities if several reagents are mixed with one droplet and allows us to vary the chemical content of each individual droplet.

6.6. Droplet splitting

For some microfluidic processing steps it is not only desirable to coalesce droplets but also to fragment droplets into several smaller compartments for incubation or screening purposes or to increase the droplet production frequency. Because

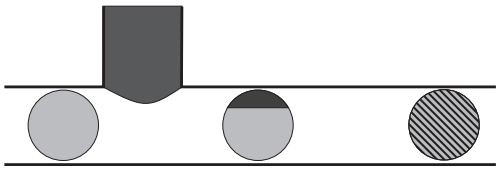

Figure 25. Schematic of dispensing a second liquid into a passing droplet.

many droplet manipulation and organizing steps rely on the degree of confinement, i.e. the relative size of the droplets with respect to the microfluidic channel width, as discussed in sections 5.1 and 5.9 [240, 263, 264]. It might also be important to split coalesced droplets just after droplet coalescence to be able to feed the droplets back into the same microfluidic processing and to guarantee the same function during each repeated process cycle.

Except for straightforward fragmenting of droplets using pneumatic valve actuators which allows us to split droplets independent of flow rate and fairly independent of size [125], essentially all of the splitting geometries elongate droplets and rely on the Rayleigh–Plateau instability. This process is similar to droplet generation, and accordingly the typical geometries used for droplet fragmentation are very similar to the geometries used for droplet generation, cf section 3.

It has been shown that droplet breakup can be mediated by microfluidic geometries like T-junctions [112, 238, 242] or Y-junctions [241, 484], cf figure 26(*a*). The fragmentation of droplets depends on the effective flow resistance of each channel or around obstacles provided the flow velocity is sufficiently high, cf figure 26(*b*). A detailed analysis of the flow resistance and the identification of a critical capillary number for droplet splitting flowing in narrow gaps around obstacles is given in [479]. Adjustable droplet splitting by variable geometries using an inflatable chamber was also realized [125]. Forcing droplets through orifices might also break them into smaller ones depending on orifice dimensions, cf figure 26(*c*). Alternatively to the mediation of droplet breakup by channel geometry, the breakup of droplets can be mediated by symmetric microfluidic cross flow leading to droplet elongation and finally to droplet breakup in the direction of the fluid flow [346] similar to hydrodynamic flow focusing.

During droplet splitting experiments it turned out that droplets of viscoelastic liquids are less stable against droplet splitting than droplets of Newtonian liquids of similar viscosity [345]. Thus, the droplet deformation at a junction may even be used to characterize the extensional rheology of low viscoelastic liquids [345]. The effective flow resistance or surface tension and thus the fragmentation can be manipulated on demand, e.g., by thermal treatment [247], as already discussed in the context of droplet formation.

6.7. Mixing in droplets and flow profiles

To complete the microfluidic tools to perform complex microfluidic processes we continue with the fast mixing of liquids inside confined drops flowing in microfluidic

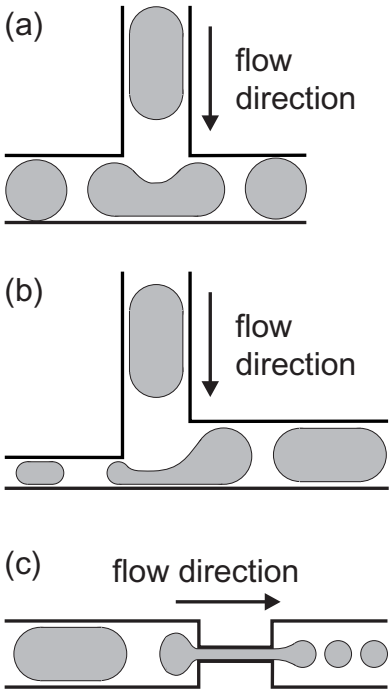

Figure 26. Sketch of various channel geometries for droplet splitting. (*a*) T-junction with symmetric channels resulting in equally sized drops. (*b*) T-junction with asymmetric channels resulting in differently sized droplet fractions, and (*c*) droplet splitting by forcing a large droplet through an orifice.

channels and explain experimental techniques to quantitatively determine those flow profiles.

The enhanced mixing in droplets was already discussed on the basis of classical studies [349–351] and demonstrated in [352, 353]. The first papers reporting on the rapid mixing in droplets and the absence of axial dispersion noticed by the growing microfluidic community were published in [96, 491]. This work started an emerging field to conduct chemical reactions in droplets and was followed by several papers quantifying the temporal resolution and reaction kinetics [354, 355], scaling laws of the chaotic advection [356], and the influence of viscosity [127]. A topical review is found in [357].

Due to the particular friction boundary condition of droplets flowing in close contact to a solid wall, a circulating flow pattern emerges within the droplets. This flow pattern exhibits a symmetry axis parallel to the flow direction. Since most of the microfluidic channel designs have a flat rectangular cross section, the two halves of a droplet—left and right with respect to the symmetry plane—will hardly mix. If thus the initial liquid gradient is perpendicular to the flow direction, as is the case when various liquids are commonly dispensed from one inlet, the symmetry axis has to be varied in time, which can easily be achieved by a back-fold channel structure, cf figure 27(*a*) and (*b*). The influence of various channel geometries on the mixing behavior was tested for, e.g., zigzag type structures having different angle [358], rectangular corners [359], or structured serpentine-like channels [355]. The mixing dynamics was typically analyzed by fluorescence microscopy but also fluorescence lifetime

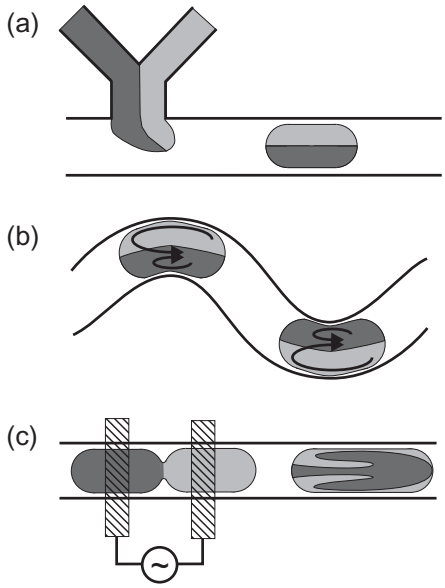

Figure 27. Schematic of liquid concentration after (*a*) common dispensing from one nozzle and (*c*) after coalescence of two droplets flowing behind each other. The drawing (*b*) sketches the varying flow pattern in droplets traveling in a serpentine channel.

imaging was employed to reconstruct mixing patterns with up to 5 μs [360] and 1 μs time resolution [361]. If, however, the concentration gradient is parallel to the flow direction, as is the case for certain droplet coalescence geometries, the symmetry axis parallel to the flow direction does not matter and the mixing proceeds very fast without back-fold channel geometries, cf figure 27(*b*).

The flow pattern and the mixing in droplets was also considered in numerical simulations of straight channels [362, 363, 368, 369] and of serpentine channels [370]. It was shown that the friction between the droplet and the channel wall increased with decreasing thickness of the fluid layer of the continuous phase between droplet and channel wall. With increasing friction the advection velocity increases and promotes fast mixing within droplets [371].

Alternatively to the friction induced motion inside a droplet, a very similar circulating flow pattern and thus mixing inside static droplets can be achieved by a local temperature variation using the thermocapillary effect, e.g., induced by a laser spot [213, 372], cf figure 20. And even a 'mechanical stirrer' inside droplets was realized by a microscopic assembly of superparamagnetic beads driven by a temporarily varying magnetic field [373, 374].

6.7.1. Measuring flow profiles by PIV. Fluid flows can be determined experimentally by adding small fluorescent tracer particles and following their movements. For the choice of particles it is on the one hand important that the particles and the density difference is sufficiently small so that the particles follow the fluid flow without any delay. On the other hand, it is also important that the tracer particles are sufficiently large to achieve a sufficiently strong fluorescent signal which allows for sufficient short exposure times which are needed to capture the desired flow velocities. If the movements of individual

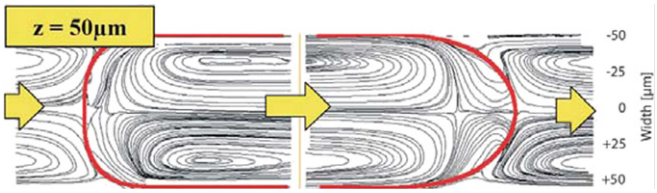

Figure 28. Flow profile in a droplet flowing in a microfluidic channel as measured by PIV. The channel height ($z = 50\ \mu$m) is half the channel width. (Image courtesy of R Lindken *et al* [197]; reproduced by permission of the Royal Society of Chemistry.)

tracers are tracked, the technique is called particle tracking and usually lacks statistics to determine an entire flow profile without averaging over many traces. PIV, however, does not track individual tracers but correlates the position of tracers in two consecutive images which are captured within a short time interval. Provided the time interval is chosen appropriately and the density of the tracers is sufficient, a flow profile can be determined from one set of those double images [197, 198] and offers a great possibility to determine flow profiles in microfluidic settings.

The emerging flow pattern in droplets flowing in straight channels [362, 363], in serpentine channels [364], in back-fold channels with square turns [359], and after coalescence [365] was studied qualitatively and quantitatively using PIV [198], cf figure 28. Recent PIV data even resolved the flow in a droplet in three dimensions [366, 367].

7. Applications of droplet based microfluidics

In addition to the fundamental physical and technical aspects of droplet production, one of the central aims of droplet based microfluidics is to develop methods for reliable manipulation of droplets to fabricate special materials or to screen and analyze (bio-)chemical reaction products.

In this section we mention some applications of droplet based microfluidics in chemistry, material science, biology, and medicine which demonstrate the usage of some of the above explained principles. The focus shall be again on commonly used microfluidic schemes and principles. For a more complete account, the reader is referred to existing review papers in the various fields dedicated to more specialized topics, such as the fabrication and usage of droplet based microfluidics for *in vitro* compartmentalization [505, 506] and the development and screening of biological assays [443, 472], the production of polymer particles [185, 376, 437], microgel particles [377], nanoparticles [378, 379], inorganic particles [438], or other special materials [439]. The fabrication of non-spherical particles and microgel particles from synthetic and natural oligomers is reviewed in [440] and [441], respectively. We consider two widely found types of systems to exemplify applications of droplet based microfluidics, the formation of special material particles, and the manipulation of biological material.

7.1. Fabrication of special materials

The typical reaction schemes to generate solid or gel particles can be grouped roughly into four reaction categories depending

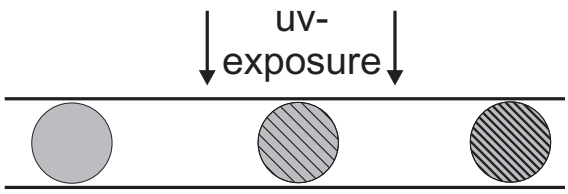

Figure 29. Schematic of droplet solidification by photo-polymerization.

on the particular technique that is employed to dispense the liquid and to initiate the reaction. Typically, a certain type of reaction also requires a certain microfluidic scheme. Reactions are frequently initiated by time delay, temperature or photo-initialization, (inter-)diffusion of molecules, or by mixing different species. While the first three options of reaction control are quite flexible considering the required microfluidic schemes, the initialization of reactions by mixing different compounds requires techniques to coalescence droplets or to dispense liquid into passing droplets.

The following text is organized in terms of the different microfluidic schemes. It is obvious that with some restrictions all of these reaction schemes can be applied in a similar manner to double emulsions where, e.g., an oily phase is surrounded by an aqueous phase which are both dispensed in a second oily phase. For that, two subsequent droplet formation processes and appropriate liquids and surfactants have to be employed which add some complexity to the microfluidic processing but the underlying principles, however, remain untouched.

7.1.1. Dispensing reactive mixtures from a single nozzle. The easiest scheme to generate particles by droplet based microfluidics is to form droplets of reactive mixtures and pre-polymers having a well-defined volume and a special shape that are solidified with time while traveling along a microfluidic channel. The potential difficulty of injecting reactive mixtures is that the liquid unavoidably comes in contact with the channel walls which might lead to channel clogging. These difficulties can be circumvented by activating the reaction after droplet formation, e.g., by photo-polymerization, temperature activated polymerization, or exchange of molecules with the surrounding carrier phase as will be discussed in the following.

The general idea is to dispense a pre-polymer into droplets containing starter molecules which can be initiated by an external stimulus like UV-exposure or heating. Alternatively a reaction can be initiated by a change in pH or by the diffusion of ions or molecules in or out of the droplet phase.

Photo-polymerization can be employed to generate spherical polymer or gel particles, see [375], cf figure 29. This microfluidic scheme was optimized for particle monodispersity [390] and more complex chemical routes were explored where the polymerization is triggered by UV-exposure and continued by the generated heat during that chemical reaction [391]. Using Raman spectroscopy the degree of polymerization during photo-polymerization was studied as a function of travel distance, respectively, of time [392].

The large freedom in shaping optical beams and droplets was utilized to polymerize particles of almost any shape like periodic arrays of polymer discs [380] and molecular imprinted polymer beads [391]. To increase the yield highly parallelized geometries were also realized for high-throughput particle production in either circular [116] or parallel [393] geometries.

In addition to the formation of particles consisting of a homogeneous material, recent developments were driven by the desire to fabricate particles with variable chemical composition or shape to achieve desired particle properties. Janus beads and ternary particles were fabricated from two or more photocurable liquid phases which are commonly dispensed from one nozzle in an immiscible carrier phase and directly polymerized [394, 395, 478], cf figure 27(*a*). Similarly, homogeneous and colloid filled hydrogel granules of various geometry [396] have been produced in this way. Even particles with a permanent magnetic moment can be generated if ferromagnetic nanoparticles are added and aligned during the curing process [477]. If only one of the two dispensed phases is photocurable and the two dispensed liquids form an interface with a finite interfacical tension, photo-polymerization will result in anisotropically shaped polymer particles [397]. When applying this technique to an appropriate combination of aqueous and organic phases the produced polymerosomes will form a double emulsion [398].

Alternatively to photo-polymerization, chemical reactions can be controlled and accelerated by increased temperatures, e.g., in the production of CdSe nanocrystals at about 300 °C [165]. Also advanced microfluidic reactors equipped with several controlled temperature zones have been designed [399]. In these approaches it is crucial that the individual droplets are always clearly separated from each other since temperature gradients drive thermocapillary flows which destabilize an emulsion very effectively.

Another frequently used scheme to initiate reactions is based on the exchange of molecules or ions between the continuous phase and the dispersed phase. The advantage of this approach is that rather complex materials (core-shell particles) can be fabricated with a fairly small microfluidic effort. In either case, some of the involved components need to be soluble in both phases posing a certain risk of cross contamination between the particles or the formation of precipitates at the channel wall.

The diffusion of gas from bubbles into the continuous phase can be utilized to adjust the size of the gas bubbles [400]. The diffusion of one solvent into the carrier phase can also be exploited to generate an ordering effect like surfactant templating [492, 493]. Generally, the effect of gas or solvent evaporation from the dispersed phase into the continuous phase or, alternatively, the exchange of ions or any other inter-diffusion between the dispersed phase and the continuous phase leads to a concentration of the droplet content [401–403], a change of the pH or to a transport of particles or molecules from one liquid phase to the other liquid phase [404, 405], or the liquid/liquid interface, cf figure 30. The time scales of these exchange processes depends on the liquid phases, the surfactants, and their concentration [406]. This technique can be applied to crystallize membrane proteins

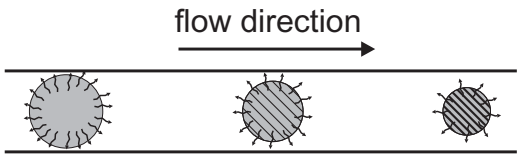

Figure 30. Schematic of reaction control by diffusion between the continuous phase and the dispersed phase.

in lipid mesophases which can be screened in individual droplets [407] and spray dry danazol nanoparticles [485]. CO_2 evaporation from bubbles into a continuous aqueous phase containing lysozyme triggers the buildup of a gas bubble with a lysozyme-alginate shell [408].

Macroporous polymer particles have been fabricated by mixing the initial pre-polymer with a solvent of the pre-polymer [409] or nanoparticles which are selectively dissolved in the continuous phase [410]. The effect of solvent evaporation was also utilized to anchor nanoparticles at the liquid/liquid interface creating particles with a raspberry-like surface structure [411]. Similarly, hollow polymer capsules and spheres can be produced. Choosing the experimental parameters like flow rate and diffusion rate properly, even toroidal polymer particles can be produced by evaporating the polymer solvent [412]. Cells can be encapsulated in alginate hydrogels [413] and hollow polymer spheres can be generated enclosing ionic liquids [414]. By adsorbing polymers at the liquid/liquid interface, polymer coated droplets [137] and biodegradable polymer microparticles for drug delivery can be fabricated [415].

A cross linking reaction can also be started after droplet formation by exchanging the dispersed phase with a continuous phase containing accelerator molecules that diffuse into the dispersed phase. Following this scheme, e.g., alginate microgel particles have been generated by diffusion of CaI_2 ions from the surrounding undecanol phase into aqueous droplets of an alginate solution [419] and thermoresponsive microgels have been produced with tunable volume-phase transition kinetics [420, 421]. Also droplets from complex fluids like liquid crystals can be formed [422, 423]. These droplets can then be coated with polymer multilayers by repeating coating and washing steps providing a microfluidic device with a sequence of sections flushed by various continuous phases [424].

But also particles or microgel particles can adsorb at the liquid/liquid interface allowing us to produce stimuli-responsive colloidosomes [425]. As another step towards tailoring special materials it was shown that bovine serum albumin (BSA) can be encapsulated in chitosan microspheres by solvent extraction allowing for a controlled drug (BSA) release [426].

Not only organic particles or hollow spheres but also inorganic particles can be produced by solvent diffusion, or by interdiffusion of ions or other substances between the dispersed phase and the continuous phase. Silica particles were produced by a metal-organic sol–gel synthesize route where the organic solvent is soluble in the continuous phase and $BaSO_4$ nanoparticles have been produced by supersaturating an aqueous solution of $BaCl_2$ by evaporating water into an alcohol solution mixed with sulfuric acid [416]. Silica spheres have been generated by interdiffusion and hydrolysis/condensation of tetraethoxy-orthosilane under a strong acidic condition provided in acidified aqueous droplets [417]. Polycaprolactone incorporating quantum dots, nanoparticles, and tamoxifen could be fabricated by evaporation of chloroform into the continuous phase [418].

7.1.2. Initiating reactions by mixing of liquids. And last but not least, chemical reactions can be initiated by coalescing droplets and mixing their contents inside droplets similar to bulk reactions where the content of one beaker is poured into another beaker and stirred. This approach involves a complex microfluidic process but it allows us to precisely control the volume of each liquid and to use an ambient phase where none of the dispensed chemicals is soluble which avoids cross contaminations and clogging.

The miscible reactants can be dispensed from a single nozzle and mixed inside plugs [96, 427, 428] as already mentioned in section 6.7, cf also figure 27(*a*). In this approach the volume of each phase that is commonly dispensed is not known precisely for each droplet and a small fraction of the dispensed liquid is already mixed and reactive at the nozzle before or right at droplet formation and will touch the microfluidic channels. Fast chemical reactions that form precipitates or sticky gels might form traces at the microfluidic channel which might clog the inlet.

The problem of clogging can be reduced when plugs are combined with a second liquid forming a meniscus just out of a side channel, see figure 25. The second fluid is miscible with the dispersed fluid and initiates the chemical reaction. This scheme has been first demonstrated to synthesize colloid CdS and CdS/CdSe core-shell nanoparticles [327]. It has also been used to synthesize azo dyes as examples of organic reactions [429] and 4-chloro-*N*-methylbenzamine [430].

This type of microfluidic scheme suffers from two difficulties. First, the merging of droplets with a liquid tip only works reliably for droplets which are either not or only poorly stabilized by surfactant. And second, the volume of the droplets already flowing in the channel is precisely known where the amount of reactant added by the liquid finger can be controlled only up to a certain extend. This becomes obvious if we consider that a fraction of the droplet's liquid will stay in the liquid meniscus after the pinch-off also adding a certain uncertainty to the reaction kinetics of each individual droplet. The first difficulty can be easily overcome by facilitating the direct dispensing of liquid into surfactant stabilized droplets by electrocoalescence [490], and represents a very flexible and high-throughput technique if the added volume is not absolutely critical.

To account for the mentioned difficulties on the cost of the reduced flexibility, a microfluidic scheme has been developed combining the synchronized production of droplet pairs containing the respective reactants (see section 3), their controlled fusion (see section 6), and fast mixing inside the fused drop (see section 6.7), cf figure 31. This reaction scheme was used to synthesize CdS nanoparticles [131] but without the use of surfactant which leads to an increased polydispersity of

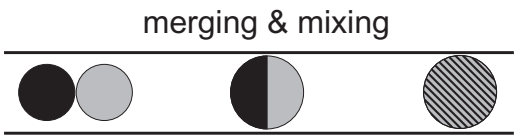

Figure 31. Schematic of reaction initiation by merging and mixing two drops.

the produced droplets. A synchronized production of droplet pairs that are surfactant stabilized and subsequently fused by electrocoalescence was demonstrated in [431] for the synthesis of magnetic iron oxide nanoparticles. Similar microfluidic schemes based on an alternative approach to generate and fuse droplet pairs were employed to fabricate silica particles from a sol–gel synthesize route [317, 318] and to fabricate poly(lactide-*co*-glycolide) micro- and nanospheres combined with solvent evaporation and extraction [432].

Pre- or post-processing at elevated temperatures of the reactants was already demonstrated by heating or cooling the entire device or larger parts of it [165, 433]. Recently it was even shown that the content of individual droplets can also be thermally processed: the temperature of individual droplets can be increased by microwave dielectric heating [434] or reducing and droplets can be even frozen by thermoelectric manipulation [435]. If emulsion droplets are frozen and docked at appropriated places in a microfluidic device, the surrounding continuous phase, and even the surfactant stabilizing the droplets, can be exchanged [436].

7.2. Biology and biophysics in droplets

Let us finally turn to applications of droplet based microfluidic systems to biological systems, where they appear particularly promising. The ability to generate precise sample aliquots of picoliter volumes, advanced sample handling, and high throughput dramatically increases the productivity of bioassays and combinatorial biochemical reactions. Experiments on this scale allow fine control in studies of complex biomolecular processes and provide a more efficient and cost-effective experimental design. Important applications for *in vitro* compartmentalization [505, 506] and the development and screening of biological assays [443, 472, 504] are already explained in depth in recent reviews and will not be considered here. In the following we present two exemplary exciting topics from the rapidly growing field of droplet-based biology and biophysics: (*a*) single cell experiments and (*b*) imaging and manipulating of protein networks.

7.2.1. Single cells in picoliter volumes. Droplet based microfluidics provide well-defined environments for individual cells. The droplet content can be varied systematically during droplet generation and can be modified subsequently by fusion with another droplet. Microfluidic assays seem to be much faster than conventional assay techniques. Different cells from bacteria [448, 449] to yeast [450] and to mammalian cells [451] have been encapsulated in microdroplets. Using gas permeable perfluorocarbon oils keeps the cells alive for several days [452]. Suspension and adherent cells as well as organisms (*C. elegans*) are not only alive for long times but also can be recovered and recultivated with comparable viability to cultures under conventional conditions.

In typical single cell-based microdroplet assays, prior to a cell lysis step the expression of proteins and activity of enzymes has been analyzed using fluorescence techniques [453]. As long as the volume of the droplet is kept constant during the experiment, the fluorescence intensity allows for a quantitative analysis [443]. On-chip lysis of cells in droplets is an alternative way to access the cell contents, but also opens a route to introduce material into cells. Electroporation of cells in microfluidic droplets can be achieved when cell-containing droplets flow through a pair of microelectrodes with a constant voltage established in between [454]. Studies on stationary droplets containing single cells show the potential of droplet based microfluidics for studies into stochastic phenotypic variations within populations of genetically identical cells [455]. In order to perform these experiments not only single cells have to be encapsulated but also the cell-containing droplets have to be stored for long time studies and droplets may be re-injected for further manipulation. Moreover, droplet sorting seems to be an essential element for integrated on-chip devices.

Normal encapsulation of single cells from solutions leads to a Poisson distribution with empty droplets as well as one or more cells in the droplet compartment. This effect leads to a large fraction of empty droplets and reduction in effective throughput. In order to overcome this drawback several methods have been developed. Edd *et al* have been able to form droplet compartments with single cells using self-organization process of the cells before droplet generation [456]. A high density suspension of cells flows rapidly through a high aspect ratio microchannel, where cell diameter is a large fraction of the channel's narrow dimension. The cells organize into two evenly spaced streams whose longitudinal order is shifted by half the particle–particle spacing. The droplet formation coincides with a cell entering the flow-focusing region of the microdevice and almost every drop contains exactly one cell, thereby overcoming the intrinsic limitations set by Poisson statistics. Another method sorts single-cell-containing droplets from smaller empty droplets after each cell triggers its own encapsulation (Rayleigh–Plateau instability) upon entering a narrow aqueous jet formed in a flow-focusing device [457].

For studies of biological matter involving incubation of cells or *in vitro* expression of proteins the residence times of microfluidic droplets have to be extended to a range from hours to days [443]. The simplest method for increasing the residence times seems to be an increase in channel length. Unfortunately, delay channels lead to a proportional increase in back-pressure and disruption in droplet formation. Several alternative methods have been developed in order to slow down, park, or trap the droplets on the microfluidic device. Specific geometrical features of the microfluidic device, such as integrated reservoirs [458], sections of channels with slightly higher aspect ratios leading to a minimization of the droplet surface tension (becoming more spherical) [402], or an array of round chambers connected by narrow constrictions [450], enable the trapping and storage of microdroplets. In

the latter device, droplets squeeze through the constrictions under flow conditions. In the absence of flow, surface tension drives the droplets to their lowest energy shape and ensures a single droplet per chamber. An increase in the carrier flow rate recovers the droplets.

In order to separate active or reactive droplets from the rest of the droplets a droplet sorting setup should be integrated into the microfluidic device. Therefore, electric fields have been used to deflect droplets by dielectrophoresis into a separate channel, while non-deflected droplets travel along the path of least hydrodynamic resistance [210]. In an alternative approach, surface acoustic wave devices have also been embedded in microfluidic devices and are capable of moving droplets by locally compressing fluids at high frequencies (about 150 MHz) [255]. Magnetic fields to manipulate droplets loaded with magnetic particles [260] and laser-induced localized heating have been used to sort droplets as well [237]. The sorting criterion of the droplets is the fluorescence light emitted from the droplet. The signal obtained from the emitted fluorescence can be used to trigger sorting of the droplets, which is similar to flow cytometry. Baret *et al* realized such a fluorescence-activated cell sorting (FACS) setup to isolate encapsulated mutant *E. coli* bacteria based on their enzymatic activity [214].

7.2.2. High resolution imaging in microdroplets: encapsulating, manipulating, and squeezing of fibrin networks. A specific droplet based microfluidics platform has been used to study the real-time assembly of three-dimensional protein networks and analyze the mechanical properties of the networks [459]. The in detail studied fibrin networks are initially catalyzed by the presence of thrombin, which selectively cleaves fibrinopeptides located in the central domain of fibrinogen, and form via the assembly of subunits of fibrinogen. Fibrin networks are not only involved in hemostasis or healing of injured blood vessels via blood clotting but also show remarkable elastic behavior, e.g., the high elastic modulus increases with increasing strain (i.e. strain-stiffen) [460, 461]. In contrast to a high-throughput approach to determine drug dosages based on blood clotting times in droplets [462], utilizing this microfluidics platform rather focuses on details of the network formation within a droplet and elucidates the influence of the microflow and confinement on the protein network by means of high resolution microscopy.

This has been achieved using tailored microfluidic devices, containing sites for droplet formation, electrocoalescence, *in situ* observation, and mechanical manipulation of the fibrin networks. The formation of fibrin was initiated in a droplet by coalescing two droplets, one with the fibrinogen monomer and the other containing the enzyme thrombin. The development of fibrin fibers within the resulting droplet required time for activation and fibril growth, and eventually neighboring fibers interacted to form a three-dimensional network. These isotropic networks were then driven through repeated geometric confinements to study the elasticity of the networks. The incorporation of geometric structures into the microchannels enables the controlled mechanical deformation and relaxation of individual droplets containing

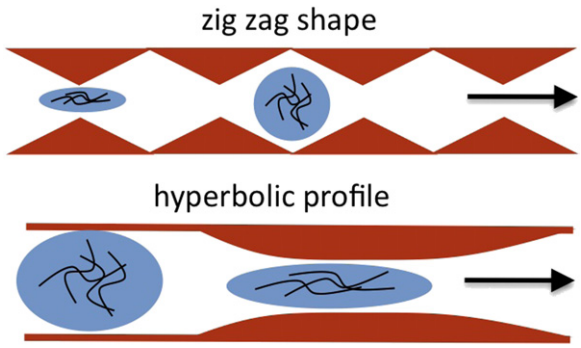

Figure 32. Schematic representation of geometric microchannel designs probing the elastic properties of protein networks encapsulated in droplets: zigzag shape for periodic deformation and relaxation, hyperbolic profile for constant acceleration at the center line of the droplet.

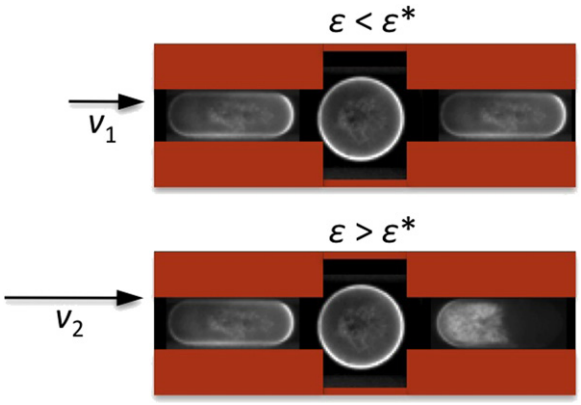

Figure 33. Protein networks are driven through repeated geometric confinements to study the elasticity of the networks (collage). Above a critical rate of deformation ϵ^* a densification of the fibrin network can be observed. Fibrin-rich and fibrin-poor regions appear within the droplet.

fibrin networks, cf figure 32. Analysis of the fibrin networks at low rates of deformation, which can be controlled by the dimension of the geometric constraints and the flow velocity, has not shown any evidence of inelastic deformations, despite undergoing repeated cycles of compression. However, a critical rate of deformation ϵ^* has been identified, above which fibrin-rich and fibrin-poor regions appear within the droplet, cf figure 33. In this case, the densification of fibrin into a dense pellet within the droplet occurs as a result of surpassing a critical hydrodynamic force on the network. From an analysis of this densification behavior the Young's modulus of the network can be estimated.

In a next step, extending experiments of micro-focused small angle x-ray scattering and diffraction in combination with microfluidics [463–465] to droplet based microfluidic systems will not only allow for studies of biomolecular reactions with reaction times in the range of minutes to days but also to study the influence of hydrodynamic flow, shear, and mechanical deformations on soft materials on the nano- and mesoscale.

8. Conclusions

Droplet based microfluidics has rapidly emerged as a versatile tool with a large spectrum of applications, while at the

same time it provides a table top platform for investigating problems of fundamental interest. In particular, the advances in the integration of tools to create, analyze, and manipulate droplets have made microfluidic devices increasingly flexible. Here, a large variety of methods for specific applications are available ranging from droplet sorting by electrophoretic or thermocapillary forces, to targeted droplet fusion induced by laser pulses.

Not only have technical applications such as the production of specific materials been the focus of microfluidic applications but also important physical questions of fluid dynamics at small length scales, soft matter physics, chemistry, and biology have been recently addressed in microfluidic experiments. Although governed by the linear Stokes equations, the dynamics of droplets in microfluidic systems may display non-linear behavior. Hydrodynamic interactions and confinement lead to interesting phenomena such as shock waves and intermittent flows. The deformation of droplets in complex flow geometries can be utilized to probe mechanical properties of soft and biological materials. Controlling the deformation of droplets has also raised questions linked to the fundamental mechanisms governing the coalescence of fluid interfaces. The increased ability to manipulate and analyze biochemical processes in isolated droplets naturally leads to the design of larger artificial biomimetic systems. A natural first step in this direction is to generate aqueous compartments separated by lipid bilayers similar to cellular networks in biology [498, 500–502]. Spontaneously formed lipid bilayers in high volume fraction droplet packings provide a promising approach to creating reconfigurable artificial networks [302, 499], or even complex self-assembled soft functional devices [503].

References

[1] Weibel D B and Whitesides G M 2006 Applications of microfluidics in chemical biology *Curr. Opin. Chem. Biol.* **10** 584–91

[2] Haeberle S and Zengerle R 2007 Microfluidic platforms for lab-on-a-chip applications *Lab Chip* **7** 1094–110

[3] Madou M, Zoval J, Jia G, Kido H, Kim J and Kim N 2006 Lab on a CD *Annu. Rev. Biomed. Eng.* **8** 601–28

[4] Squires T M and Quake S R 2005 Microfluidics: fluid physics at the nanoliter scale *Rev. Mod. Phys.* **77** 977–1025

[5] Tabeling P 2009 A brief introduction to slippage, droplets and mixing in microfluidic systems *Lab Chip* **9** 2428–36

[6] Tabeling P 2010 Investigating slippage, droplet breakup, and synthesizing microcapsules in microfluidic systems *Phys. Fluids* **22** 021302

[7] Ajdari A, Bontoux N and Stone H A 2006 *Anal. Chem.* **78** 387–92

[8] Ottino J M 1990 Mixing, chaotic advection, and turbulence *Annu. Rev. Fluid Mech.* **22** 207–53

[9] Mensinger H, Richter T, Hessel V, Döpper J and Ehrfeld W 1995 Microreactor with integrated static mixer and analysis system *Proc. Micro Analysis Systems 94* (*Enschede, The Netherlands, 21–22 November*) pp 237–43

[10] Branebjerg J, Gravesen P, Krog J P and Nielsen C R 1996 Fast mixing by lamination *Proc. IEEE Micro Electro Mechanical Systems 96* (*San Diego, CA, 11–15 February*) pp 441–6

[11] Evans J, Liepmann D and Pisano A P 1997 Planar laminar mixer *Proc. IEEE Micro Electro Mechanical Systems 97* (*Nagoya, Japan, 26–30 January*) pp 96–101

[12] Miyake R, Tsuzuki K, Takagi T and Imai K 1997 A highly sensitive and small flow-type chemical analysis system with integrated absorptiometric micro-flowcell *Proc. IEEE Micro Electro Mechanical Systems 97* (*Nagoya, Japan, 26–30 January*) pp 102–7

[13] Fujii T, Hosokawa K, Shoji S, Yotsumoto A, Nojima T and Endo I 1998 Development of a microfabricated biochemical workbench—improving the mixing efficiency *Proc. Micro Analysis Systems 98* (*Banff, Canada, 13–16 October*) pp 173-6

[14] Manz A, Bessoth F and Kopp M U 1998 Continuous flow versus batch process—a few examples *Proc. Micro Analysis Systems 98* (*Banff, Canada, 13–16 October*) pp 235–40

[15] Stroock, A D, Dertinger S K W, Ajdari A, Mezić I, Stone H A and Whitesides G M 2002 Chaotic mixer for microchannels *Science* **295** 647–51

[16] Aref H 2002 The development of chaotic advection *Phys. Fluids* **14** 1315–25

[17] Jen C P, Wu C Y, Lin Y C and Wu C Y 2003 Design and simulation of the micromixer with chaotic advection in twisted microchannels *Lab Chip* **3** 77–81

[18] Wiggins S and Ottino J M 2004 Foundations of chaotic mixing *Phil. Trans. R. Soc. Lond.* A **362** 937–70

[19] Liu Ying Zheng, Kim B J and Sung H J 2004 Two-fluid mixing in a microchannel *Int. J. Heat Fluid Flow* **25** 986–95

[20] Jiang F, Dress K S, Hardt S, Kupper M and Schonfeld F 2004 Helical flows and chaotic mixing in curved micro channels *AIChE J.* **50** 2297–305

[21] Kim D S, Lee S W, Kwon T H and Lee S S 2004 A barrier embedded chaotic micromixer *J. Micromech. Microeng.* **14** 798–805

[22] Nguyen N T and Wu Z 2005 Micromixers—a review *J. Micromech. Microeng.* **15** R1–R16

[23] Hessel V, Lowe H and Schonfeld F 2005 Micromixers—a review on passive and active mixing principles *Chem. Eng. Sci.* **60** 2479–501

[24] Hardt S, Drese K S, Hessel V and Schönfeld F 2005 Passive micromixers for applications in the microreactor and μTAS fields *Microfluid. Nanofluid.* **1** 108–18

[25] Kim D S, Lee S H, Kwon T H and Ahn C H 2005 A serpentine laminating micromixer combining splitting/recombination and advection *Lab Chip* **5** 739–47

[26] Chang C C and Yang R J 2007 Electrokinetic mixing in microfluidic systems *Microfluid. Nanofluid.* **3** 501–25

[27] Khan S A, Günther A, Schmidt M A and Jensen K F 2004 Microfluidic synthesis of colloidal silica *Langmuir* **20** 8604–11

[28] Trachsel F, Günther A, Khan S and Jensen K F 2005 Measurement of residence time distribution in microfluidic systems *Chem. Eng. Sci.* **60** 5729–37

[29] Khan S A and Jensen K F 2007 Microfluidic synthesis of titania shells on colloidal silica *Adv. Matter.* **19** 2556–60

[30] Axel G and Jensen K F 2006 Multiphase microfluidics: from flow characteristics to chemical and materials synthesis *Lab Chip* **6** 1487–503

[31] El-Ali J, Gaude S, Günther A, Sorge P K and Jensen K F 2005 Cell stimulus and lysis in a microfluidic device with segmented gas–liquid flow *Anal. Chem.* **77** 3629–36

[32] Sahoo R, Kralj J G and Jensen K F 2007 Multistep continuous-flow microchemical synthesis involving multiple reactions and separations *Angew. Chem. Int. Edn Engl.* **46** 5704–8

[33] Hartman R I, Sahoo H R, Yen B C and Jensen K F 2009 Distillation in microchemical systems using capillary forces and segmented flow *Lab Chip* **9** 1843–9

[34] Wang M, Roman G T, Perry M L and Kennedy R T 2009 Microfluidic chip for high efficiency electrophoretic analysis of segmented flow from a microdialysis probe and *in vivo* chemical monitoring *Anal. Chem.* **81** 9072–8

[35] Hartman R L, Naber J R, Buchwald S L and Jensen K F 2010 Multistep microchemical synthesis enabled by microfluidic distillation *Angew. Chem. Int. Edn Engl.* **49** 899–903

[36] Hartman R L and Jensen K F 2009 Microchemical systems for continuous-flow synthesis *Lab Chip* **9** 2495–507

[37] Günther A, Khan S A, Thalmann M, Trachsel F and Jensen K F 2004 Transport and reaction in microscale segmented gas–liquid flow *Lab Chip* **4** 278–86

[38] Günther A, Jhunjhunwala M, Thalmann M, Schmidt M A and Jensen K F 2005 Micromixing of miscible liquids in segmented gas-liquid flow *Langmuir* **21** 1547–55

[39] Fries D M, Waelchli S and von Rohr P R 2008 Gas-liquid two-phase flow in meandering microchannels *Chem. Eng. J.* **135S** 37–45

[40] Kreutzer M T, Günther A and Jensen K F 2008 Sample dispersion for segmented flow in microchannels with rectangular cross section *Anal. Chem.* **80** 1558–67

[41] Fries D M and von Rohr P R 2009 Liquid mixing in gas–liquid two-phase flow by meandering microchannels *Chem. Eng. Sci.* **64** 1326–35

[42] Kralj J G, Sahoo H R and Jensen K F 2007 Integrated continuous microfluidic liquid–liquid extraction *Lab Chip* **7** 256–63

[43] Niu X Z, Zhang B, Marszalek R T, Ces O, Edel J B, Klug D R and deMello A J 2009 Droplet-based compartmentalization of chemically separated components in two-dimensional separations *Chem. Commun.* **41** 6159–61

[44] Marre S and Jensen K F 2010 Synthesis of micro and nanostructures in microstructures in microfluidic systems *Chem. Soc. Rev.* **39** 1183–202

[45] Henkel T, Bermig T, Kielpinski M, Grodrian A, Metze J and Köhler M 2004 Chip modules for generation and manipulation of fluid segments for micro serial flow processes *Chem. Eng. J.* **101** 439–45

[46] Quake S R and Scherer A 2000 From micro- to nanofabrication with soft materials *Science* **290** 1536–9

[47] Sia S K and Whitesides G M 2003 Microfluidic devices fabricated in poly(dimethylsiloxane) for biological studies *Electrophoresis* **24** 3563–76

[48] Weibel D B, Diluzio W R and Whitesides G M 2007 Microfabrication meets microbiology *Nature Rev.* **5** 209–18

[49] Ziaie B, Baldi A, Lei M, Gu Y and Siegel R A 2004 Hard and soft micromachining for BioMEMS: review of techniques and examples of applications in microfluidics and drug delivery *Adv. Drug Deliv. Rev.* **56** 145–72

[50] Abgrall P and Gu A M 2007 Lab-on-chip technologies: making a microfluidic network and coupling it into a complete microsystem—a review *J. Micromech. Microeng.* **18** R15–R49

[51] Mijatovic D, Eijkel J C T and van den Berg A 2005 Technologies for nanofluidic systems: top-down vs. bottom-up—a review *Lab Chip* **5** 492–500

[52] Heckele M and Schomburg W K 2004 Review on micro molding of thermoplastic polymers *J. Micromech. Microeng.* **14** R1–R14

[53] Delamarche E, Bernard A, Schimd H, Michel B and Biebuyck H 1997 Patterned delivery of immunoglobulins to surfaces using microfluidic networks *Science* **276** 779–81

[54] Effenhauser C S, Bruin G J M, Paulus A and Ehrat M 1997 Integrated chip-based capillary electrophoresis *Anal. Chem.* **69** 3451–7

[55] Duffy D C, McDonald J C, Schueller O J A and Whitesides G M 1998 Rapid prototyping of microfluidic systems in poly(dimethylsiloxane) *Anal. Chem.* **70** 4974–84

[56] Bohl B, Steger R, Zengerle R and Koltay P 2005 Multi-layer SU-8 lift-off technology for microfluidic devices *J. Micromech. Microeng.* **15** 1125–30

[57] Jia Y, Jiang J, Ma X, Li Y, Huang H, Cai H, Cai S and Wu Y 2008 PDMS microchannel fabrication technique based on microwire-molding *Chin. Sci. Bull.* **53** 3928–36

[58] Easly C J, Benninger R K P, Shaver J H, Head W S and Piston D W 2009 Rapid and inexpensive fabrication of polymer microfluidic devices via toner transfer masking *Lab Chip* **9** 1119–27

[59] Chae S K, Lee C H, Lee S H, Kim T S and Kang J Y 2009 Oil droplet generation in PDMS microchannel using an amphiphilic continuous phase *Lab Chip* **9** 1957–61

[60] Barbier V, Tatoulian M, Li H, Arefi-Khonsari F, Ajdari A and Tabeling P 2006 Stable modification of PDMS surface properties by plasma polymerization: application to the formation of double emulsions in microfluidic systems *Langmuir* **22** 5230–2

[61] Bauer W A C, Fischlechner M, Abell C and Huck W T S 2010 Dydrophilic PDMS microchannels for high-throughput formation of oil-in-water microdroplets and water-in-oil-in-water double emulsions *Lab Chip* **10** 1814–19

[62] Lee M, Park W, Chung C, Lim J, Kwon S, Ahn K H, Lee S J and Char K 2010 Multilayer deposition on patterned posts using alternating polyelectrolyte droplets in a microfluidic device *Lab Chip* **10** 1160–6

[63] Gervais T, El-Ali J, Günther A and Jensen K F 2006 Flow-induced deformation of shallow microfluidic channels *Lab Chip* **6** 500–7

[64] McDonald J C, Duffy D C, Anderson J R, Chiu D T, Wu H, Schueller O J A and Whitesides G M 2000 Fabrication of microfluidic systems in poly(dimethylsiloxane) *Electrophoresis* **21** 27–40

[65] McDonald J C and Whitesides G M 2002 Poly(dimethylsiloxane) as a material for fabricating microfluidic devices *Acc. Chem. Res.* **35** 491–9

[66] Lee J N, Park C and Whitesides G M 2003 Solvent compatibility of poly(dimethylsiloxane)-based microfluidic devices *Anal. Chem.* **75** 6544–54

[67] Cygan Z T, Cabral J T, Beers K L and Amis E J 2005 Microfluidic platform for the generation of organic-phase microreactors *Langmuir* **21** 3629–34

[68] Abate A R, Lee D, Do T, Holtze C and Weitz D A 2008 Glass coating for PDMS microfluidic channels by sol–gel methods *Lab Chip* **8** 516–18

[69] Abate A R, Krummel A T, Lee D, Marquez M, Holze C and Weitz D A 2008 Photoreactive coating for high-contrast spatial patterning of microfluidic device wettability *Lab Chip* **8** 2157–60

[70] Zhao B, Moore J S and Beebe D J 2001 Surface-directed liquid flow inside microchannels *Science* **291** 1023–6

[71] Fiddes L K, Raz N, Srigunapalan S, Tumarkan E, Simmons C A, Wheeler A R and Kumacheva E 2010 A circular cross-section PDMS microfluidics system for replication of cardiovascular flow conditions *Biomaterials* **31** 3459–64

[72] Bartolo D, Degré G, Nghe P and Studer V 2008 Microfluidic stickers *Lab Chip* **8** 274–9

[73] Hung L H, Lin R and Lee A P 2008 Rapid microfabrication of solvent-resistant biocompatible microfluidic devices *Lab Chip* **8** 983–7

[74] Gu H, Duits M H G and Mugele F 2010 A hybrid microfluidic chip with electrowetting functionality using ultraviolet (UV)-curable polymer *Lab Chip* **10** 1550–6
[75] Leech P W, Wu N and Zhu Y 2009 Application of dry films resists in the fabrication of microfluidic chips for droplet generation *J. Micromech. Microeng.* **19** 065019
[76] Tsao C W and DeVoe D L 2009 Bonding of thermoplastic polymer microfluidics *Microfluid. Nanofluid.* **6** 1–16
[77] Greener J, Li W, Ren J, Voicu D, Pakharenko V, Tang T and Kumacheva E 2010 Rapid, cost-efficient fabrication of microfluidic reactors in thermoplastic polymers by combining photolithography and hot embossing *Lab Chip* **10** 522–4
[78] Holtze S *et al* 2008 Biocompatible surfactants for water-in-fluorocarbon emulsions *Lab Chip* **10** 1632–9
[79] Nie Z, Park J, Li W, Bon S A F and Kumacheva E 2008 An 'Inside-Out' microfluidic approach to monodisperse emulsions stabilized by solid particles *J. Am. Chem. Soc.* **130** 16508–9
[80] Subramaniam A B, Abkarian M and Stone H A 2005 Controlled assembly of jammed colloidal shells on fluid droplets *Nature Mater.* **4** 553–6
[81] Park J, Nie Z, Kumachev A, Abdelrahman A I, Binks B P, Stone H A and Kumacheva E 2009 A microfluidic approach to chemically driven assembly of colloidal particles at gas–liquid interfaces *Angew. Chem. Int. Edn Engl.* **48** 5300–4
[82] Muschiolik 2007 Multiple emulsions for food use *Curr. Opin. Colloid. Interface Sci.* **12** 213–20
[83] Bibette J 1991 Depletion interactions and fractionated crystallization for polydisperse emulsion purification *J. Colloid. Interface Sci.* **147** 474–8
[84] Mason T G and Bibette J 1996 Emulsification in viscoelastic media *Phys. Rev. Lett.* **77** 3481–4
[85] Liu H, Nakajima M and Kimura T 2004 Production of monodispersed water-in-oil emulsions using polymer microchannels *J. Am. Oil Chem. Soc.* **81** 705–11
[86] Sugiura S, Nakajima M, Iwamoto S and Seki M 2001 Interfacial tension driven monodispersed droplet formation from microfabricated channel array *Langmuir* **17** 5562–6
[87] Kobayashi I, Uemura K and Nakajima M 2006 Controlled generation of monodisperse discoid droplets using microchannel arrays *Langmuir* **22** 10893–7
[88] Kobayashi I, Neves M A, Yokota T, Uemura K and Nakajima M 2009 Generation of geometrically confined droplets using microchannel arrays effects of channel and step structure *Ind. Eng. Chem. Res.* **48** 8848–55
[89] Kobayashi I, Wada Y, Uemura K and Nakajima M 2010 Microchannel emulsification for mass production of uniform fine droplets: integration of microchannel arrays on a chip *Microfluid. Nanofluid.* **8** 255–2
[90] Kobayashi I, Mukataka S and Nakajima M 2005 Novel asymmetric through-hole array microfabricated on a silicon plate for formulating monodisperse emulsions *Langmuir* **21** 7629–32
[91] Kobayashi I, Takano T, Maeda R, Wada Y, Uemura K and Nakajima M 2008 Straight-through microchannel devices for generating monodisperse emulsion droplets several micrometers in size *Microfluid. Nanofluid.* **4** 167–77
[92] Vladisavljević G T, Kobayashi I and Nakajima M 2008 Generation of highly uniform droplets using asymmetric microchannels fabricated on a single crystal silicon plate: effect of emulsifier and oil types *Powder Technol.* **183** 37–45
[93] Xu S L J, Wang Y and Luo G 2009 Liquid–liquid two-phase flow in pore array microstructured devices for scaling-up of nanoparticle preparation *AIChE J.* **55** 3041–51
[94] Sato H, Matsumura H, Keino S and Shoji S 2006 An all SU-8 microfluidic chip with built-in 3D fine microstructures *J. Micromech. Microeng.* **16** 2318–22
[95] Thorsen T, Roberts R W, Arnold F H and Quake S R 2001 Depletion interactions and fractionated crystallization for polydisperse emulsion purification *Phys. Rev. Lett.* **86** 4163–66
[96] Song H, Tice J D and Ismagilov R F 2003 A microfluidic system for controlling reaction networks in time *Angew. Chem. Int. Edn Engl.* **42** 767–72
[97] Guillot P and Colin A 2005 Stability of parallel flows in a microchannel after a T junction *Phys. Rev.* E **72** 066301
[98] Xu J H, Li S W, Tan J and Luo G S 2008 Correlations of droplet formation in T-junction microfluidic devices: from squeezing to dripping *Microfluid. Nanofluid.* **5** 711–17
[99] Malsch D, Gleichmann N, Kielpinski M, Mayer G, Henkel T, Mueller D, van Steijn V, Kleijn C R and Kreutzer M T 2010 Dynamics of droplet formation at T-shaped nozzles with elastic feed lines *Microfluid. Nanofluid.* **8** 497–507
[100] Xu J H, Luo G S, Li S W and Chen G G 2006 Shear force induced monodisperse droplet formation in a microfluidic device by controlling wetting properties *Lab Chip* **6** 131–6
[101] Wang K, Lu Y C, Xu J H and Luo G S 2009 Determination of dynamic interfacial tension and its effect on droplet formation in the T-shaped microdispersion process *Langmuir* **25** 2153–8
[102] Steegmans M L J, Schroën K G P H and Boom R M 2009 Characterization of emulsification at flat microchannel Y junctions *Langmuir* **25** 3396–3401
[103] Xu J H, Li S W, Tan J, Wang Y J and Luo G S 2006 Preparation of highly monodisperse droplet in a T-junction microfluidic device *AIChE J.* **52** 3005–10
[104] Xu J H, LI S W, Tan J, Wang Y J and Luo G S 2006 Controllable preparation of monodisperse O/W and W/O emulsions in the same microfluidic device *Langmuir* **22** 7943–6
[105] Shui L, van den Berg A and Eijkel J C T 2009 Interfacial tension controlled W/O and O/W 2-phase flows in microchannel *Lab Chip* **9** 795–801
[106] Baret J C, Kleinschmidt F, El Harrak A and Griffiths A D 2009 Kinetic aspects of emulsion stabilization by surfactants: a microfluidic analysis *Langmuir* **25** 6088–93
[107] Zhao Y, Chen G and Yuan Q 2006 Liquid–liquid two-phase flow patterns in a rectangular microchannel *AIChE J.* **52** 4052–60
[108] Herrada M A, Ferrera C, Montanero J M and Gañan-Calvo A M 2010 Absolute lateral instability in capillary coflowing jets *Phys. Fluids* **22** 064104
[109] Ménétrier-Deremble L and Tabeling P 2006 Droplet breakup in microfluidic junctions of arbitrary angles *Phys. Rev.* E **74** 034303 (R)
[110] Abate A R, Poitzsch A, Hwang Y, Lee J, Czerwinska J and Weitz D A 2009 Impact of inlet channel geometry on microfluidic drop production *Phys. Rev.* E **80** 026310
[111] Garstecki P, Fuerstman, Stone H A and Whitesides G M 2006 Formation of droplets and bubbles in a microfluidic T-junction—scaling and mechanism of break-up *Lab Chip* **6** 437–46
[112] Jullien M C, Ching M J M M, Cohen C, Menetrier L and Tabeling P 2009 Droplet breakup in microfluidic T-junctions at small capillary numbers *Phys. Fluids* **21** 072001
[113] Christopher G F, Noharuddin N N, Taylor J A and Anna S L 2008 Experimental observations of the squeezing-to dripping transition in T-shaped microfluidic junctions *Phys. Rev.* E **78** 036317

[114] Wang K, Lu Y C, Tan J, Yang B D and Luo G S 2010 Generating gas/liquid/liquid three-phase microdispersed systems in double T-junctions microfluidic device *Microfluid. Nanofluid.* **8** 813–21
[115] Zeng Y, Novak R, Shuga J, Smith M T and Mathies R A 2010 High-performance single cell genetic analysis using microfluidic emulsion generator arrays *Anal. Chem.* **82** 3183–90
[116] Nisisako T and Torii T 2008 Microfluidic large-scale integration on a chip for mass production of monodisperse droplets and particles *Lab Chip* **8** 287–93
[117] Wang K L, Jones T B and Raisanen A 2009 DEP actuated nanoliter droplet dispensing using feedback control *Lab Chip* **9** 901–9
[118] Zheng B, Tice J D and Ismagilov R F 2004 Formation of droplets of alternating composition in microfluidic channels and applications to indexing of concentrations in droplet-based assays *Anal. Chem.* **76** 4977–82
[119] Woodward A, Cosgrove T, Espidel J, Jenkins P and Shaw N 2007 Monodisperse emulsions from a microfluidic device, characterised by diffusion NMR *Soft Matter* **3** 627–33
[120] Shui L, Mugele F, van den Berg A and Eijkel J C T 2008 Geometry-controlled droplet generation in head-on microfluidic devices *Appl. Phys. Lett.* **93** 153113
[121] GU H, Murade C U, Duits M H G and Mugele F 2011 A microfluidic platform for on-demand formation and merging of microdroplets using electric control *Biomicrofluidics* **5** 011101
[122] Shui L, van den Berg A and Eijkel J C T 2009 Capillary instability, squeezing, and shearing in head-on microfluidic devices *J. Appl. Phys.* **106** 124305
[123] Lin Y H, Lee C H and Lee G B 2008 Droplet formation utilizing controllable moving-wall structures for double-emulsion applications *J. Microelectromech. Syst.* **17** 573–81
[124] Wu H W, Huang Y C, Wu C L and Lee G B 2009 Exploitation of a microfluidic device capable of generating size-tunable droplets for gene delivery *Microfluid. Nanofluid.* **7** 45–56
[125] Choi J H, Lee S K, Lim J M, Yang S M and Yi G R 2010 Designed pneumatic valve actuators for controlled deoplet breakup and generation *Lab Chip* **10** 456–61
[126] Murshed S M S, Tan S H, Nguyen N T, Wong T N and Yobas L 2009 Microdroplet formation of water and nanofluids in heat-induced microfluidic T-junction *Microfluid. Nanofluid.* **6** 253–9
[127] Tice J D, Lyon A D and Ismagilov R F 2004 Effects of viscosity on droplet formation and mixing in microfluidic channels *Anal. Chim. Acta* **507** 73–7
[128] Lee W S, Jambovane S, Kim D and Hong J W 2009 Predictive model on micro droplet generation through mechanical cutting *Microfluid. Nanofluid.* **7** 431–8
[129] Churski K, Michalski J and Garstecki P 2010 Droplet on demand system utilizing a computer controlled microvalve integrated into a stiff polymeric microfluidic device *Lab Chip* **10** 512–18
[130] Barbier V, Willaime H, Tabeling P and Jousse F 2006 Producing droplets in parallel microfluidic systems *Phys. Rev.* E **74** 046306
[131] Hung L H, Choi K M, Tseng W Y, Tan Y C, Shea K J and Lee A P 2006 Alternating droplet generation and controlled dynamic droplet fusion in microfluidic device for CdS nanoparticle synthesis *Lab Chip* **6** 174–8
[132] Frenz L, Blouwolff J, Griffith A D and Baret J C 2008 Microfluidic production of droplet pairs *Langmuir* **24** 12073–6
[133] Hong J, Choi M, Edel J B and deMellow A 2010 Passive self-synchronized two-droplet generation *Lab Chip* **10** 2702–9
[134] Gañán-Calvo A M 1998 Generation of steady liquid microthreads and micron-sized monodisperse sprays in gas streams *Phys. Rev. Lett.* **80** 285–8
[135] Umbanhovar P B, Prasad V and Weitz D A 2000 Monodisperse emulsion generation via drop break off in a coflowing stream *Langmuir* **16** 347–51
[136] Anna S L, Bontoux N and Stone H A 2003 Formation of dispersions using 'flow focusing' in microchannels *Appl. Phys. Lett.* **82** 364–6
[137] Takeuchi S, Garsteck P, Weibel D B and Whitesides G M 2005 An axisymmetric flow-focusing microfluidic device *Adv. Matter.* **17** 1067–72
[138] Huang S H, Tan W H, Tseng F G and Takeuchi S 2006 A monolithically three-dimensional flow-focusing device for formation of single/double emulsions in closed/open microfluidic systems *J. Micromech. Microeng.* **16** 2336–44
[139] Collins J and Lee A P 2007 Control of serial microfluidic droplet size gradient by step-wise ramping of flow rates *Microfluid. Nanofluid.* **3** 19–25
[140] Ward T, Faivre M, Abkarian M and Stone H A 2005 Microfluidic flow focusing: drop size and scaling in pressure versus flow-rate-driven pumping *Electrophoresis* **26** 3716–24
[141] Utada A S, Fernandez-Nieves A, Stone H A and Weitz D A 2007 Dripping to jetting trasnsitions in coflowing liquid streams *Phys. Rev. Lett.* **99** 094502
[142] Cubaud T and Mason T G 2008 Capillary threads and viscous droplets in square microchannels *Phys. Fluids* **20** 053302
[143] Tan Y C, Cristini V and Lee A P 2006 Monodispersed microfluidic droplet generation by shear focusing microfluidic device *Sensors Actuators* B **114** 350–6
[144] Nie Z, Seo M, Xu S, Lewis P C, Mok M, Kumacheva E, Whitesides G M, Garstecki P and Stone H A 2008 Emulsification in a microfluidic flow-focusing device: effect of the viscosities of the liquids *Microfluid. Nanofluid.* **5** 585–94
[145] Li W, Nie Z, Zhang H, Paquet C, Seo M, Garstecki P and Kumacheva E 2007 Screening of the effect of surface energy of microchannels on microfluidic emulsification *Langmuir* **23** 8010–14
[146] Anna S L and Mayer H C 2006 Microscale tipstreaming in a microfluidic flow focusing device *Phys. Fluids* **18** 121512
[147] Lee W, Walker L M and Anna S L 2009 Role of geometry and fluid properties in droplet and thread formation processes in planar flow focusing *Phys. Fluids* **21** 032103
[148] He P, Barthès-Biesel D and Leclere E 2010 Flow of two immiscible liquids with low viscosity in Y shaped microfluidic systems: effect of geometry *Microfluid. Nanofluid.* **9** 293–301
[149] Yobas L, Martens S, Ong W L and Ranganathan N 2006 High-performance flow-focusing geometry for spontaneous generation of monodispersed droplets *Lab Chip* **6** 1073–9
[150] Ong W L, Hua J, Zhang B, Teo Y, Zhuo J, Nguyen N T, Ranganathan N and Yobs L 2007 Experimental and computational analysis of droplet formation in a high-performance flow-focusing geometry *Sensors Actuators* A **138** 203–12
[151] Wang W H, Zhang Z L, Xie Y N, Wang L, Yi S, Liu K, Liu J, Pang D W and Zhao X Z 2007 Flow-focusing generation of monodisperse water droplets wrapped by ionic liquid on microfluidic chips: from plug to sphere *Langmuir* **23** 11924–31
[152] Edmond W L, Young W K, Seo M, Nie Z, Garstecki P, Simmons C A and Kumacheva E 2008 Simultaneous generation of droplets with different dimensions in parallel integrated microfluidic droplet generators *Soft Matter* **4** 258–62

[153] Hashimoto M, Shevkoplyas S S, Zasoniska B, Szymborski T, Garstecki P and Whitesides G M 2008 *Small* **4** 1795–805
[154] Funfschilling D, Debas H, Li H Z and Mason T G 2009 Flow-field dynamics during droplet formation by dripping in hydrodynamic-focusing microfluidics *Phys. Rev.* E **80** 015301
[155] Hua J, Zhang R and Lou J 2007 Numerical simulation of microdroplet formation in coflowing immiscible liquids *AIChE J.* **53** 2534–48
[156] Harvie D J E, Davidson M R, Cooper-White J J and Rudman M 2006 A parametric study of droplet deformation through a microfluidic contraction: low viscosity Newtonian droplets *Chem. Eng. Sci.* **61** 5149–58
[157] Kim L S, Jeong H K, Ha M Y and Kim K C 2008 Numerical simulation of droplet formation in a micro-channel using the lattice Boltzmann method *J. Mech. Sci. Technol.* **22** 770–9
[158] Hsiung S K, Chen C T and Lee G B 2006 Micro-droplet formation utilizing microfluidic flow focusing and controllable moving-wall chopping techniques *J. Micromech. Microeng.* **16** 2403–10
[159] Lee C Y, Lin Y H and Lee G B 2009 A droplet-based microfluidic system capable of droplet formation and manipulation *Microfluid. Nanofluid.* **9** 599–610
[160] Abate A R, Romanowsky M B, Agresti J J and Weitz D A 2009 Valve-based flow focusing for drop formation *Appl. Phys. Lett.* **94** 023503
[161] Miller E, Rotea M and Rothstein J P 2010 Microfluidic device incorporating closed loop feedback control for uniform and tunable production of micro-droplets *Lab Chip* **10** 1293–301
[162] Bransky A, Korin N, Khoury M and Levenberg S 2009 A microfluidic droplet generator bases on a piezoelectric actuator *Lab Chip* **9** 516-520
[163] Tan S H, Murshed S M S, Nguyen N T, Wong T N and Yobas L 2008 Thermally controlled droplet formation in flow focusing geometry: formation regimes and effect of nanoparticle suspension *J. Phys. D: Appl. Phys.* **41** 165501
[164] Stan C A, Tang S K Y and Whitesides G M 2009 Independent control of drop size and velocity in microfluidic flow-focusing generators using variable temperature and flow rate *Anal. Chem.* **81** 2399–402
[165] Chan E M, Alivisators A P and Mathies R A 2005 High-temperature microfluidic synthesis of CdSe nanocrystals in nanoliter droplets *J. Am. Chem. Soc.* **127** 13854–61
[166] Priest C, Herminghaus S and Seemann R 2006 Generation of monodisperse gel emulsions in a microfluidic device *Appl. Phys. Lett.* **88** 024106
[167] Chokkalingam V, Herminghaus S and Seemann R 2008 Self-synchronizing pairwise production of monodisperse droplets by microfluidic step emulsification *Phys. Rev. Lett.* **93** 254101
[168] Saeki D, Sugiura S, Kanamori T, Sato S, Mukataka S and Ichikawa S 2008 Highly productive droplet formation by anisotropic elongation of a thread flow in a microchannel *Langmuir* **24** 13809–13
[169] Humphry K J, Ajdari A, Fernández-Nieves A, Stone H A and Weitz D A 2009 Supression of instabilities in multiphase flow by geometric confinement *Phys. Rev.* E **79** 056310
[170] Malloggi F, Pannacci N, Attia R, Monti F, Mary P, Willaime H and Tabeling P 2010 Monodisperse colloids synthesized with nanofluidic technology *Langmuir* **26** 2369–73
[171] van Dijke K, Veldhuis G, Schroën K and Boom R 2009 Parallelized edge-based droplet generation (EDGE) devices *Lab Chip* **9** 2824–30
[172] van Dijke K C, Veldhuis G, Schroën K and Boom R M 2010 Simultaneous formation of many droplets in a single microfluidic droplet formation unit *AIChE J.* **56** 833–6
[173] van Dijke K, de Ruiter R, Schroën and Boom R 2010 The mechanism of droplet formation in microfluidic EDGE systems *Soft Matter* **6** 321–30
[174] Chen C T and Lee G B 2006 Formation of microdroplets in liquids utilizing active pneumatic choppers on a microfluidic chip *J. Microelectromech. Syst.* **15** 1492–8
[175] Lai C W, Lin Y H and Lee G B 2008 A microfluidic chip for formation and collection of emulsion droplets utilizing active pneumatic micro-choppers and micro-switches *Biomed. Microdevices* **10** 749–56
[176] Wu L, Li G P, Xu W and Bachman M 2006 Droplet formation in microchannels under static conditions *Appl. Phys. Lett.* **89** 144106
[177] He M, Kuo J S and Chiu D T 2005 Electro-generation of single femtoliter- and picoliter-volume aqueous droplets in microfluidic systems *Appl. Phys. Lett.* **87** 031916
[178] He M, Kuo J S and Chiu D T 2006 Effects of ultrasmall orifices on the electrogeneration of femtoliter-volume aqueous droplets *Langmuir* **22** 6408–13
[179] Kim H, Luo D, Link D, Weitz D A, Marquez M and Cheng Z 2007 Controlled production of emulsion drops using an electric field in a flow-focusing microfluidic device *Appl. Phys. Lett.* **91** 133106
[180] Kim S J, Song Y A, Skipper P L and Han J 2006 Electrohydrodynamic generation and delivery of monodisperse picoliter droplets using a poly(dimethylsiloxane) microchip *Anal. Chem.* **78** 8011–19
[181] He P, Kim H, Luo D, Marquez M and Cheng Z 2010 Low-frequency ac electro-flow-focusing microfluidic emulsification *Appl. Phys. Lett.* **96** 174103
[182] Niu X, Zhang M, Wu J, Wen W and Sheng P 2009 Generation and manipulation of 'smart' droplets *Soft Matter* **5** 576–81
[183] Malloggi F, Vanapalli SA, Gu H, van den Ende D and Mugele F 2007 Electrowetting-controlled droplet generation in a microfluidic flow-focusing device *J. Phys.: Condens. Matter* **19** 1–7
[184] Baroud C N, Delville J P, Gallaire F and Wunenburger R 2007 Thermocapillary valve for droplet production and sorting *Phys. Rev.* E **75** 046302
[185] Christopher G F and Anna S L 2007 Microfluidic methods for generating continuous droplet streams *J. Phys. D: Appl. Phys.* **40** R319–R336
[186] Young T 1805 An essay on the cohesion of fluids *Phil. Trans. R. Soc. Lond.* **95** 65–7
[187] Tate T 1864 On the magnitude of a drop of liquid formed under different circumstances *Phil. Mag.* **27** 176–80
[188] Lord Rayleigh 1899 Investigations in capillarity: the size of drops. The liberation of gas from supersaturated solutions. Colliding jets. The tension of contaminated water-surfaces. A curious observation *Phil. Mag.* **48** 321–37
[189] Eggers J 1997 Nonlinear dynamics and breakup of free-surface flows *Rev. Mod. Phys.* **69** 865–929
[190] Lord Rayleigh 1879 On the stability, or instability, of certain fluids in motion *Proc. Lond. Math. Soc.* **10** 57–72
[191] Lord Rayleigh 1879 On the capillary phenomena of jets *Proc. R. Soc. Lond.* A **29** 71–9
[192] Tomotika S 1935 On the instability of a cylindrical threat of a viscous liquid liquid surrounded by another viscous fluid *Proc. R. Soc. Lond.* A **150** 322–37
[193] Guillot P, Colin A and Ajdari A 2008 Stability of a jet in confined pressure-driven biphasic flows at low Reynolds number in various geometries *Phys. Rev.* E **78** 016307
[194] Garstecki P, Gitlin I, DiLuzio W, Whitesides G M, Kumacheva E and Stone H A 2004 Formation of

monodisperse bubbles in a microfluidic flow-focusing device *Appl. Phys. Lett.* **85** 2649–51
[195] Tan J, Li S W, Wang K and Luo G S 2009 Gas-liquid flow in T-junction microfluidic devices with a new perpendicular rupturing flow route *Chem. Eng. J.* **146** 428–33
[196] Fu T, Funfschilling D, Ma Y and Li H Z 2010 Scaling the formation of slug bubbles in microfluidic flow-focusing devices *Microfluid. Nanofluid.* **8** 467–75
[197] Lindken R, Gui L and Merzkirch W 1999 Velocity measurements in multiphase flow by means of particle image velocimetry *Chem. Eng. Technol.* **22** 202–6
[198] Lindken R, Rossi M, Große S and Westerweed J 2009 Micro-particle image velocimetry (μPIV): recent developments, applications, and guidelines *Lab Chip* **9** 2551–67
[199] Xu J H, Li S W, Wang Y L and Luo G S 2006 Controllable gas–liquid phase flow patterns and monodisperse microbubbles in a microfluidic T-junction device *Appl. Phys. Lett.* **88** 133506
[200] Xu J H, Li S W, Chen G G and Luo G S *Bioeng. Natural Prod.* **52** 2254–9
[201] van Steijn V, Kreutzer M T and Kleijn C R 2007 μ-PIV study of the formation of segmented flow in microfluidic T-junctions *Chem. Eng. Sci.* **62** 7505–14
[202] Xiong R, Bai M and Chung J N 2007 Formation of bubbles in a simple co-flowing micro-channel *J. Micromech. Microeng.* **17** 1002–11
[203] Fu T, Ma Y, Funschilling D and Li H Z 2009 Bubble formation and breakup mechanism in a microfluidic flow-focusing device *Chem. Eng. Sci.* **64** 2392–400
[204] Dietrich N, Poncin S, Midoux N and Li H Z 2008 Bubble formation dynamics in various flow-focusing microdevices *Langmuir* **24** 13904–11
[205] Liu H and Zhang Y 2009 Droplet formation in a T-shaped microfluidic junction *J. Appl. Phys.* **106** 034906
[206] De Menech M, Garstecki P, Jousse F and Stone H A 2008 Transition from squeezing to dripping in a microfluidic T-shaped junction *J. Fluid. Mech.* **595** 141–61
[207] Sang L, Hong Y and Wang F 2009 Investigation of viscosity effect on droplet formation in T-shaped microchannels by numerical and analytical methods *Microfluid. Nanofluid.* **9** 621–35
[208] Gupta A, Murshed S M S and Kumar R 2009 Droplet formation and stability of flows in a microfluidic T-junction *Appl. Phys. Lett.* **94** 164107
[209] Gupta A and Kumar R 2010 Effect of geometry on droplet formation in the squeezing regime in a microfluidic T-junction *Microfluid. Nanofluid.* **8** 799–812
[210] Ahn K, Kerbage C, Hunt T P, Link D R and Weitz D A 2006 Dielectrophoretic manipulation of drops for high-speed microfluidic sorting devices *Appl. Phys. Lett.* **88** 024104
[211] Hunt T P, Issadore D and Westervelt R M 2008 Integrated circuit/microfluidic chip to programmably trap and move cells and droplets with dielectrophoresis *Lab Chip* **8** 81–7
[212] Fidalgo L M, Whyte G, Bratton D, Kaminski C F, Abell C and Huch W T S 2008 From microdroplets to microfluidics: selective emulsion separation in microfluidic devices *Angew. Chem. Int. Edn Engl.* **47** 2042–5
[213] Basu A S and Gianchandani Y B 2008 Virtual microfluidic traps, filters, channels and pumps using Marangoni flows *J. Micromech. Miroeng.* **18** 115031
[214] Baret J C *et al* 2009 Fluorescence-activated droplet sorting (FADS): efficient microfluidic cell sorting based on enzymatic activity *Lab Chip* **9** 1850–8
[215] Guo F, Ji X H, Liu K, He R X, Zhao L B, Guo Z X, Liu W, Guo S S and Zhao X Z 2010 Droplet electric separator microfluidic device for cell soring *Appl. Phys. Lett.* **96** 193701
[216] Selva B, Miralles V, Cantat I and Jullien M C 2010 Thermocapillary actuation by optimized resistor pattern: bubbles and droplets displacing, switching and trapping *Lab Chip* **10** 1835–40
[217] Chiou P Y, Ohta A T and Wu M 2005 Massively parallel manipulation of single cells, and microparticles using optical images *Nature* **436** 370–2
[218] Ohta A T, Chiou P Y, Han T H, Liao J C, Bhardwaj U McCabe E R B, Fuqu Y, Ren S and Wu M 2007 Dynamic cell and microparticle control via optoelectronic tweezers *J. Microelectromech. Syst.* **16** 491–500
[219] Park S Y, Kalim S, Callahan C, Teitell M A and Chiou E P Y 2009 A light-induced dielectrophoretic droplet manipulation platform *Lab Chip* **9** 3228–35
[220] Lee D H, Hwang H and Park J K 2009 Generation and manipulation of droplets in an optoelectrofluidic device integrated with microfluidic channels *Appl. Phys. Lett.* **95** 164102
[221] Ajaev V S and Homsy G M 2006 Modeling shapes and dynamics of confined bubbles *Annu. Rev. Fluid Mech.* **38** 277–307
[222] Nguyen N T, Wang C and Wong T N 2006 A silicon/glass-based microfluidic device for investigation of Lagrangian velocity field in microdroplets *J. Phys.: Conf. Ser.* **34** 130–5
[223] Santiago J G, Wereley S T, Meinhart C D, Beebe D J and Adrian R J 1998 A particle image velocimetry system for microfluidics *Exp. Fluids* **25** 316–9
[224] Meinhart C D, Wereley S T and Santiago J G 1999 PIV measurements of a microchannel flow *Exp. Fluids* **27** 414–9
[225] Stone S W, Meinhard C D and Wereley S T 2002 A microfluidic-based nanoscope *Exp. Fluids* **33** 613–9
[226] Devasenathipathy 2002 Particle tracking techniques for electrokinetic microchannel flows *Anal. Chem.* **74** 3704–13
[227] Sato Y, Irisawa G, Ishizuka M, Hishida K and Maeda M 2003 Visualization of convective mixing in microchannels by fluorescence imaging *Meas. Sci. Technol.* **14** 114–21
[228] Shinohara K, Sugii Y, Aota A, Hibara A, Tokeshi M, Kitamori T and Okamoto K 2004 High-speed micro-PIV measurements of transient flow in microfluidic devices *Meas. Sci. Technol.* **15** 1965–70
[229] Devasenathipathy S, Santiago J G, Wereley S T, Meinhart C D and Takehara K 2003 Particle imaging techniques for microfabricated fluidic systems *Exp. Fluids* **34** 504–14
[230] Lindken R, Westerweel J and Wieneke B 2006 Stereoscopic micro particle image velocimetry *Exp. Fluids* **41** 161–71
[231] Klank H, Goranović G, Kutter J P, Gjelstrup H, Michelsen J and Westergaard C H 2002 PIV measurements in a microfluidic 3D-sheathing structure with three-dimensional flow behaviour *J. Micromech. Microeng.* **12** 862–9
[232] Hung S H, Lin Y H and Lee G B 2010 A microfluidic platform for manipulation and separation of oil-in-water emulsion droplets using optically induced dieletrohoresis *J. Micromech. Microeng.* **20** 045026
[233] Delville J P, de Saint Vincent M R, Schroll R D, Chraïbi H, Issenmann B, Wunenburger R, Lasseux D, Zhang W W and Brasselet E 2009 Laser microfluidics: fluid actuation by light *J. Opt. A: Pure Appl. Opt.* **11** 034015
[234] Darhuber A A and Troian S M 2005 Principles of microfluidic actuation by modulation of surface stresses *Annu. Rev. Fluid Mech.* **37** 425–55
[235] Berge B, Konovalov O, Lajzerowicz J, Renault A, Rieu J P, Vallade M, Als-Nielsen J, Grübel G and Legrand J F 1994 Melting of short 1-alcohol monolayers on water: thermodynamics and x-ray scattering studies *Phys. Rev. Lett.* **73** 1652–5

[236] Sloutskin E, Bain C D, Ocko B M and Deutsch M 2005 Surface freezing of chain molecules at liquid–liquid and liquid–air interfaces *Faraday Discuss.* **129** 1–14
[237] Baroud C N, de Saint Vincent M R and Delville J P 2007 An optical toolbox for total control of droplet microfluidics *Lab Chip* **7** 1029–33
[238] Link D R, Anna S L, Weitz D A and Stone H A 2004 Geometrically mediated breakup of drops in microfluidic devices *Phys. Rev. Lett.* **92** 054503
[239] Surenjav E, Priest C, Herminghaus S and Seemann R 2009 Manipulation of gel emulsions by variable microchannel geometry *Lab Chip* **9** 325–30
[240] Surenjav E, Herminghaus S, Priest C and Seemann R 2009 Discrete microfluidics: reorganizing droplet arrays at a bend *Appl. Phys. Lett.* **95** 154104
[241] Hsieh A T H, Hori N, Massoudi R, Pan P J H, Sasaki H, Lin Y A and Lee A P 2009 Nonviral gene vector formation in monodispersed picolitre incubator for consistent gene delivery *Lab Chip* **9** 2638–43
[242] Leshansky A M and Pismen L M 2009 Breakup of drops in a microfluidic T junction *Phys. Fluids* **21** 023303
[243] Wang W, Yang C and Li C M 2009 On-demand microfluidic droplet trapping and fusion for on-chip static droplet assays *Lab Chip* **9** 1504–6
[244] Jung Y-M and Kang I S 2009 A novel actuation method of transporting droplets by using electrical charging of droplets in a dielectric fluid *Biomicrofluidics* **3** 022402
[245] Wang W W, Yang C, Liu Y S and Li C M 2010 On-demand droplet release for droplet-based microfluidic system *Lab Chip* **10** 559–62
[246] Tan Y C and Lee A P 2005 Microfluidic separation of satellite droplets as the basis of a monodispersed micron and submicron emulsification system *Lab Chip* **5** 1178–83
[247] Ting T H, Yap Y F, Nguyen N T, Wong T N and Chai J C K 2006 Thermally mediated breakup of drops in microchannels *Appl. Phys. Lett.* **89** 234101
[248] Tan Y C, Ho Y L and Lee A P 2008 Microfluidic sorting of droplets by size *Microfluid. Nanofluid.* **4** 343–8
[249] Mazutis L and Griffiths A D 2009 Preparation of monodisperse emulsions by hydrodynamic size fractionation *Appl. Phys. Lett.* **95** 204103
[250] Rhee M and Burns M A 2009 Microfluidic pneumatic logic circuits and digital pneumatic microprocessors for integrated microfluidic systems *Lab Chip* **9** 3131–43
[251] Abbyad P, Dangla R, Alexandrou A and Baroud C N 2011 Rails and anchors: guiding and trapping droplet microreactors in two dimensions *Lab Chip* **11** 813–21
[252] Ahn B, Lee K, Louge R and Oh K W 2009 Concurrent droplet charging and sorting by electrostatic actuation *Biomicrofluidics* **3** 044102
[253] Cordero M L, Burnham D R, Baroud C N and McGloin D 2008 Thermocapillary manipulation of droplets using holographic beam shaping: microfluidic pin ball *Appl. Phys. Lett.* **93** 034107
[254] Manneberg O, Hagsäter S M, Svennebring J, Hertz H M, Kutter J P, Bruus H and Wiklund M 2009 Spatial confinement of ultrasonic force fields in microfluidic channels *Ultrasonics* **49** 112–19
[255] Franke T, Abate A R, Weitz D A and Wixforth A 2009 Surface acoustic wave (SAW) directed droplet flow in microfluidics for PDMS devices *Lab Chip* **9** 2625–7
[256] Franke T, Braunmüller S, Schmid L, Wixforth A and Weitz D A 2010 Surface acoustic wave actuated cell sorting (SAWACS) *Lab Chip* **10** 789–94
[257] Wixforth A 2006 Acoustically driven programmable microfluidics for biological and chemical applications *J. Assoc. Lab. Autom.* **11** 399–405
[258] Yeo L Y and Friend J R 2009 Ultrafast microfluidics using surface acoustic waves 2009 *Biomicrofluidics* **3** 012002
[259] Beer N R, Rose K A and Kennedy I M 2009 Monodisperse droplet generation and rapid trapping for single molecule detection and reaction kinetics measurement *Lab Chip* **9** 841–4
[260] Zhang K, Liang Q, Ma S, Mu X, Hu P, Wang Y and Luo G 2009 On-chip manipulation of continuous picoliter-volume superparamagnetic droplets using a magnetic force *Lab Chip* **9** 2992–9
[261] Unger M A, Chou H P, Thorsen T, Scherer A and Quake S R 2000 Monolithic microfabricated valves and pumps by multilayer soft lithography *Science* **288** 113–6
[262] Thorsen T, Maerkl S J and Quake SR 2002 Microfluidic large-scale integration *Science* **298** 580–5
[263] Hutzler S, Weaire D, Elias F and Janiaud E 2002 Juggling with bubbles in cylindrical ferrofluid foams *Phil. Mag. Lett.* **82** 297–301
[264] Weaire D *et al* 2003 The fluid dynamics of foams *J. Phys.: Condens. Matter* **15** S65–S73
[265] Niu X Z, Zhang M Y, Peng S L, Wen W J and Sheng P 2007 Real-time detection, control, and sorting of microfluidic droplets *Biomicrofluidics* **1** 044101
[266] Luo C, Yang X, Fu Q, Sun M, Ouyang Q, Chen Y and Ji H 2007 Picoliter-volume aqueous droplets in oil: electrochemical detection and yeast cell electroporation *Electrophoresis* **27** 1977–83
[267] Srivastava N and Burns M A 2006 Electronic drop sensing in microfluidic devices: automated operation of a nanliter viscometer *Lab Chip* **6** 744–51
[268] Wang F and Burns M A 2010 Multiphase bioreaction microsystem with automated on-chip droplet operation *Lab Chip* **10** 1308–15
[269] Liu S, Gu Y, Le Roux R B, Matthews S M, Bratton D, Yunus K, Fisher A C and Huck W T 2008 The electrochemical detection of droplets in microfluidic devices *Lab Chip* **8** 1937–42
[270] Grad M, Tsai C C, Yu M, Kwong D L, Wong C W and Attinger D 2010 Transient sensing of liquid films in microfluidic channels with optofluidic microresonators *Meas. Sci. Technol.* **21** 075204
[271] Klingenberg D G, Van Swol F and Zukoski C F 1989 Dynamic simulations of electrorheological suspensions *J. Chem. Phys.* **91** 7888–95
[272] Tao R and Sun J M 1991 Three-dimensional structure of induced electrorheological solid *Phys. Rev. Lett.* **67** 398–401
[273] Hass K C 1993 Computer-simulations of nonequilibrium structure formation in electrorheological fluids *Phys. Rev.* E **47** 3362–73
[274] Davis L C 1992 Finite-element analysis of particle–particle forces in electrorheological fluids *Appl. Phys. Lett.* **60** 319–21
[275] Davis L C 1992 Polarization forces and conductivity effects in electrorheological fluids *J. Appl. Phys.* **72** 1334–40
[276] Ma H R, Wen W J, Tam W Y and Sheng P 1996 Frequency dependent electrorheological properties: origin and bounds *Phys. Rev. Lett.* **77** 2499–502
[277] Tam W Y, Yi G H, Wen W J, Ma H R, Loy M M T and Sheng P 1997 New electrorheological fluid: theory and experiment *Phys. Rev. Lett.* **78** 2987–90
[278] Chen T J, Zitter R N and Tao R 1992 Laser diffraction determination of the crystalline-structure of an electrorheological fluid *Phys. Rev. Lett.* **68** 2555–8
[279] Chen Y, Sprecher A E and Conrad H 1991 Electrostatic particle-particle interactions in electrorheological fluids *J. Appl. Phys.* **70** 6796–803

[280] Niu X Z, Liu L Y, Wen W J and Sheng P 2006 Hybrid approach to high-frequency microfluidic mixing *Phys. Rev. Lett.* **97** 044501
[281] Liu L Y, Chen X Q, Niu X Z, Wen W J and Sheng P 2006 Electrorheological fluid-actuated microfluidic pump *Appl. Phys. Lett.* **89** 083505
[282] Willaime H, Barbier W, Kloul L, Maine S and Tabeling P 2006 Arnold tongues in a microfluidic drop emitter *Phys. Rev. Lett.* **96** 054501
[283] Tan S H, Nguyen N T, Yobas L and Kang T G 2010 Formation and manipulation of ferrofluid droplets at a microfluidic T-junction *J. Micromech. Microeng.* **20** 045004
[284] Zhang M, Wu J, Niu X Z, Wen W and Sheng P 2008 Manipulation of microfluidic droplets using electrorheological carrier fluids *Phys. Rev.* E **78** 066305
[285] Prakash M and Gershenfeld N 2007 Microfluidic bubble logic *Science* **315** 832–5
[286] Fuerstman M J, Garstecki P and Whitesides G M 2007 Coding/decoding and reversibility of droplet trains in microfluidic networks *Science* **315** 828–32
[287] Zhang K, Gong X and Wen W 2009 Manipulation of microfluidic droplets by electrorheological fluid *Electrophoresis* **30** 3116–23
[288] Pittet N, Rivier N and Weaire D 1995 Cylindrical packings of foams cells *Forma* **10** 65–73
[289] Reinelt D, Boltenhagen P and Rivier N 2001 Deformed foam structure and transitions in a tube *Eur. Phys. J.* E **4** 299–304
[290] Hutzler S, Barry J, Grasland-Mongrain P, Smyth D and Weaire D 2009 Ordered packings of bubbles in columns of square cross-section *Colloids Surf.* A **344** 37–41
[291] Zhang HP and Makse 2005 Jamming transition in emulsions and granular materials *Phys. Rev.* E **72** 011301
[292] Vanapalli S A, Iacovella C R, Sung K E, Mukhija D, Millunchick J M, Burns M A, Glotzer S C and Solomon M J 2008 Fluidic assembly and packing of microspheres in confined channels *Langmuir* **24** 3661–70
[293] Shui L, Kooij E S, Wijnperle D, van den Berg A and Eijkel J C T 2009 Liquid crystallography: 3D microdroplet arrangements using microfluidics *Soft Matter* **5** 2708–12
[294] van der Net A, Drenckhan W, Weaire D and Hutzler S 2006 The crystal structure of bubbles in the wet foam limit *Soft Matter* **2** 129–34
[295] Mehrotra R, Jing N and Kameoka J 2008 Monodispersed polygonal water droplets in microchannel *Appl. Phys. Lett.* **92** 213109
[296] Bayley H, Cronin B, Heron A, Holden M A, Hwang W L, Syeda R, Thompson J and Mark Wallace M 2008 Droplet interface bilayers *Mol. BioSyst.* **4** 1191–208
[297] Hwang W L, Holden M A, White S and Bayley H 2007 Electrical behavior of droplet interface bilayer networks: experimental analysis and modeling *J. Am. Chem. Soc.* **129** 11854–64
[298] Holden A, Needham D and Bayley H 2007 Functional bionetworks from nanoliter water droplets *J. Am. Chem. Soc.* **129** 8650–55
[299] Maglia G, Heron A J, Hwang W L, Holden M A, Mikhailova E, Li Q, Cheley S and Bayley H 2009 Droplet networks with incorporated protein diodes show collective properties *Nature Nanotechnol.* **4** 437–40
[300] Funakoshi K, Suzuki H and Takeuchi S 2006 Lipid bilayer formation by contacting monolayers in a microfluidic device for membrane protein analysis *Anal. Chem.* **78** 8169–74
[301] Malmstadt N, Nash M A, Purnell R F and Schmidt J J 2006 Automated formation of lipid-bilayer membranes in a microfluidic device *Nano Lett.* **6** 1961–5
[302] Stanley C E, Elvira K S, Niu X Z, Gee A D, Ces O, Edel J B and deMello A J 2010 A microfluidic approach for high-throughput droplet interface bilayer (DIB) formation *Chem. Commun.* **46** 1620–22
[303] Thutupalli S, Seemann R and Herminghaus S 2011 Bilayer membranes in micro-fluidics: from gel emulsions to soft functional devices *Soft Matter* **7** 1312–20
[304] Cui B, Diamant H, Lin B and Rice S A 2004 Anomalous hydrodynamic interaction in a quasi-two-dimensional suspension *Phys. Rev. Lett.* **92** 258301
[305] Beatus T, Tlusty T and Bar-Ziv R 2006 Phonons in a one-dimensional microfluidic crystal *Nature Phys.* **2** 743–8
[306] Champagne N, Vasseur R, Montourcy A and Bartolo D 2010 Traffic jams and intermittent flows in microfluidic networks *Phys. Rev. Lett.* **105** 044502
[307] Beatus T, Bar-Ziv R and Tlusty T 2007 Anomalous microfluidic phonons induced by the interplay of hydrodynamic screening and incompressibility *Phys. Rev. Lett.* **99** 124502
[308] Beatus T, Tlusty T and Bar-Ziv R 2009 Burgers shock waves and sound in a 2D microfluidic droplets ensemble *Phys. Rev. Lett.* **103** 114502
[309] Hashimoto M, Garstecki P, Stone H A and Whitesides G M 2008 Interfacial instabilities in a microfluidic Hele–Shaw cell *Soft Matter* **4** 1403–13
[310] Tan Y C, Fisher J S, Lee A I, Cristini V and Phillip A 2004 Design of microfluidic channel geometries for the control of droplet volume, chemical concentration, and sorting *Lab Chip* **4** 292–8
[311] Tan Y C, Ho Y L and Lee A P 2007 Droplet coalescence by geometrically mediated flow in microfluidic channels *Microfluid. Nanofluid.* **3** 495–9
[312] Liu K, Ding H, Chen Y and Zhao X Z 2007 Droplet-based synthetic method using microflow focusing and droplet fusion *Microfluid. Nanofluid.* **3** 239–43
[313] Bremond N, Thiam A R and Bibette J 2008 Decompressing emulsion droplets favors coalescence *Phys. Rev. Lett.* **100** 024501
[314] Yoon Y, Baldessari F, Ceniceros H D and Leal L G 2007 Coalescence of two equali-sized deformable drops in an axisymmetric flow *Phys. Fluid* **19** 102102
[315] Manica R, Conner J N, Clasohm L Y, Carnie S L, Horn R G and Chan D Y C 2008 Transient responses of a wetting film to mechanical and electrical pertubations *Langmuir* **24** 1381–90
[316] Lai A, Bremond N and Stone H A 2009 Separation-driven coalescence of droplets: an anaytical criterion for the approach to contact *J. Fluid Mech.* **632** 97–107
[317] Chokkalingam V, Weidenhof B, Krämer M, Maier W F, Herminghaus S and Seemann R 2010 Optimized droplet-based microfluidics scheme for sol–gel reactions *Lab Chip* **10** 1700–5
[318] Chokkalingam V, Weidenhof B, Krämer M, Herminghaus S, Seemann R and Maier W F 2010 Template-free preparation of mesoporous silica spheres through optimized microfluidics *ChemPhysChem* **11** 2091–5
[319] Niu X, Gulati S, Edel J B and deMello A J 2008 *Lab Chip* **8** 1837–41
[320] Lin B C and Su C Y 2008 On-demand liquid-in-liquid droplet metering and fusion utilizing pneumatically actuated membrane valves *J. Micromech. Microeng.* **18** 115005
[321] Christopher G F, Bergstein J, End N B, Poon M, Nguyen C and Anna S L 2009 Coalescence and splitting of confined droplets at microfluidic junctions *Lab Chip* **9** 1102–9
[322] Um E and Park J K 2009 A microfluidic abacus channel for controlling the addition of droplets *Lab Chip* **9** 207–12
[323] Jin B J, Kim Y W and Lee Y 2010 Droplet merging in a straight microchannel using droplet size or viscosity difference *J. Micromech. Microeng.* **20** 035003

[324] Hong J, Choi M, deMello A J and Edel J B 2009 Interfacial tension-mediated droplet fusion in rectangular microchannels *Biochip J.* **3** 203–7
[325] Fidalgo L M, Abell C and Huck T S 2007 Surface-induced droplet fusion in microfluidic devices *Lab Chip* **7** 984–6
[326] Kusumaatmaja H and Yeomans J M 2007 Controlling drop size and polydispersity using chemically patterned surfaces *Langmuir* **23** 956–9
[327] Shestopalov I, Tice J D and Ismagilov R F 2004 Multi-step synthesis of nanoparticles performed on millisecond time scale in a microfluidic droplet-based system *Lab Chip* **4** 316–21
[328] Li Liang, Boedicker J Q and Ismagilov R F 2007 Using a multijunction microfluidic device to inject substrate into an array of preformed plugs without cross-contamination: comparing theory and experiments *Anal. Chem.* **79** 2756–61
[329] Sivasamy J, Chim Y C, Wong T N, Nguyen N T and Yobas L 2010 Reliable addition of reagents into microfluidic droplets *Microfluid. Nanofluid.* **8** 409–16
[330] Mazutis L, Baret J C and Griffiths A D 2009 A fast and efficient microfluidic system for highly selective one-to-one droplet fusion *Lab Chip* **9** 2665–72
[331] Lorenz R M, Edgar S, Jeffries G D M, Zhao Y, McGloin D and Chiu D T 2007 Vortex-trap-induced fusion of femtoliter-volume aqueous droplets *Anal. Chem.* **79** 224–8
[332] Zagnoni M and Cooper J M 2009 One-chip electrocoalescence of microdroplets as a function of voltage, frequency and droplet size *Lab Chip* **9** 2652–8
[333] Zagnoni M, Baroud C N and Cooper J M 2009 Electrically initiated upstream coalescence cascade of droplets in a microfluidic flow *Phys. Rev.* E **80** 046303
[334] Eow J S, Ghadiri M, Sharif A O and Williams T J 2001 Electrostatic enhancement of coalescence of water droplets in oil: a review of the current understanding *Chem. Eng. J* **84** 173–92
[335] Kralj J G, Schmidt M A and Jensen K F 2005 Surfactant-enhanced liquid–liquid extraction in microfluidic channels with inline electric-field enhanced coalescence *Lab Chip* **5** 531–5
[336] Chabert M, Dorfman K D and Viovy J L 2005 Droplet fusion by alternating current (ac) field electrocoalescence in microchannels *Electrophoresis* **26** 3706–15
[337] Tan W H and Takeuchi S 2006 Timing controllable electrofusion device for aqueous droplet-based microreactors *Lab Chip* **6** 757–63
[338] Ahn K, Agresti J, Chong H, Marquez M and Weitz D A 2006 Electrocoalescence of drops synchronized by size-dependent flow in microfluidic channels *Appl. Phys. Lett.* **88** 264105
[339] Thiam A R, Bremond N and Bibette J 2009 Breaking of an emulsion under an ac electric field *Phys. Rev. Lett.* **102** 188304
[340] Zagnoni M, Le Lain G and Cooper J M 2010 Electrocoalescence mechanisms of microdroplets using localized electric fields in microfluidic channels *Langmuir* **26** 14443–9
[341] Link D R, Grasland-Mongrain E, Duri A, Sarrazin F, Cheng Z, Cristobal G, Marquez M and Weitz D A 2006 Electric control of droplets in microfluidic devices *Angew. Chem. Int. Edn Engl.* **45** 2556–60
[342] Vrij A 1966 Possible mechanism for spontaneous rupture of thin free liquid films *Disc. Faraday Soc.* **42** 23–33
[343] Herminghaus S 1999 Dynamical instability of thin liquid films between conducting media *Phys. Rev. Lett.* **83** 2359–61
[344] Priest C, Herminghaus S and Seemann R 2006 Controlled electrocoalescence in microfluidics: targeting a single lamella *Appl. Phys. Lett.* **89** 134101
[345] Christopher G F and Anna S L 2009 Passive breakup of viscoelastic droplets and filament self-thinning at a microfluidic T-junction *J. Rheol.* **53** 663–83
[346] Cubaud T 2009 Deformation and breakup of high-viscosity droplets with symmetric microfluidic cross flows *Phys. Rev.* E **80** 026307
[347] Garstecki P, Fischbach M A and Whitesides G M 2005 Design for mixing using bubbles in branced microfluidic channels *Appl. Phys. Lett.* **86** 244108
[348] Garstecki P, Fuerstman M J, Fischbach M A, Sia S K and Whitesides G M 2006 Mixing with bubbles: a practical technology for use with portable microfluidic devices *Lab Chip* **6** 207–12
[349] Duda J L and Vrentas J S 1971 Steady flow in region of closed streamlines in a cylindrical cavity *J. Fluid Mech.* **45** 247–60
[350] Snyder L R and Adler H J 1976 Dispersion in segmented flow through glass tubing in continuous-flow analysis—ideal model *Anal. Chem.* **48** 1017–22
[351] Snyder L R and Adler H J 1976 Dispersion in segmented flow through glass tubing in continuous-flow analysis—nonideal model *Anal. Chem.* **48** 1022–7
[352] Anderson R C, Bogdan G J, Puski A and Su X 1998 Genetic analysis systems: improvements and methods *Proc. Micro Analysis Systems 98* (*Banff, Canada, 13–16 October*) pp 11–16
[353] Hosokawa K, Fujii T and Endo I 1999 Handling of picoliter liquid samples in a poly(dimethylsiloxane)-based microfluidic device *Anal. Chem.* **71** 4781–5
[354] Song H and Ismagilov R F 2003 Millisecond kinetics on a microfluidic chip using nanoliters of reagents *J. Am. Chem. Soc.* **125** 14613–9
[355] Liau A, Karnik R, Majumdar A and Cate J H D 2005 Mixing crowded biological solutions in milliseconds *Anal. Chem.* **77** 7618–25
[356] Song H, Bringer M R, Tice J D, Gerdts C J and Ismagilov R F 2003 Experimental test of scaling of mixing by chaotic advection in droplets moving through microfluidic channels *Appl. Phys. Lett.* **83** 4664–6
[357] Bringer M R, Gerdts C J, Song H, Tice J D and Ismagilov R F 2004 Microfluidic systems for chemical kinetics that rely on chaotic mixing in droplets *Phil. Trans. R. Soc. Lond.* A **362** 1087–104
[358] Sarrazin F, Prat L, Di Miceli N, Cristobal G, Link D R and Weitz D A 2007 Mixing characterization inside microdroplets engineered on a microcoalescer *Chem. Eng. Sci.* **62** 1042–8
[359] Tung K Y, Li C C and Yang J T 2009 Mixing and hydrodynamic analysis of a droplet in a planar serpentine micromixer *Microfluid. Nanofluid.* **7** 545–57
[360] Srisa-Art M, deMello A J and Edel J B 2008 Fluorescence lifetime imaging of mixing dynamics in continuous-flow microdroplet reactors *Phys. Rev. Lett.* **101** 014502
[361] Solvas X C, Srisa-Art M, deMello A j and Edel J B 2010 Mapping of fluidic mixing in microdroplets with 1+ μs time resolution using fluorescence lifetime imaging *Anal. Chem.* **82** 3950–6
[362] Sarrazin F, Loubière K, Prat L and Gourdon C 2006 Experimental and numerical study of droplets hydrodynamics in microchannels *AIChE J.* **52** 4061–70
[363] Rhee M and Burns M A 2008 Drop mixing in a microchannel for lab-on-a-chip platforms *Langmuir* **24** 590–601
[364] Malsch D, Kielpinski M, Merhan R, Albert J, Mayer G, Köhler J M, Süße H, Stahl M and Henkel T 2008 PIV-analysis of Taylor flow in micro channel *Chem. Eng. J.* **135** S166–S172
[365] Wang C, Nguyen N T and Wong T N 2007 Optical measurement of flow field and concentration field inside a moving nanoliter droplet *Sensors Actuators* A **133** 317–22

[366] Miessner U, Lindken R and Westerweel J 2008 3D-velocity measurements in microscopic two-phase flows by means of micro PIV *14th Int. Symp. on Applications of Laser Techniques to Fluid Mechanics* (*Lisbon, Portugal, 7–10 July 2008*) pp 1–11

[367] Kinoshita H, Kaneda S, Fujii T and Oshima M 2007 Three-dimensional measurement and visualization of internal flow of a moving droplet using confocal micro-PIV *Lab Chip* **7** 338–46

[368] Chabreyrie R, Vainchtein D, Chandre C, Singh P and Aubry N 2008 Tailored mixing inside a translating droplet *Phys. Rev.* E **77** 036314

[369] Chabreyrie R, Vainchtein D, Chandre C, Singh P and Aubry N 2009 Robustness of tuned mixing within a droplet for digital microfluidics *Mech. Res. Commun.* **36** 130–6

[370] Stone Z B and Stone H A 2005 Imaging and quantifying mixing in a model droplet micromixer *Phys. Fluids* **17** 063103

[371] Verguet S, Duan C, Liau A, Verk V, Cate J H, Majumdar A and Szeri A J 2010 Mechanics of liquid–liquid interfaces and mixing enhancement in microscale flows *J. Fluid Mech.* **62** 207–40

[372] Cordero M L, Rolfsnes H O, Burnham D R, Campbell P A, McGloin D and Baroud C N 2009 Mixing via thermocapillary generation of flow patterns inside a microfluidic drop *New J. Phys.* **11** 075033

[373] Roy T, Sinha A, Chakraborty S, Ganguly R and Puri I K 2009 Magnetic microsphere-based mixers for microdroplets *Phys. Fluids* **21** 027101

[374] Franke T, Schmid L, Weitz D A and Wixforth A 2009 Magneto-mechanical mixing and manipulation of picoliter volumes in vesicles *Lab Chip* **9** 2831–5

[375] Nisisako T, Torii T and Higuchi T 2004 Novel microreactors for functional polymer beads *Chem. Eng. J.* **101** 23–9

[376] Seo M, Nie Z, Xu S, Mok M, Lewis P C, Graham R and Kumacheva E 2005 Continuous microfluidic reactors for polymer particles *Langmuir* **21** 11614–22

[377] Zhang H, Tumarkin E, Sullan R M A, Walker G C and Kumacheva E 2007 Exploring microfluidic routes to microgels of biological polymers *Macromol. Rapid Commun.* **28** 527–38

[378] Jahn A, Reiner J E, Vreeland W N, DeVoe D L, Locascio L E and Baitan M 2008 Preparation of nanoparticles by continuous-flow microfluidics *J. Nanopart. Res.* **10** 925–34

[379] Song Y, Hormes J and Kumar C S S R 2008 Microfluidic synthesis of nanomaterials *Small* **8** 698–711

[380] Seo M, Nie Z, Xu S, Lewis P C and Kumacheva E 2005 Microfluidics: from dynamic lattices to periodic arrays of polymer discs *Langmuir* **21** 4773–5

[381] Teh S Y, Lin R, Hung L H and Lee A P 2008 Droplet microfluidics *Lab Chip* **8** 198–220

[382] Baroud CN, Gallaire F and Dangla R 2010 Dynamics of microfluidic droplets *Lab Chip* **10** 2032–45

[383] Griffiths A D and Tawfik D S 2006 Miniaturising the laboratory in emulsion droplets *Trends Biotechnol.* **24** 395–402

[384] Song H, Chen D L and Ismagilov R F 2006 Reactions in droplets in microfluidic channels *Angew. Chem. Int. Edn Engl.* **45** 7336–56

[385] Schaerli Y and Hollfelder F 2009 The potential of microfluidic water-in-oil droplets in experimental biology *Mol. BioSyst.* **51** 1392–404

[386] Theberge A B, Courtouis F, Schaerli Y, Fischlechner M, Abell C, Hollfelder F and Huck W T S 2010 Microdroplets in microfluidics: an evolving platform for discoveries in chemistry and biology *Angew. Chem. Int. Edn Engl.* **49** 2–25.

[387] Salieb-Beugelaar G B, Simone G, Arora A, Philippi A and Manz A 2010 Latest developments in microfluidic cell biology and analysis systems *Anal. Chem.* **82** 4848–64

[388] Arora A, Simone G, Salieb-Beugelaar B, Kim J T and Manz A 2010 Latest developments in micro total analysis systems *Anal. Chem.* **82** 4830–47

[389] Skurtys O and Aguilera J M 2008 Applications of microfluidic devices in food engineering *Food Biophys.* **3** 1–15

[390] Lewis P C, Graham R R, Nie Z, Xu S, Seo M and Kumacheva E 2005 Continuous synthesis of copolymer particles in microfluidic reactors *Macromolecules* **38** 4536–8

[391] Zourob M, Mohr S, Mayes A G, Macaskill A, Pérez-Moral N, Fielden P R and Goddard N J 2006 A micro-reactor for preparing uniform molecularly imprinted polymer beads *Lab Chip* **6** 296–301

[392] Barnes S E, Cygan Z T, Yates J K, Beers K I and Amis E J 2006 Raman spectroscopic monitoring of droplet polymerization in a microfluidic device *Analyst* **131** 1027–33

[393] Li W, Greener J, Voicu D and Kumacheva E 2009 Multiple modular microfluidic (M^3) reactors for the synthesis of polymer particles *Lab Chip* **9** 2715–21

[394] Nie Z, Li W, Seo M, Xu S and Kumacheva E 2006 Janus and ternary particles generated by microfluidic synthesis: design, synthesis, and self-assembly *J. Am. Chem. Soc.* **128** 9408–12

[395] Chen C H, Shah R K, Abate A R and Weitz D A 2009 Janus particles templated from double emulsion droplets generated using microfluidics *Langmuir* **25** 4320–3

[396] Shepherd R F, Conrad J C, Rhodes S K, Link D R, Marquez M, Weitz D A and Lewis J A 2006 Microfluidic assembly of homogeneous and Janus colloid-filled hydrogel granules *Langmuir* **22** 8618–22

[397] Nisisako T and Hatsuzawa T 2010 A microfluidic cross-flowing emulsion generator for producing biphasic droplets and anisotropically shaped polymer particles *Microfluid. Nanofluid.* **9** 427–37

[398] Shum H C, Kim J W and Weitz D A 2008 Microfluidic fabrication of monodisperse biocompatible and biodegradable polymersomes with controlled permeability *J. Am. Chem. Soc.* **130** 9543–9

[399] Winterton J D, Myers D R, Lippmann J M, Pisano A P and Doyle F M 2008 A novel continuous microfluidic reactor design for the controlled production of high-quality semiconductor nanocrystals *J. Nanopart. Res.* **10** 893–905

[400] Park J, Nie Z, Kumachev A and Kumacheva E 2010 A microfluidic route to small CO_2 microbubbles with narrow size distribution *Soft Matter* **6** 630–4

[401] He M, Sun C and Chiu D T 2004 Concentrating solutes and nanoparticles within individual aqueous microdroplets *Anal. Chem.* **76** 1222–7

[402] Shim J U, Cristobal G, Link D R, Torsen T, Jia Y, Piattelli K and Fraden S 2007 Control and measurement of the phase behavior of aqueous solutions using microfluidics *J. Am. Chem. Soc.* **129** 8825–35

[403] Shim J U, Cristobal G, Link D R, Thorsen T and Fraden S 2007 Using microfluidics to decouple nucleation and growth of protein crystals *Crystal Growth Des.* **70** 2192–4

[404] Mary P, Studer V and Tabeling P 2008 Microfluidic droplet-based liquid-liquid extraction *Anal. Chem.* **80** 2680–7

[405] Xu J H, Tan J, Li S W and Luo G S 2008 Enhancement of mass transfer performance of liquid–liquid system by droplet flow in microchannels *Chem. Eng. J.* **141** 242–9

[406] Courtois F, Olguin L F, Whyte G, Theberge A B, Huck W T S, Hollfelder F and Abell C 2009 Controlling

the retention of small molecules in emulsion microdroplets for use in cell-based assays *Anal. Chem.* **81** 3008–16
[407] Li L, Fu Q, Kors C A, Stewart L, Nollert P, Laible P D and Ismagilov R F 2010 A plug-based microfluidic system for dispensing lipidic cubic phase (LCP) material validated by crystallizing membrane proteins in lipidic mesophases *Microfluid. Nanofluid.* **8** 789–98
[408] Park J I, Tumarkin E and Kumacheva E 2010 Small, stable, and monodispersed bubbles encapsulated with biopolymers *Macromol. Rapid Commun.* **31** 222–7
[409] Dubinsky S, Zhang H, Nie Z, Gourevich I, Voicu D, Deetz M and Kumacheva E 2008 Microfluidic synthesis of macroporous copolymer particles *Macromolecules* **41** 3555–61
[410] Hu J, Zhao Y J, Li J, Xu W Y, Wen Z Y, Xu M and Gu Z Z 2009 Photonic crystal hydrogel beads used for multiplex biomolecular detection *Lab Chip* **19** 5730–6
[411] Kim S H, Shim J W, Lim J M, Lee S Y and Yang S M 2009 Microfluidic fabrication of microparticles with structural complexity using photocurable emulsion droplets *New J. Phys.* **11** 075014
[412] Wang B, Shum H C and Weitz D A 2009 Fabrication of monodisperse torpoidal particles by polymer solidification in microfluidics *Chem. Phys. Chem.* **10** 641–5
[413] Tan W H and Takeuchi S 2007 Monodisperse alginate hydrogel microbeads for cell encapsulation *Adv. Matter.* **19** 2696–701
[414] Yang W W, Lu Y C, Xiang Z Y and Luo G S 2007 Monodispersed microcapsules enclosing ionic liquid of 1-butyl-3-methylimidazolium hexafluorophosphate *Reactive Funct. Polym.* **67** 81–6
[415] Xu Q, Hashimoto M, Dang T T, Haare T, Kohane D A, Whitesides G M, Langer R and Anderson D G 2009 Preparation of monodisperse biodegradable polymer microparticles using a microfluidic flow-focusing device for controlled drug delivery *Small* **13** 1575–81
[416] Li S, Xu J, Wang Y and Luo G 2008 Controllable preparation of nanoparticles by drops and plugs flow in a microchannel device *Langmuir* **24** 4194-4199
[417] Tachibana M, Engel W, Panizza P, Deleuze H, Lecommandoux S, Ushiki H and Backov R 2008 Combining sol–gel chemistry and millifluidic toward engineering microporous silica ceramic final sizes and shapes: an integrative chemistry approach *Chem. Eng. Process.* **47** 1317–22
[418] Yang C H, Huang K S, Lin Y S, Lu K, Tzeng C C, Wang E C, Lin C H, Hsu W Y and Chang J Y 2009 Microfluidic assisted synthesis of multi-functional polycarprolactone microcapsules: incorporation of CdTe quantum dots, Fe_3O_4 superparamagnetic nanoparticles and tamoxifen anticancer drugs *Lab Chip* **9** 961–5
[419] Zhang H, Tumarkin E, Peerani R, Nie Z, Sullan R M A, Walker G C and Kumacheva E 2006 Microfluidic production of biopolymer microxcapsules with controlled morphology *J. Am. Chem. Soc.* **128** 12205–10
[420] Chu L Y, Kim J W, Shah R K and Weitz D A 2007 Monodisperse thermoresponsive microgels with tunable volume-phase transition kinetics *Adv. Funct. Matter* **17** 3499–504
[421] Shah R K, Kim J W, Agresti J J, Weitz D A and Chu L Y 2008 Fabrication of monodisperse thermosensitive microgels and gel capsules in microfluidic devices *Soft Matter* **4** 2303–9
[422] Hamlington B D, Steinhaus B, Feng J J, Links D, Shelley M J and Shen A Q 2007 Liquid crystal droplet production in a microfluidic device *Liq. Cryst.* **34** 861–70
[423] Shklyaev O E and Shen A Q 2009 Microfluidics enhanced control of the microstructure and flow of complex fluids *Mech. Res. Commun.* **36** 121–4
[424] Pries C, Quinn A, Postma A, Zelikin A N, Ralston J and Caruso F 2008 Microfluidic polymer multilayer adsorption on liquid crystal droplets for microcapsule synthesis *Lab Chip* **8** 2185–7
[425] Shah R K, Kim J W and Weitz D A 2010 Monodisperse stimuli-responsive colloidosomes by self-assembly of microgels in droplets *Langmuir* **26** 1561–5
[426] Xu J H, Li S W, Tostado C, Lan W J and Luo G S 2009 Preparation of monodispersed chitosan microspheres and *in situ* encapsulation of BSA in a co-axial microfluidic device *Biomed. Microdevices* **11** 243–9
[427] Duraiswamy S and Khan S A 2009 Droplet-based microfluidic synthesis of anisotropic metal nanocrystals *Small* **5** 2828–34
[428] Churski K, Korczyk P and Garstecki P 2010 High-throughput automated droplet microfluidic system for screening of reaction conditions *Lab Chip* **10** 816–18
[429] Günther P M, Müller F, Henkel T, Köhler J M and Groß G A 2005 Formation of monomeric and Novolak azo dyes in nanofluid segments by use of a double injector chip reactor *Chem. Eng. Technol.* **28** 520–7
[430] Poe S L, Cummings M A, Haaf M P and McQuade D T 2006 Solving the clogging problem: precipitate-forming reactions in flow *Angew. Chem. Int. Edn Engl.* **45** 1544–8
[431] Frenz L, Harrak A E, Pauly M, Bégin-Colin S, Griffiths D and Baret J C 2008 Droplet-based microreactors for the synthesis of magnetic iron oxide nanoparticles *Angew. Chem. Int. Edn Engl.* **47** 6817–20
[432] Hung L H, Teh S Y, Jester J and Lee A P 2010 PLGA micro/nanosphere synthesis by droplet microfluidic solvent evaporation and extraction approaches *Lab Chip* **10** 1820–5
[433] Park J H, Derfus A M, Segal E, Vecchio K S, Bhatita S N and Sailor M J 2006 Local heating of discrete droplets using magnetic porous silicon-based photonic crystals *J. Am. Chem. Soc.* **128** 7938–46.
[434] Issadore D, Humphry K J, Brown K A, Sandberg L, Weitz D A and Westervelt R M 2009 Microwave dielectric heating of drops in microfluidic devices *Lab Chip* **9** 1701–6
[435] Sgro A E, Allen P B and Chiu D T 2009 Thermoelectric manipulation of aqueous droplets in microfluidics devices *Anal. Chem.* **79** 4845–51
[436] Sgro A E and Chiu D T 2010 Droplet freezing, docking, and the exchange of immiscible phase and surfactant around frozen droplets *Lab Chip* **10** 1873–7
[437] Dendukuri D and Doyle P 2009 The synthesis and assembly of polymeric microparticles using microfluidics *Adv. Matter* **21** 4071–86
[438] Park J I, Saffari A, Kumar S, Günther A and Kumacheva E 2010 Microfluidic synthesize of polymer and inorganic particulate materials *Annu. Rev. Mater. Res.* **40** 415–43
[439] About-Hassan A, Sandre O and Cabuil V 2010 Microfluidics in inorganic chemistry *Angew. Chem. Int. Edn Engl.* **49** 6268–86
[440] Shum H C, Abate A R, Lee D, Studart A R, Wang B, Chen C H, Thiele J, Shah R K, Krummel A and Weitz D A 2010 Droplet microfluidics for fabrication of non-spherical particles *Macromol. Rapid. Commun.* **31** 108–18
[441] Tumarkin E and Kumacheva E 2009 Microfluidic generation of microgels from synthetic and natural polymers *Chem. Soc. Rev.* **9** 2161–8
[442] Abate A R, Chen C H, Agresti J J and Weitz D A 2009 Beating Poisson encapsulation statistics using close-packed ordering *Lab Chip* **9** 2628–31
[443] Theberge A B, Courtois F, Schaerli F, Fischlechner M, Abell C, Hollfelder F and Huck W T S 2010 Microdroplets in microfluidics: an evolving platform for

discoveries in chemistry and biology *Angew. Chem. Int. Edn Engl.* **49** 5846–68
[444] Vogelstein B and Kinzler K W 1999 Digital PCR *Proc. Natl Acad. Sci. USA* **96** 9236–41
[445] Beer N R, Wheeler E K, Lee-Houghton L, Watkins N, Nasarabadi S, Hebert N, Leung P, Arnold D W, Bailey C G and Colston B W 2008 On-chip single-copy real-time reverse-transcription PCR in isolated picoliter droplets *Anal. Chem.* **80** 1854–8
[446] Kiss M M, Ortoleva-Donnelly L, Beer N R, Warner J, Bailey C G, Colston B W, Rothberg J M, Link D R and Leamon J H 2008 High-throughput quantitative polymerase chain reaction in picoliter droplets *Anal. Chem.* **80** 8975–81
[447] Schaerli Y, Wootton R C, Robinson T, Stein V, Dunsby C, Neil M A A, French P M W, deMello A J, Abell C and Hollfelder F 2009 Continuous-flow polymerase chain reaction of single-copy dna in microfluidic microdroplets *Anal. Chem.* **81** 302–6
[448] Huebner A, Srisa-Art M, Holt D, Abell C, Hollfelder F, Demello A J and Edel J B 2007 Quantitative detection of protein expression in single cells using droplet microfluidics *Chem. Commun.* 1218–20
[449] Boedicker J Q, Li L, Kline T R and Ismagilov R F 2008 Detecting bacteria and determining their susceptibility to antibiotics by stochastic confinement in nanoliter droplets using plug-based microfluidics *Lab Chip* **8** 1265–72
[450] Schmitz C H J, Rowat A C, Köster S and Weitz D A 2009 Dropspots: a picoliter array in a microfluidic device *Lab Chip* **9** 44–9
[451] Köster S *et al* 2008 Drop-based microfluidic devices for encapsulation of single cells *Lab Chip* **8** 1110–15
[452] Clausell-Tormos J *et al* 2008 Droplet-based microfluidic platforms for the encapsulation and screening of mammalian cells and multicellular organisms *Chem. Biol.* **15** 427–37
[453] He M Y, Edgar J S, Jeffries G D M, Lorenz R M, Shelby J P and Chiu D T 2005 Selective encapsulation of single cells and subcellular organelles into picoliter- and femtoliter-volume droplets *Anal. Chem.* **77** 1539–44
[454] Zhan Y H, Wang J, Bao N and Lu C 2009 Electroporation of cells in microfluidic droplets *Anal. Chem.* **81** 2027–31
[455] Rowat A C, Bird J C, Agresti J J, Rando O J and Weitz D A 2009 Tracking lineages of single cells in lines using a microfluidic device *Proc. Natl Acad. Sci. USA* **106** 18149–54
[456] Edd J F, Di Carlo D, Humphry K J, Köster S, Irimia D, Weitz D A and Toner M 2008 Controlled encapsulation of single-cells into monodisperse picolitre drops *Lab Chip* **8** 1262
[457] Chabert M and Viovy J L 2008 Microfluidic high-throughput encapsulation and hydrodynamic self-sorting of single cells *Proc. Natl Acad. Sci. USA* **105** 3191–6
[458] Courtois F, Olguin L F, Whyte G, Bratton D, Huck W T S, Abell C and Hollfelder F 2008 An integrated device for monitoring time-dependent *in vitro* expression from single genes in picolitre droplets *ChemBioChem* **9** 439–46
[459] Evans H M, Surenjav E, Priest C, Herminghaus S and Seemann R 2009 *In situ* formation, manipulation, and imaging of droplet-encapsulated fibrin networks *Lab Chip* **9** 1933–41
[460] Liu W, Jawerth L M, Sparks E A, Falvo M R, Hantgan R R, Superfine R, Lord S T and Guthold M 2006 Fibrin fibers have extraordinary extensibility and elasticity *Science* **313** 634
[461] Wen Q, Basu A, Winer J P, Yodh A and Janmey P A 2007 Local and global deformations in a strain-stiffening fibrin gel *New J. Phys.* **9** 428
[462] Song H, Li H W, Munson M S, VanHa T G and Ismagilov R F 2006 On-chip titration of an anticoagulant argatroban and determination of the clotting time within whole blood or plasma using a plug-based microfluidic system *Anal. Chem.* **78** 4839–49.
[463] Pfohl T, Otten A, Köster S, Dootz R, Struth B and Evans H M 2007 Highly packed and oriented DNA mesophases identified using *in situ* microfluidic x-ray microdiffraction *Biomacromolecules* **8** 2167–72
[464] Köster S, Evans H M, Wong J Y and Pfohl T 2008 An *in situ* study of collagen self-assembly processes *Biomacromolecules* **9** 199–207
[465] Evans H M, Dootz R, Köster S, Struth B and Pfohl T 2007 X-ray microdiffraction on flow-controlled biomolecular assemblies *Bull. Polish Acad. Sci.* **55** 217–27
[466] Köhler J M, Henkel Th Grodrian A, Kirner Th, Roth M, Martin K and Metze J 2004 Digital reaction technology by micro segmented flow—components, concepts and applications *Chem. Eng. J.* **101** 201–16
[467] Shikida M, Takayanagi K, Inouchi K, Honda H and Sato K 2006 Using wettability and interfacial tension to handle droplets of magnetic beads in a micro-chemical-analysis system *Sensors Actuators* B **113** 563–9
[468] Mukhopadhyay R 2007 When PDMS isn't the best. What are its weaknesses, and which other polymers can researchers add to their toolboxes? *J. Am. Chem. Soc.* **79** 3248–53
[469] Wu N, Zhu Y, Brown S, Oakeshott J, Peat T S, Surjadi R, Easton C, Leech P W and Sexton B A 2009 A PMMA microfluidic droplet platform for *in vitro* protein expression using crude *E. coli* S30 extract *Lab Chip* **9** 3391–8
[470] Wu N, Courtois F, Zhu Y, Oakeshott J, Easton C and Abell C 2010 Management of the diffusion of 4-methylumbelliferone across phases in microdroplet-based systems for *in vitro* protein evolution *Electrophoresis* **31** 3121–8
[471] Nguyen N T, Lassemoto S and Chollet F A 2006 Optical detection for droplet size control in microfluidic droplet-based analysis systems *Sensors Actuators* B **117** 431–6
[472] Vyawahara S, Griffiths A D and Merten C A 2010 Miniaturization and parallelization of biological and chemical assays in microfluidic devices *Chem. Biol.* **17** 1052–6
[473] Abate A R, Hung T, Mary P, Agresti J J and Weitz D A 2010 High-throughput injection with microfluidics using picoinjectors *Proc. Natl Acad. Sci. USA* **107** 19163–6
[474] Abate A R, Agresti J J and Weitz D A 2010 Microfluidic sorting with high-speed single-layer membrane valves *Appl. Phys. Lett.* **96** 203509
[475] Romanowsky M B, Heymann M, Abate A R, Krummel A T, Fraden S and Weitz D A 2010 Functional patterning of PDMS microfluidic devices using integrated chemo-masks *Lab Chip* **10** 1521–4
[476] Abate A R, Thiele J, Weinhart M and Weitz D A 2010 Patterning microfluidic device wettability using flow confinement *Lab Chip* **10** 1774–6
[477] Seiffert S, Romanowsky M B and Weitz D A 2010 Janus microgels produced from functional precursor polymers *Langmuir* **26** 14842–7
[478] Seiffert S and Weitz D A 2010 Microfluidic fabrication of smart microgels from macromolecular precursors *Polymer* **51** 5883–9
[479] Protière S, Bazant M Z, Weitz D A and Stone H A 2010 Droplet breakup in flow past an obstacle: a capillary instability due to permeability variations *Europhys. Lett.* **92** 54002
[480] Datta S S, Shum H C and Weitz D A 2010 Controlled buckling and crumpling of nanoparticle-coated droplets *Langmuir* **26** 18612–6

[481] Abate A R and Weitz D A 2011 Syringe-vacuum microfluidics: a portable technique to create monodisperse emulsions *Biomicrofluidics* **5** 14107
[482] Seiffert S, Dubbert J, Richtering W and Weitz D A 2011 Reduced UV light scattering in PDMS microfluidic devices *Lab Chip* **11** 966–8
[483] Abate A R and Weitz D A 2011 Air-bubble-triggered drop formation in microfluidics *Lab Chip* **11** 1713–16
[484] Abate A R and Weitz D A 2011 Faster multiple emulsification with drop splitting *Lab Chip* **11** 1911–15
[485] Thiele J, Windbergs M, Abate A R, Trebbin M, Shum H C, Förster S and Weitz D A 2011 Early development drug formulation on a chip: fabrication of nanoparticles using a microfluidic spray dryer *Lab Chip* **11** 2362–8
[486] Goluch E D, Nam J-M, Georganopoulou D G, Chiesl T N, Shaikh K A, Ryu K S, Barron A E, Mirkin C A and Liu C 2006 A bio-barcode assay for on-chip attomolar-sensitivity protein detection *Lab Chip* **6** 1293–9
[487] Psaltis D, Quake S R and Yang C 2006 Developing optofluidic technology through the fusion of microfluidics and optics *Nature* **442** 381–6
[488] Klostranec J M, Xiang Q, Farcas G A, Lee J A, Rhee A, Lafferty E I, Perrault S D, Kain K C and Chan W C W 2007 Convergence of quantum dot barcodes with microfluidics and signal processing for multiplexed high-throughput infectious disease diagnostics *Nano Lett.* **7** 2812–18
[489] Zhao Y, Shum H C, Chen H, Adams L L A, Gu Z and Weitz D A 2011 Microfluidic generation of multifunctional quantum dot barcode particles *J. Am. Chem. Soc.* **133** 8790–3
[490] Agresti J J, Antipov E, Abate A R, Ahn K, Rowat A C, Baret J-C, Marquez M, Klibanov A M, Griffiths A D and Weitz D A 2010 Ultrahigh-throughput screening in drop-based microfluidics for directed evolution *Proc. Natl Acad. Sci. USA* **107** 4004–9
[491] Tice J D, Song H, Lyon A D and Ismagilov R F 2003 Formation of droplets and mixing in multiphase microfluidics at low values of the Reynolds and the capillary numbers *Langmuir* **19** 9127–33
[492] Carroll N J, Rathod S B, Derbins E, Mendez S, Weitz D A and Petsev D N 2008 Letter droplet-based microfluidics for emulsion and solvent evaporation synthesis of monodisperse mesoporous silica microspheres *Langmuir* **24** 658–61
[493] Lee I, Yoo Y, Cheng Z and Jeong H-K 2008 Generation of monodisperse mesoporous silica microspheres with controllable size and surface morphology in a microfluidic device *Adv. Funct. Matter* **18** 4014–21
[494] Krüger J, Singh K, O'Neill A, Jackson C, Morrison A and O'Brien P 2002 Development of a microfluidic device for fluorescence activated cell sorting *J. Micromech. Microeng.* **12** 486–94
[495] Studer V, Jameson R, Pellereau E, Pépin A and Chen Y 2004 A microfluidic mammalian cell sorter based on fluorescence detection *Microelectron. Eng.* **73** 852–7
[496] Yang S Y, Hsiung S K, Hung Y C, Chang C M, Liao T L and Lee G B 2006 A cell counting/sorting system incorporated with a microfabricated flow cytometer chip *Meas. Sci. Technol.* **17** 2001–9
[497] Lee S J, Chan J C Y, Maung K J, Rezler E and Sundararajan N 2007 Characterization of laterally deformable elastomer membranes for microfluidics *J. Micromech. Microeng.* **17** 843–51
[498] Ota S, Yoshizawa S and Takeuchi S 2009 Microfluidic formation of monodisperse, cell-sized, and unilamellar vesciles *Angew. Chem. Int. Edn Engl.* **48** 6533–7
[499] Noireaux V and Libchaber A 2004 A vesicle bioreactor as a step towards an artificial cell assembly *Proc. Natl Acad. Sci. USA* **101** 17669–74
[500] Pautot S, Frisken B J and Weitz D A 2003 Engineering asymmetric vesicles *Proc. Natl Acad. Sci. USA* **100** 10718–21
[501] Stachowiak J C, Richmond D L, Li T H, Liu A P, Parekh S H and Fletcher D A 2008 Unilamellar vesicle formation and encapsulation by microfluidic jetting *Proc. Natl Acad. Sci. USA* **105** 4697–702
[502] Stachowiak J C, Richmond D L, Li T H, Brochard-Wyart F and Fletcher D A 2009 Inkjet formation of unilamellar lipid vesicles for cell-like encapsulation *Lab Chip* **9** 2003–9
[503] Thutupalli S, Herminghaus S and Seemann R 2011 Bilayer membranes in micro-fluidics: from gel emulsions to soft functional devices *Soft Matter* **7** 1312–20 and references therein
[504] Kelly B T, Baret J-C, Taly V and Griffiths A D 2007 Miniaturizing chemistry and biology in microdroplets *Chem. Commun.* 1773–88
[505] Zhu Y and Power B E 2008 Lab-on-a-chip *in vitro* compartmentalization technologies for protein studies *Protein–Protein Interaction* (*Advances in Biochemical Engineering/Biotechnology* vol 110) (Berlin: Springer) pp 81–114
[506] Wu N, Oakeshott J, Brown S, Easton C and Zhu Y 2010 Microfluidic droplet technique for *in vitro* direct evolution *Aust. J. Chem.* **63** 1313–25
[507] Shum C H, Carreras E S, Kim J-W, Ehrlicher A, Bibette J and Weitz D A 2011 Dewetting-induced membrane formation by adhesion of amphiphile-laden interfaces *J. Am. Chem. Soc.* **133** 4420–6
[508] Shum H C, Zhao Y-J, Kim S-H and Weitz D A 2011 Multicompartment polymersomes from double emulsions *Angew. Chem. Int. Edn Engl.* **50** 1648–51
[509] Chen Y, Wang Y J, Yang L A and Luo G S 2008 Micrometer-sized monodispersed silica spheres with advanced adsorption properties *AIChE J.* **54** 298–309
[510] Mary P, Chen A, Chen I, Abate A R and Weitz D A 2011 On-chip background noise reduction for cell-based assays in droplets *Lab Chip* **11** 2066–70